Electrostatic field theory and measurement

Learn to infer a field from charges, potentials or boundary measurements. Build the mathematics of flux, uniqueness and Green functions as each problem requires it.

Contents

1. **From a force reading to Poisson's equation**
   Imagine trying to infer an invisible charge distribution with a force probe and a voltmeter. Coulomb's law, Gauss's law and the electrostatic potential describe the same experiment in three different ways. Deriving the connections also exposes the measurements a single probe cannot make.
2. **Vector calculus through flux, circulation and singular sources**
   A closed-surface flux and a closed-path circulation answer different experimental questions. Starting from small physical collecting surfaces shows why the associated differential operators look different in Cartesian, cylindrical and spherical coordinates.
3. **When do boundary measurements determine a unique electrostatic field?**
   A boundary-value solver may converge while solving the wrong electrical experiment. Establishing which potentials, charges and fluxes are fixed gives a uniqueness proof and a way to turn an approximate field into an upper bound.
4. **Images in wedges, cylinders and dielectric interfaces**
   An image source is a construction for a particular physical domain and boundary condition. Three examples show how geometry determines the image position, how material response sets its amplitude, and why an apparent success on part of a boundary is insufficient.
5. **Green functions, the Poisson kernel and what a small electrode can influence**
   A Green function is the response of an entire boundary-value problem to a unit source. Once that response is known, a continuous charge distribution and a patterned boundary voltage can both be treated by integration. The two integrations require different kernels.
6. **Rectangular geometries, orthogonality and sources that drive individual modes**
   Fourier modes are solutions selected by their electrode walls. On a rectangle they turn a boundary-voltage problem into independent vertical equations. When a charge fills the rectangle the same eigenfunctions give a different denominator and a different physical response.

7. Cylindrical geometry, coaxial boundaries and Bessel spectra

The radial coordinate of a cylinder leads to logarithms in one experiment and to Bessel functions in another. The difference is set by the variation along the axis and around the circumference. Recovering the radial weight from flux clarifies both.

8. Normalised spherical harmonics and the field of an arbitrary three-dimensional source

An axial voltage scan can determine Legendre coefficients only if the source is rotationally symmetric. A general spherical electrode or molecule needs angular modes with two indices. Their normalisation fixes the conversion from a measured multipole coefficient to a physical voltage.

9. Capacitance matrices, floating nodes and controlled approximation bounds

A multi-electrode device generally has no single capacitance until the other terminals have been connected or isolated. An energy identity determines the matrix that relates voltages to charges, and a complementary flux identity can certify estimates even when the exact field is unknown.

10. Anisotropic and nonlinear dielectrics from local measurements to global fields

A single dielectric constant cannot describe a crystal whose displacement tilts away from its electric field, or a reversible material whose incremental response changes with bias. Starting with the constitutive measurement clarifies which parts of ordinary electrostatics survive.

11. From mobile ions to screening lengths and differential double-layer capacitance

A charged planar wall in an electrolyte can be studied without assuming a capacitance in advance. Diffusion and electrostatic drift first establish an ion cloud. The charge–voltage slope of that cloud is an experimental output of the model.

12. Reconstructing a source from noisy voltage measurements

A forward electrostatic calculation can be unique and stable while the inverse problem constructed from it is unstable or nonunique. A scanned electrode, a finite collecting area and an explicitly chosen noise level make these statements experimentally testable.

13. Which electrode sees a charge moving above a detector?

A point charge moves without touching the electrodes. Derive the induced charge on one strip from a second, source-free boundary problem. Use the two-dimensional map to distinguish motion across the detector from motion away from it.

14. Build the field operators in curved coordinates

Derive the geometric factors in gradient, divergence, curl and Laplacian, then use dimensional conversion to compare electromagnetic conventions.

Electrostatic field theory and measurement · 1. From a force reading to Poisson’s equation

Imagine trying to infer an invisible charge distribution with a force probe and a voltmeter. Coulomb’s law, Gauss’s law and the electrostatic potential describe the same experiment in three different ways. Deriving the connections also exposes the measurements a single probe cannot make.

Calibrate a probe before calling its reading a field

Place a small charged bead on an insulating support, sufficiently far from other objects for the effect of surrounding matter to be negligible. At a known point nearby, hold a much smaller probe charge q_t on a force balance. If the only force changing when the source is introduced is electrical, the difference in force readings is $q_t\mathbf{E}$. Operationally one should repeat the measurement with decreasing probe charge and extrapolate the ratio $\mathbf{F}/q_t$. Otherwise a mobile source or a nearby conductor might rearrange in response to the probe itself. A field at a point means the force per unit positive test charge in this limiting preparation.

In SI units the vacuum force between stationary point charges is parallel to their separation. A convenient convention places the source at $\mathbf{y}$, the detector at $\mathbf{x}$, and defines $\mathbf{R} = \mathbf{x} - \mathbf{y}$. Then $\mathbf{E} = q\mathbf{R}/(4\pi\epsilon_0 R^3)$. The factor $\mathbf{R}/R^3$ contains a unit direction vector and an inverse square in magnitude. Reversing source sign reverses the vector. Doubling distance reduces its magnitude to one quarter. Doubling source and test charge together increases the force fourfold while doubling the field only twice relative to the original experiment.

For $q = 40$ pC at distance 60 mm the magnitude is 99.9 V/m. A positive 2 pC test bead experiences 0.200 nN away from the source. A negative probe gives the opposite force at the same field. This example also establishes why reporting a force in newtons and a field in volts per metre are physically different measurements. Making the test charge twice as large can improve the force signal but can increase disturbance of the original experiment.

Replace a sum by an integral without losing the direction

For two sources superposition adds forces on the same probe, so the electric fields add as vectors. In a continuous charge distribution divide space into cells small on the scale of the observation distance and assign each cell $dq = \rho(\mathbf{y}) d^3y$. Refining the partition gives

$$\mathbf{E}(\mathbf{x}) = \frac{1}{4\pi\epsilon_0} \int \frac{\mathbf{x} - \mathbf{y}}{|\mathbf{x} - \mathbf{y}|^3} \rho(\mathbf{y})\, d^3y.$$

Surface or filament models replace dq by $\sigma\, dA$ or $\lambda\, ds$, respectively. Their densities have different units. A wire of radius a may be modelled as a line at observation distances large compared with a, while the field right at the ideal line diverges. Replacing a physical distribution with a lower-dimensional source is an approximation about distances. It is not a claim that metal contains literal curves with zero area.

Take a straight filament extending along z from $-L$ to $+L$, with constant λ. On the perpendicular bisector at $x = s > 0$, terms from z and $-z$ cancel their axial components. A slice contributes $dE_x = \lambda s\, dz/[4\pi\epsilon_0 (s^2 + z^2)^{3/2}]$. Using $d[z/\sqrt{s^2 + z^2}]/dz = s^2/(s^2 + z^2)^{3/2}$ yields

$$E_x = \frac{\lambda}{2\pi\epsilon_0 s}\frac{L}{\sqrt{s^2+L^2}}.$$

At $s \ll L$ this is the infinite-line expression. At $s \gg L$ it becomes $2L\lambda/(4\pi\epsilon_0 s^2)$, exactly the point-charge field for the full segment. The same model changes apparent radial power law between two limits. For $s = L$ the long-line formula would overpredict by a factor $\sqrt{2}$. Fitting an observed power law over a limited range does not identify the microscopic source shape.

Discover why inverse-square strength produces a flux law

Choose a patch of surface at distance R from a point charge. Its oriented area is $\hat{\mathbf{n}}\,dA$. Only the component projected perpendicular to the ray contributes to radial-field flux. That projected area is $\hat{\mathbf{n}}\cdot\hat{\mathbf{R}}\,dA = R^2 d\Omega$, where $d\Omega$ is an oriented solid angle. Consequently $d\Phi_E = q\,d\Omega/(4\pi\epsilon_0)$. The decrease with R^2 exactly cancels the spread of a fixed cone. An enclosing sphere covers total solid angle 4π, and any smooth closed surface surrounding the point gives the same oriented total because each outward ray leaves once more than it re-enters. For a charge lying outside, entering and leaving contributions cancel.

Superposition extends this argument to arbitrary bounded sources. For a closed surface with no point source on the surface,

$$\oint \mathbf{E}\cdot d\mathbf{A} = Q_{\text{inside}}/\epsilon_0.$$

This equation returns one scalar from an entire field map. It determines pointwise E only where symmetry fixes directions and makes the relevant component constant over the chosen pieces. Draw a cube around an off-centre charge. The six face fluxes still sum to q/ϵ_0, but symmetry cannot divide that sum by six. Draw the same cube centred on that charge and all six face integrals become equal even though the field is not uniform across an individual face.

Gauss's law also explains the field of a thick spherical distribution without integrating the Coulomb kernel. For $\rho(r)$ in a sphere centred at the origin, invariance under all rotations forces $\mathbf{E} = E_r(r)\hat{\mathbf{r}}$. A spherical collecting surface gives

$$E_r = Q(<r)/(4\pi\epsilon_0 r^2),$$

with $Q(<r) = 4\pi\int_0^r \rho(s)s^2 ds$. A hollow shell in vacuum therefore has zero interior field; its potential there may still be large relative to infinity. Changing the reference of the voltmeter affects its number but cannot change the force probe.

Why a line integral can be reduced to its endpoints

For a static point charge,

$$d(1/R) = -\hat{\mathbf{R}} \cdot d\mathbf{x}/R^2.$$

The work per unit test charge along a path from A to B is $\int_A^B \mathbf{E} \cdot d\mathbf{x} = q[1/R_A - 1/R_B]/(4\pi\epsilon_0)$. It depends only on endpoints. Superposing static sources preserves this property. We define $V(B) - V(A) = -\int_A^B \mathbf{E} \cdot d\mathbf{x}$. With a reference at infinity for a compact distribution, direct integration gives

$$V(\mathbf{x}) = \int \rho(\mathbf{y})/(4\pi\epsilon_0|\mathbf{x} - \mathbf{y}|)\, d^3y.$$

A numerical evaluation adds scalar potentials; a directional derivative recovers the desired force component. Differentiating local data can amplify noise, so a voltage map and a force map are equivalent descriptions mathematically but different experiments.

An infinitesimal displacement yields

$$\mathbf{E} = -\nabla V.$$

To see the sign, move a positive probe in the field direction. The field does positive work and the potential decreases. Surfaces of constant V are perpendicular to $\mathbf{E}$ wherever its magnitude is nonzero. Uniformly spaced contour values on a map denote equally spaced voltages, not equal physical intervals. Where those contours crowd together the component normal to them has greater magnitude.

For the finite filament, integrating $dz/\sqrt{s^2 + z^2}$ on the perpendicular bisector gives

$$V(s) = \lambda \operatorname{arsinh}(L/s)/(2\pi\epsilon_0).$$

Its negative derivative recovers the field above. If L tends to infinity at fixed s, the field reaches a finite limit but V diverges logarithmically when referenced to infinity. A measured difference $V(s_2) - V(s_1)$ stays finite, tending to $-\lambda \ln(s_2/s_1)/(2\pi\epsilon_0)$. The failure is in the proposed reference for the infinite model. Real finite conductors and return paths supply physically well-defined voltage references.

From integral measurements to a boundary problem

Apply the divergence theorem to Gauss's law in a smooth region: $\int_\Omega (\nabla \cdot \mathbf{E} - \rho/\epsilon_0) d^3x = 0$. It holds for arbitrary small volumes, so $\nabla \cdot \mathbf{E} = \rho/\epsilon_0$ there. Combining it with the potential gives Poisson's equation $-\epsilon_0 \nabla^2 V = \rho$, reducing to Laplace's equation in empty space. At point or sheet sources this statement has an integral, or distributional, interpretation. A single derivative at the singularity is not an ordinary finite number.

The equation alone is insufficient to compute a laboratory voltage. Adding any harmonic function changes the field while preserving the same charge density inside the region. Installing external electrodes changes those harmonic contributions. To predict a unique measurement, supply boundary potentials, conductor charges, flux conditions or an appropriate condition at infinity. For example, $V(x) = \rho x(L - x)/(2\epsilon_0)$ solves a one-dimensional region of uniform charge between grounded planes

at 0 and L. Raising the right plane to V_b adds $V_b x/L$. The curvature and inferred density remain identical, while the force throughout the gap acquires a uniform extra component.

How does this fit time-dependent Maxwell theory? A static source satisfies a zero-curl electric field and the Gauss constraint. With a varying magnetic flux, Faraday changes the circulation to $-d\Phi_B/dt$, so a purely scalar, path-independent description of the complete electric field can fail. A slowly driven experiment can remain close to an electrostatic sequence when induction corrections and propagation delays are negligible. Compare the system flight time L/c with its driving timescale, but also check any imposed magnetic flux. A small device placed around a deliberately changing magnetic circuit can have appreciable induced circulation even when its own dimensions are small.

A finite charged sheet and the solid angle it subtends

An insulating rectangle spans $-a \le x' \le a$, $-b \le y' \le b$ in the horizontal plane, carrying prescribed uniform surface charge σ. The sides need not be equal. Measure the field directly above its centre at $(0, 0, h)$, $h > 0$. Reflection suppresses the two lateral components but there is no sufficiently symmetric closed Gaussian surface that supplies the remaining field from flux alone. Instead each patch contributes $dE_z = \sigma h\, dx'dy'/[4\pi\epsilon_0(x'^2 + y'^2 + h^2)^{3/2}]$. The factor $h\,dx'dy'/R^3$ is the positive solid angle of the patch as seen from the detector. Thus $E_z = \sigma\Omega/(4\pi\epsilon_0)$, where Ω is the solid angle of the whole rectangle. This reverses the usual flux picture: the detector is the point from which the source surface is viewed.

The integral can be evaluated without a solid-angle table. By symmetry integrate one quadrant and multiply by four. First integrate along x' using the antiderivative $x'/[(h^2 + y'^2)\sqrt{x'^2 + h^2 + y'^2}]$. This leaves $\int_0^b ah\, dy'/[(h^2 + y'^2)\sqrt{a^2 + h^2 + y'^2}]$. Differentiating $\arctan[ay'/(h\sqrt{a^2 + h^2 + y'^2})]$ recovers precisely this integrand. Consequently

$$E_z = \frac{\sigma}{\pi\epsilon_0}\arctan\left(\frac{ab}{h\sqrt{a^2 + b^2 + h^2}}\right).$$

Before inserting numbers, examine both extreme geometries. When $h \to 0^+$ at fixed a, b, the arctangent tends to $\pi/2$. A small probe above the interior sees the infinite-sheet field $\sigma/(2\epsilon_0)$. Reverse h to obtain its opposite below the sheet, giving the correct normal jump. If $h \gg a, b$, the arctangent argument is small and $E_z \simeq \sigma ab/(\pi\epsilon_0 h^2) = Q/(4\pi\epsilon_0 h^2)$ for $Q = 4ab\sigma$. A finite source with sheet-like near field therefore regains a point-like field without needing a second physical law.

For a square of half-width 4.0 cm, at $h = 4.0$ cm its solid angle is

$$4\arctan(1/\sqrt{3}) = 2\pi/3.$$

The field is only one third of the infinite-sheet estimate. If $\sigma = 2.0$ nC/m², that is 37.6 V/m instead of 113 V/m. A cube of side 8.0 cm drawn around a point at its centre has exactly the same solid angle on each face. Six copies of $2\pi/3$ close to 4π; this checks the integral's normalisation without referring back to the same antiderivative. At the same h, replacing the entire charged square by a point would instead give 71.9 V/m. Its error has the other sign because the approximation concentrates all charge at the closest radial location.

The same formula can be used for a point above a rectangular sensor away from its centre. Break the rectangle into four axis-aligned pieces whose common corner lies at the projected point. Add their signed quadrant solid angles with their actual edge distances, taking care of sign when the projection lies outside the detector. A useful numerical strategy is to integrate the near patch analytically and the smooth distant patches by quadrature. A uniform mesh chosen only to match the physical electrode widths may entirely miss the sharply peaked angular kernel at small h. Refine around the projection while checking the total field against the measured large-distance and small-distance limits.

What a differential voltage measurement rejects

A voltmeter spanning two nearby points measures an integral of the field rather than a pointwise derivative. Put two identical probes at $x = \pm s/2$ on an axis and report $\Delta V = V(-s/2) - V(+s/2)$. Taylor expansion around the origin gives

$$\Delta V / s = -V'(0) - s^2 V'''(0)/24 + O(s^4).$$

It cancels a common voltage offset and the quadratic term. The estimate approaches the centre field with an error set by curvature of the field itself, not by the local voltage magnitude. A common reference shift can be huge and still disappear exactly, while spatially varying disturbances remain.

Take a small source charge q on the same axis at $x = d > s/2$. The exact potential is $kq/(d - x)$,

$$k = 1/(4\pi\epsilon_0).$$

Substitution gives a signed differential estimate $\Delta V / s = -kq/[d^2 - (s/2)^2]$. The true field at the midpoint is $-kq/d^2$, pointing away from a positive charge to the left. A probe of finite separation overestimates its magnitude by $1/[1 - (s/2d)^2]$. For $s = 10$ mm, $d = 25$ mm the bias is 4.17%. Reducing s to 5 mm gives 1.01%. This systematic error does not disappear by repeating the same pair of readings many times.

Measurement noise produces the opposite trend. If each voltage reading has independent standard deviation δV, their difference divided by s has standard deviation $\sqrt{2}\,\delta V / s$. Halving probe separation doubles the field uncertainty even as it quarters the leading geometrical bias. With $\delta V = 0.5$ mV, a 10 mm baseline gives 0.071 V/m uncertainty. At a true field of 10 V/m and the preceding geometry, the systematic 0.417 V/m is larger; at 5 mm it falls to 0.101 V/m while random uncertainty grows to 0.141 V/m. Comparing both scales helps choose a practical probe spacing. Correlated noise from a common reference changes the variance calculation and may cancel more completely than independent probe noise.

This distinction persists when measurements are replaced by a grid of computed potentials. A finite-difference derivative measures change over a cell, while the Coulomb integral can give the field directly at a point. Agreement of the raw potential to many digits does not guarantee a comparably accurate local field if neighbouring numerical errors vary rapidly. Use a known analytic source, vary the sampling baseline separately from the underlying field mesh, and compare the measured scaling with the predicted s^2 truncation and $1/s$ noise behaviour. That procedure checks an actual numerical reading of the physical observable rather than simply refining every parameter together.

Can a bead of nonzero size measure the field at one point?

Consider a rigid insulating bead of radius a_t, carrying a fixed spherically symmetric probe charge density $\rho_t(r)$ and total charge q_t. The external sources all lie outside the bead and do not move when the bead is introduced. These assumptions exclude rearrangement of either the probe's own charge or the external conductors. Its net electric force is the volume integral $\int \rho_t(\mathbf{s})\mathbf{E}_{\text{ext}}(\mathbf{x}_0+\mathbf{s})d^3s$. It might appear necessary to treat every nonzero bead radius as a source of measurement bias. In this particular experiment the result equals $q_t\mathbf{E}_{\text{ext}}(\mathbf{x}_0)$ exactly.

To see why, the external potential is harmonic throughout the enclosing ball. Each Cartesian component of its field is also harmonic there, because a Cartesian derivative commutes with the Laplacian in a smooth uniform vacuum. The mean-value property says that the angular average of a harmonic field component on each spherical shell equals its value at the centre. Pull this value through the remaining radial integral of $\rho_t(r)\,4\pi r^2 dr$ and the result follows. The field can change strongly across the bead. What matters is the combination of a source-free exterior solution within its volume and a rigid radially symmetric charge weight. A probe that averages along a straight baseline, as above, does not possess this spherical mean-value property.

What changes if the source charge distribution lies partly inside the sampling ball? In a charged region $\nabla^2 E_i = \partial_i \rho/\epsilon_0$, so a density gradient can produce a finite-size correction. For a uniform spherical probe a Taylor expansion gives $\langle s_i s_j\rangle = (a_t^2/5)\delta_{ij}$, hence leading force per total charge $E_i(\mathbf{x}_0) + (a_t^2/10)\nabla^2 E_i(\mathbf{x}_0)$. In a locally uniform volume charge even this correction vanishes, since an electric field linear in position averages to its central value under any centred symmetric probe. Material interfaces or singular sources require separate treatment; the smooth expansion cannot be extended through them by taking more terms.

A conducting sensor is a different preparation. A neutral conducting bead carries an induced dipole in an external field and can feel a force in a field gradient even with lab-calibrated net charge zero. One experimental check is to reverse the deliberately deposited test charge while keeping its magnitude fixed. In a weakly perturbing regime the desired force changes sign with q_t; a charge-independent polarisation force contributes to the even part. Dividing a single force measurement by q_t without checking such an offset may produce an apparent field that changes with probe charge. A physically meaningful field measurement begins by deciding what the actual sensor averages and which parts of its signal follow the calibration law.

Measure the field of a finite source

Move along the axis of an annulus and compare the integrated source with its distant point-charge limit. Identify the length scale that controls the difference.

Open this experiment online

Try the calculation

Hole / outer radius **0.5**

Radial integration cells **8**

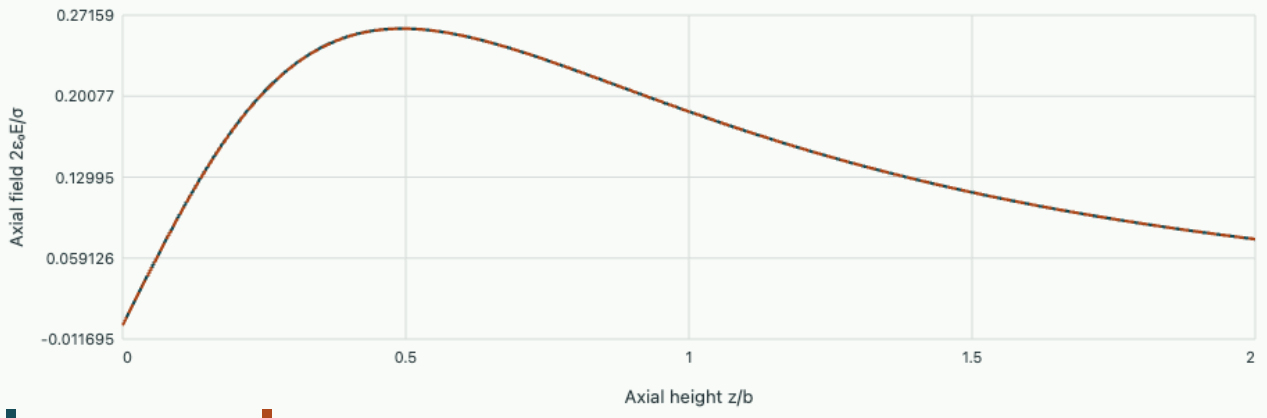

Analytic integral Ring quadrature

The analytic peak is at z/b = 0.4934 with field 0.2599. At that location the quadrature differs by -0.01507%.

Tutorial · design measurements that distinguish sources

A finite line mistaken for an infinite one

A filament extends from −40 to +40 mm. A probe is placed 10 mm from its midpoint on the perpendicular bisector. Find the fractional error from using the infinite-line formula. How close must the probe be for that approximation to overstate the exact field by less than 1%?

▼ **Work through the solution**

The ratio of the approximation to the exact field is $\sqrt{1+(s/L)^2}$. At $s/L = 1/4$ this is 1.0308, so the overestimate is 3.08%. Requiring the ratio below 1.01 gives $s/L < \sqrt{1.01^2 - 1} = 0.1418$, or $s < 5.67$ mm. The proximity criterion must coexist with the condition that the physical filament radius be much smaller than s. No universal sensor distance satisfies both criteria for every wire.

A second check is to take two radial readings. Their ratio cancels any unknown absolute calibration of λ. The infinite-line prediction is simply the inverse distance ratio, whereas the exact result contains the two end correction factors. With finite signal noise a reading very near the source may not be necessary if the probe is stable enough to resolve the predicted ratio difference.

Can an external cage identify a hollow charge distribution?

A spherical shell at radius a and a solid sphere of radius a carry the same spherically symmetric total charge. Compare external voltage, centre voltage, and electrostatic work on a positive probe from the centre to the surface for uniform charge in each model.

▼ **Work through the solution**

Outside both, the field is $q/(4\pi\epsilon_0 r^2)$ and the potential with zero at infinity is $q/(4\pi\epsilon_0 r)$. No exterior electrostatic measurement can distinguish these sources within the spherical model. For the shell the interior field vanishes, so centre and surface potentials are equal and the journey does no electrical work on the probe. For a solid uniform sphere $E_r = qr/(4\pi\epsilon_0 a^3)$, so $V(0) - V(a) = q/(8\pi\epsilon_0 a)$. The centre potential becomes $3q/(8\pi\epsilon_0 a)$ and the outward electrical work on test charge q_t is $q_t q/(8\pi\epsilon_0 a)$.

At fixed radius the solid's higher centre voltage coexists with zero centre field, because the potential slope vanishes there by symmetry. An internal probe may itself disturb the charges in a liquid or conductor. The comparison assumes the specified source profiles stay fixed as measurements are taken.

Further reading

- Integrate a finite annulus and compare its field with the analytic integral
- Reconstruct a screened charge from two voltage readings
- MIT, Electromagnetic Fields and Energy, chapter 4 · source integrals
- Griffiths, 5th ed., chapters 1–2 · vector analysis and electrostatics

Electrostatic field theory and measurement · 2. Vector calculus through flux, circulation and singular sources

A closed-surface flux and a closed-path circulation answer different experimental questions. Starting from small physical collecting surfaces shows why the associated differential operators look different in Cartesian, cylindrical and spherical coordinates.

How a short displacement detects a derivative

A voltmeter measures a difference between endpoints. If a small displacement $d\boldsymbol{\ell}$ changes a smooth potential by dV, the gradient is the unique vector satisfying $dV = \nabla V \cdot d\boldsymbol{\ell}$ for every displacement. Its component along an arbitrary unit vector is the slope in that direction. Its largest rate of increase occurs when the displacement is parallel to the gradient. A unit step in a coordinate label does not necessarily mean a unit physical displacement. This distinction is the source of the metric factors in curvilinear coordinates.

At position (s, ϕ, z) in cylindrical coordinates, the three physical components of displacement are ds, $s\,d\phi$, dz. Equating the general dot product to $\partial_s V\,ds + \partial_\phi V\,d\phi + \partial_z V\,dz$ gives

$$\nabla V = \hat{\mathbf{s}}\partial_s V + \hat{\boldsymbol{\phi}} s^{-1}\partial_\phi V + \hat{\mathbf{z}}\partial_z V.$$

The azimuthal factor converts a voltage change per radian into a voltage change per metre around a circle. For $V = V_0(s/a)\cos\phi$ the radial and azimuthal components of $-\nabla V$ are $-V_0\cos\phi/a$ and $+V_0\sin\phi/a$. Together they equal the constant Cartesian field $-V_0\hat{\mathbf{x}}/a$, since $s\cos\phi = x$. The apparent angular variation comes only from the rotating local unit vectors. Leaving out $1/s$ would predict a nonuniform field and components with incompatible dimensions.

Count what leaves the sides of a shrinking cell

Consider a vector $\mathbf{F}$, perhaps electric displacement measured in C/m². Define its divergence at a smooth point as the limiting outward flux per cell volume. In a Cartesian box $\Delta x\Delta y\Delta z$, the opposing x faces give $[F_x(x+\Delta x) - F_x(x)]\Delta y\Delta z$. Dividing by volume and adding the other pairs gives $\partial_x F_x + \partial_y F_y + \partial_z F_z$. The signed flux measures the local excess of outflow over inflow. A field can be large and uniform while its divergence is zero.

Repeat the count in a thin cylindrical wedge between s and $s + ds$, angular width $d\phi$, height dz. The outer curved face has larger area than the inner one. Their net flux is $\partial_s(sF_s)ds\,d\phi\,dz$. The two cuts at fixed angle each have physical area $ds\,dz$ and differ by $\partial_\phi F_\phi d\phi$. The axial faces contribute $\partial_z F_z\,s\,ds\,d\phi\,dz$. Division by the wedge volume gives

$$\nabla\cdot\mathbf{F} = \frac{1}{s}\partial_s(sF_s) + \frac{1}{s}\partial_\phi F_\phi + \partial_z F_z.$$

A radial flow $F_s = A/s$ has zero divergence at positive s because the same flux crosses every cylindrical side of fixed height. A constant radial magnitude instead has divergence A/s: larger cylinders carry greater total flux and therefore enclose additional source. Specifying that a magnitude is constant says nothing about the divergence of its direction field.

In a spherical sector the radial areas grow as r^2. For a spherically symmetric radial field $F_r(r)$, the same count gives $r^{-2}d(r^2F_r)/dr$. A sphere of radius r then has flux $4\pi r^2F_r(r)$. Choosing $F_r = Ar$ produces $3A$ everywhere instead of A; the two missing contributions in a one-dimensional derivative account for growth of transverse area. For a uniform charge density ρ, setting $3A = \rho/\epsilon_0$ immediately reconstructs the interior electrostatic field of a sphere.

Inspect a small loop before asserting that a potential exists

The component of curl normal to a surface is the limiting circulation of $\mathbf{F}$ around an oriented small loop divided by its area. In an xy rectangle the upper side is traversed oppositely to the lower one. Opposite x-directed sides leave $-\partial_y F_x$; opposite y-directed sides leave $+\partial_x F_y$. Thus

$$(\nabla \times \mathbf{F})_z = \partial_x F_y - \partial_y F_x.$$

For a planar polar loop the curved segments have different lengths, giving $(\nabla \times \mathbf{F})_z = s^{-1}[\partial_s(sF_\phi) - \partial_\phi F_s]$. Curl and divergence use different faces and signs even when their cylindrical formulas share a factor $1/s$.

Join many neighboring loops. Circulations on common edges cancel in pairs, leaving only the outer boundary; the summed area integrals of the curl give Stokes's theorem. A similar cancellation of internal face fluxes gives the divergence theorem. These are physical bookkeeping identities, and they motivate discretisations that attach oriented fluxes to shared faces and voltages to shared edges. Assigning two independent approximations to one shared face can spoil exact cancellation in a computed conservation budget.

Take $\mathbf{F} = A\hat{\boldsymbol{\phi}}/s$ outside a thin excluded cylinder. Its ordinary curl is zero there. Any circle about the cylinder has circulation $2\pi A$. A disk spanning this circle would pass through the excluded region, so a surface lying entirely inside the stated domain cannot supply the usual zero-curl conclusion. Locally $\mathbf{F} = \nabla(A\phi)$ on any small patch avoiding a branch cut, while the putative potential changes by $2\pi A$ after a full turn. This example explains the role of domain topology. A genuine static electrostatic source in ordinary free space has a globally consistent potential; a changing flux through an excluded region can instead generate precisely such an exterior circulation.

Measure curvature through neighboring voltages

Taking the divergence of a gradient defines $\nabla^2 V$. A Taylor expansion at a point gives

$$[V(x+h) - 2V(x) + V(x-h)]/h^2 = \partial_x^2 V + O(h^2).$$

Adding the three Cartesian expressions relates the six neighbouring voltage readings to the local charge density. Equivalently, averaging a potential over directions at radius h removes all terms odd in the displacement. The angular mean of $n_i n_j$ is $\delta_{ij}/3$, so for smooth V

$$\langle V(\mathbf{x} + h\mathbf{n})\rangle_\Omega = V(\mathbf{x}) + \frac{h^2}{6}\nabla^2 V(\mathbf{x}) + O(h^4).$$

In a region with positive charge, Poisson's equation makes the spherical average smaller than the centre value. An uncharged saddle can have strong curvature along each of two axes that cancels in the sum. A local maximum along a single measurement line therefore does not prove that an interior source exists. To make such an inference one needs curvature in every independent spatial direction or independent symmetry information.

Near a boundary or dielectric interface this smooth Taylor analysis may break down. Enforce the integral flux balance on a cell straddling the interface instead. In media of different permittivity the normal derivative of V can jump even where there is no free charge. The physical differential operator is then $\nabla \cdot (\epsilon \nabla V)$; simply inserting a pointwise averaged permittivity in front of a smooth Laplacian may erase the correct jump condition.

Use a test volume to give singular expressions meaning

Outside the origin the divergence of $\hat{\mathbf{r}}/r^2$ is zero, yet every sphere centred there has flux 4π. To characterize its source measure the field against a smooth test function f of compact support. Excise a ball of radius η, integrate by parts in the remaining exterior and note that its inward-facing inner boundary normal is $-\hat{\mathbf{r}}$. The zero bulk divergence eliminates the interior term, leaving $-\int (\hat{\mathbf{r}}/r^2) \cdot \nabla f \, dV \to 4\pi f(0)$ as the ball shrinks. This is the defining action of the three-dimensional delta distribution:

$$\nabla \cdot (\hat{\mathbf{r}}/r^2) = 4\pi \delta^3(\mathbf{r}),$$

$$\nabla^2 (1/r) = -4\pi \delta^3(\mathbf{r}).$$

The factors and signs follow from an ordinary finite flux calculation. A delta distribution has no finite peak height to compare with a mesh value. A convergent field computation should reproduce its integral and its action on smooth functions. In spherical coordinates a radially concentrated charge can be represented with a radial delta only when the $4\pi r^2$ integration weight and the convention for the endpoint are treated consistently. It is often safer to specify the enclosed charge directly.

For a finite regularisation take $V_a = q/(4\pi\epsilon_0\sqrt{r^2 + a^2})$. Differentiation gives

$$E_r = qr/[4\pi\epsilon_0 (r^2 + a^2)^{3/2}].$$

A spherical flux measurement encloses $Q/q = r^3/(r^2 + a^2)^{3/2}$. Its derivative divided by $4\pi r^2$ gives

$$\rho_a = 3qa^2/[4\pi (r^2 + a^2)^{5/2}].$$

For every $a > 0$ the density is smooth; its peak scales as a^{-3}, preserving a finite total charge. For fixed $r > 0$, $Q/q \to 1$ as $a \to 0$. Shrinking the collecting radius and the source core simultaneously at fixed r/a instead retains a nontrivial fraction. The resolution of the probe is part of the limiting experiment.

A sheet of dipoles produces a voltage jump without a net sheet

charge

Replace an ideal neutral polarised layer by two parallel charge sheets, one at $z = -d/2$ with density $-\sigma$, another at $z = +d/2$ with density $+\sigma$. Assume both planes extend far beyond the detectors so their fields can be treated as infinite-plane fields. The field outside cancels. Between them it points from positive to negative,

$$E_z = -\sigma/\epsilon_0.$$

A voltmeter moved from below to above the pair rises by $+\sigma d/\epsilon_0$. The result can stay finite when d shrinks provided that the dipole moment per area $p_s = \sigma d$ is fixed. The fields away from the layer then converge to zero on both sides while the voltage difference persists. This model is useful for a surface dipole layer, for example when positive and negative charge distributions are displaced by molecular-scale distances.

It is essential not to infer the voltage jump from the net charge enclosed in a pillbox, since the net is zero for every d. Write the signed density as $\rho_d = \sigma[\delta(z - d/2) - \delta(z + d/2)]$. For any smooth test voltage $f(z)$, integration gives $\sigma[f(d/2) - f(-d/2)] \to p_s f'(0)$. The distribution with action $f \mapsto p_s f'(0)$ is $-p_s \delta'(z)$. In one dimension Poisson's equation is $-\epsilon_0 V'' = \rho$, so a solution is

$$V = (p_s/\epsilon_0) H(z) + \text{constant},$$

where H is a step. Its derivative is a delta, its second derivative a delta derivative. Reversing the layer orientation reverses both the jump and the sign of this source distribution.

A conventional monopole sheet instead has $\rho = \sigma_f \delta(z)$. Its potential is continuous and its normal derivative jumps. The two types of ideal source thus leave different signatures in electrode boundary models. For a voltage jump of 20 mV, the required $p_s = \epsilon_0(0.020) = 1.77 \times 10^{-13}$ C/m in vacuum. Spreading it across 1.0 nm requires $\sigma = 1.77 \times 10^{-4}$ C/m² and an internal field of 20 MV/m in that thin-layer model. The large internal field is consistent with a small voltage step because it acts only over one nanometre. At fixed p_s the field energy per area grows as $p_s^2/(2\epsilon_0 d)$. Thus taking a perfect zero-thickness dipole layer gives useful exterior fields and voltage jumps but not a finite internal energy. A physical model of finite layer thickness is necessary for that observable.

Moving a numerical grid across the sheet illustrates how to recognise the two cases. If its potential samples resolve a continuous cusp, integrating the inferred charge across one symmetric layer gives finite sheet charge. If instead the voltage contains a step, two neighbouring density bins can acquire large opposite entries whose sum tends to zero. Their first moment stays finite. A useful verification uses both $\int \rho \, dz$ and $\int z\rho \, dz$ and compares potential readings on each side. A code that preserves charge but smooths a dipole step into an incorrect zero voltage would pass the first test but fail the others.

An explicit flux audit on a nonuniform mesh

To separate geometrical signs from a particular physical equation, take a rectangular box $0 < x < L_x,\ 0 < y < L_y,\ 0 < z < L_z$ and an exactly known displacement $\mathbf{D} = Axy\,\hat{\mathbf{x}} + By^2\,\hat{\mathbf{y}} + Cz\,\hat{\mathbf{z}}$. The constants have units making each term C/m². Its divergence is

$(A+2B)y+C$. Integrating over the volume gives total free charge $L_xL_z[(A+2B)L_y^2/2+CL_y]$. At $x=0, y=0, z=0$ the relevant normal components vanish. At $x=L_x$, integrating over the face gives $AL_xL_zL_y^2/2$. The $y=L_y$ face gives $BL_xL_zL_{y'}^2$, and the top gives $CL_xL_yL_z$. Addition reproduces the volume calculation, including its factors of two.

Choose numerical constants by specifying $L_x=L_y=L_z=1$ m, $A=2$ nC/m⁴, $B=3$ nC/m⁴ and $C=4$ nC/m³. The three positive-face contributions are 1, 3 and 4 nC, for total 8 nC. Split the volume at $y=0.30$ m. The bottom subvolume has volume charge $\int_0^{0.3}(8y+4)\,dy=1.56$ nC. Its new upper face carries $B(0.30)^2=0.27$ nC. The bottom section of the $x=L_x$ face carries 0.090 nC and that of the top carries 1.20 nC. Their sum is 1.56 nC. For the upper subvolume the same internal face must be counted with the opposite sign. Physical flux is single-valued on that shared face even if the cells on its sides have very different thicknesses.

Suppose a program evaluates the shared face once using a derivative from the lower cell and independently using another from the upper cell. A mismatch of 0.03 nC in those estimates generates a global charge defect when summing cells, although each side may display a locally plausible gradient. A conservative scheme stores one oriented face flux and uses the same number with opposite signs in both cells. Flux conservation can then hold to floating-point accuracy on any partition, without guaranteeing the shared flux is physically accurate. In our manufactured example a shared wrong value would move the two cell errors in opposite directions and leave the total exact. Compare the two individual subvolume charges as well as the global one.

Is this manufactured $\mathbf{D}$ an electrostatic vacuum solution? In a homogeneous scalar dielectric, $\nabla\times\mathbf{D}$ would have to vanish for a purely electrostatic field. Its z component here is $-Ax$. Thus the displacement tests the divergence theorem and a face-flux data structure perfectly, but it does not simultaneously test a potential-gradient solver with constant permittivity. For the latter choose $\mathbf{D}=-\epsilon\nabla V$ from an explicit potential before manufacturing the charge. This example separates validation of a mathematical operation from validation of a whole physical model, an important distinction when a beautifully closed flux budget is the only available diagnostic.

Reconstruct a field from its divergence and curl in a periodic measurement cell

Suppose a three-dimensional field map is tabulated on a periodic cube and you know two derived maps: its divergence d and its curl $\mathbf{w}$. Can these determine the original field? Fourier analysis gives a practical construction and reveals the missing information. For a nonzero spatial wavevector $\mathbf{k}$, use the convention $\mathbf{F}(\mathbf{x})=\sum_{\mathbf{k}}\mathbf{F}_{\mathbf{k}}e^{i\mathbf{k}\cdot\mathbf{x}}$. Then $d_{\mathbf{k}}=i\mathbf{k}\cdot\mathbf{F}_{\mathbf{k}}$ and $\mathbf{w}_{\mathbf{k}}=i\mathbf{k}\times\mathbf{F}_{\mathbf{k}}$. Decompose $\mathbf{F}_{\mathbf{k}}$ into its component parallel to $\mathbf{k}$ and the remaining transverse component. Elementary vector identities give

$$\mathbf{F}_{\mathbf{k}}=-\frac{i\mathbf{k}}{k^2}d_{\mathbf{k}}+\frac{i}{k^2}\mathbf{k}\times\mathbf{w}_{\mathbf{k}}\qquad(\mathbf{k}\neq0).$$

The first term supplies the requested divergence and zero curl. The second supplies the requested curl when $\mathbf{k}\cdot\mathbf{w}_{\mathbf{k}}=0$, a compatibility requirement because the divergence of a curl vanishes. At $\mathbf{k}=0$ both operations annihilate the constant field. Its mean must be measured independently. In a nonperiodic region suitable boundary data enter as well. This is a constructive version of the statement that

divergence and curl determine a field only after specifying its domain, boundary information and any harmonic freedom.

For a concrete field take $\mathbf{F} = (A\cos kx, B\sin kx, C)$. Its divergence is $-kA\sin kx$, its only curl component is $w_z = kB\cos kx$, and the constant offset $C\hat{\mathbf{z}}$ drops out of both maps. The first input alone reconstructs the x component and the second the y component. A purely electrostatic solver may legitimately require $B = 0$ but will not recover C from the local charge distribution alone. A uniform applied field can be imposed by suitable distant electrodes. A strictly periodic scalar potential cannot represent a nonzero mean field without separately adding a linear background.

A grid-based reconstruction needs its own consistency check. A centred difference on a periodic grid maps e^{ikx} to $i\sin(kh)e^{ikx}/h$, not exactly ike^{ikx}. A source plane wave at the highest alternating grid mode $k = \pi/h$ has zero centred derivative at every node despite alternating sign. Treating discrete divergence measurements as exact continuum coefficients near that grid scale would infer falsely that an oscillatory field has vanished. Use a consistent discrete operator, stagger quantities if appropriate, and restrict quantitative interpretation to adequately sampled modes. The continuous Helmholtz identity is exact; the data acquisition and differentiation scheme decides which components of that identity are actually observable.

Enclose different amounts of a regularised source

Predict how the flux of a small sphere changes as it crosses the charge cloud. Compare the enclosed fraction with the local source density.

Open this experiment online

Try the calculation

Core radius a (mm) 1

Collector radius R (mm) 2

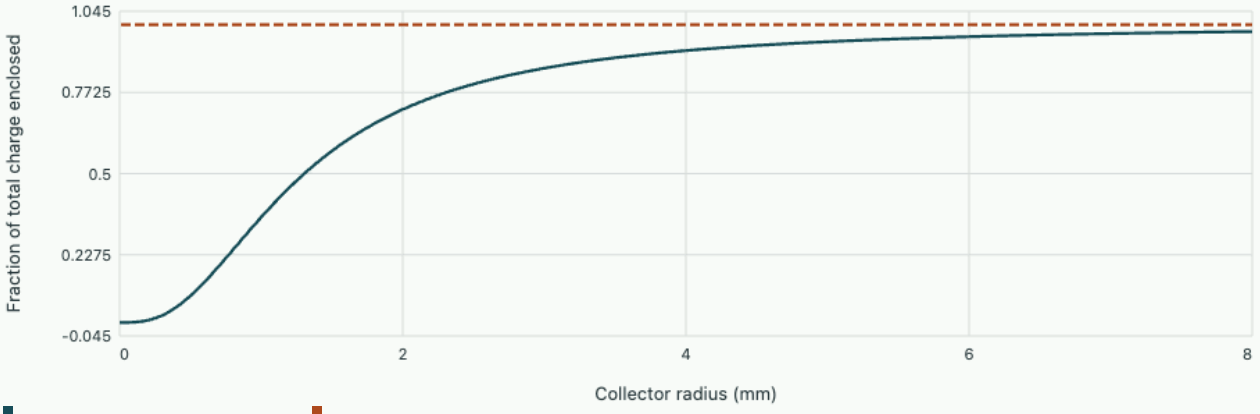

At 2 mm the collector encloses 71.6% of the charge. Doubling its radius would enclose 91.3%.

Tutorial · turn field values into reliable local measurements

Reconstruct a sheet from a voltage cusp

Two electrodes at $z = \pm L$ are grounded. Inside the gap a measured potential is $V_0(1 - |z|/L)$. Find both fields and reconstruct the source, then explain what a centred finite difference reports at the cusp.

▼ **Work through the solution**

For $z < 0$, $E_z = -V_0/L$; for $z > 0$, $E_z = +V_0/L$. The jump gives a sheet $\sigma = 2\epsilon_0 V_0/L$ at zero. A centred estimate of the first derivative there returns zero by symmetry, reflecting the arithmetic mean of the two one-sided fields. It cannot be interpreted as either physical one-sided limit. The centred second difference is $-2V_0/(Lh)$, so the inferred cell density grows as $1/h$. Multiplying by a cell width h returns the finite sheet charge. This is the correct quantity to compare when refining the grid.

With $V_0 = 2$ V and $L = 2$ mm the fields have magnitudes 1000 V/m and the sheet charge is 17.7 nC/m². Reversing V_0 reverses both field vectors and the sheet sign without moving the cusp.

Can a voltage map distinguish a saddle from a charge?

Near the origin a section shows $V(x, 0, 0) = V_c - Ax^2$, $A > 0$. Give a source-free three-dimensional extension and a second extension consistent with uniform positive charge. Propose a minimum additional measurement given no prior symmetry.

▼ **Work through the solution**

The first is $V_c - Ax^2 + Ay^2$, independent of z. Its Laplacian vanishes. The second is $V_c - A(x^2 + y^2 + z^2)$, whose Laplacian is $-6A$, giving $\rho = 6\epsilon_0 A$. Both match the entire original line. Curvatures along y, z together with the given x-curvature determine the Laplacian. A small enclosing surface measuring normal electric flux provides the same information integrated over a volume and does not require numerical second differentiation. Neither a second derivative along one line nor a visibly crowded pair of voltage contours is a universal charge detector.

Further reading

- Vary the width and collecting radius of a regularised charge
- Fließbach, chapter 3 · distributions
- Griffiths, 5th ed., chapter 1 · vector analysis and the delta function

Electrostatic field theory and measurement · 3. When do boundary measurements determine a unique electrostatic field?

A boundary-value solver may converge while solving the wrong electrical experiment. Establishing which potentials, charges and fluxes are fixed gives a uniqueness proof and a way to turn an approximate field into an upper bound.

Specify the experiment before specifying the equation

An insulating region occupies a bounded volume Ω with smooth conducting or insulating boundaries. A known free charge density ρ_f is embedded in the region. For a positive scalar linear permittivity $\epsilon(\mathbf{x})$, electrostatics reduces to

$$-\nabla \cdot (\epsilon \nabla V) = \rho_f.$$

To turn this into an experiment one must decide how each boundary is prepared. A conductor attached to a source supplies a fixed voltage; an isolated conductor keeps a fixed total charge while becoming an equipotential; an insulating surface with known displacement flux prescribes a normal component. These preparations require different mathematical data. The same electrode shape can participate in any of them.

At an interface between two ordinary dielectrics the potential is continuous in the absence of a prescribed dipole sheet. Integrating Gauss's law across the interface gives

$$(\mathbf{D}_2 - \mathbf{D}_1) \cdot \mathbf{n} = \sigma_f,$$

where $\mathbf{n}$ points from medium 1 to 2. Thus the appropriate field problem can be posed either in a weak integral form across both materials or as two equations joined by voltage and flux conditions. The latter view is especially helpful when a measured charge appears on just one internal sheet. A jump in permittivity alone does not permit an arbitrary jump in voltage.

Prove uniqueness by testing the difference, not the solution

Suppose two solutions V_1, V_2 fit identical prescribed volume sources, material data and boundary voltages. Define $w = V_1 - V_2$. It satisfies $\nabla \cdot (\epsilon \nabla w) = 0$ and vanishes at the boundary. Multiply by w and apply the product rule to $\nabla \cdot (w \epsilon \nabla w)$. Integration yields

$$\int_\Omega \epsilon |\nabla w|^2 \, dV = \oint_{\partial\Omega} w \epsilon \, \partial_n w \, dA.$$

The boundary term is zero. The integrand on the left is nonnegative and $\epsilon > 0$, so the gradient vanishes wherever the material is regular. The function must be constant on each connected component; its fixed boundary value makes it zero. This proves that at most one field solves the stated problem. It does not itself construct a solution. It converts a difficult task of checking every possible competitor into checking the PDE and boundary data for one candidate.

The same reasoning works for a symmetric positive-definite permittivity tensor: replace $\epsilon|\nabla w|^2$ by $(\nabla w)^T \boldsymbol{\epsilon} \nabla w$. It also applies with internal material interfaces. Integrate separately on either side. Their face terms cancel because w is continuous and the prescribed free sheet makes the jump in the difference flux zero. An unaccounted interface charge would supply precisely the term that invalidates this cancellation.

If only the normal flux is fixed everywhere, the boundary difference flux vanishes and the left integral again gives a constant w. Constants are now indistinguishable by the boundary data; the electric field remains unique. Gauss's law also imposes compatibility $\oint_{\partial\Omega} \mathbf{D} \cdot \mathbf{n}\, dA = \int_\Omega \rho_f\, dV$. Choosing flux values whose sum disagrees with the enclosed charge produces no solution, even after choosing a voltage reference. Numerically this can appear as a residual that never falls below a threshold, or as a solver modifying the source silently to make the equations compatible.

Prove uniqueness when only total conductor charge is known

Take a region surrounding several isolated conductors. The value on each metal is constant but initially unknown. For the difference of two candidate solutions denote these constants by w_i. Then each conductor's contribution to the right-hand side of the energy identity factors as $w_i \int_{S_i} \epsilon \partial_n w\, dA$. With outward normal from the dielectric into the metal this integral is the difference in the conductor's free charge. Prescribing total charge for each metal makes every such term vanish individually. Provided a reference conductor or condition at infinity removes an overall constant, the potential is unique.

Knowing only the sum of charges over several electrically disconnected metals can be insufficient. For two isolated spheres, allow one to take charge $+\delta q$ and the other $-\delta q$ while fixing their total at zero. Their equipotential values can change relative to each other, and an external field may appear. If instead they are joined by an ideal wire they must share one voltage, so the common boundary contribution factors against their total charge. The proof itself identifies the physical distinction between strings of electrically connected metal and separate conductors.

A functional whose variation is Gauss’s law

For fixed boundary voltage consider

$$\mathcal{I}[V] = \int_\Omega \left[\frac{1}{2} \nabla V \cdot \epsilon \nabla V - \rho_f V \right] dV.$$

The two meanings of V in this notation are distinguishable from context: $V(\mathbf{x})$ is potential and dV is a volume element. Add a trial perturbation η that vanishes on the fixed-voltage boundary. The first-order change is $\int [\nabla \eta \cdot \epsilon \nabla V - \rho_f \eta] dV$. Integrate the first term by parts. Requiring zero for every admissible η gives

$$-\nabla \cdot (\epsilon \nabla V) = \rho_f.$$

On a boundary portion where flux rather than voltage is prescribed, an additional linear boundary contribution accounts for the specified normal derivative. It is not generally correct to hold every trial

voltage zero there.

For an exact fixed-voltage solution V_* expand $\mathcal{I}[V_* + \eta]$. The first-order terms vanish, leaving

$$\mathcal{I}[V_* + \eta] - \mathcal{I}[V_*] = \frac{1}{2}\int_\Omega \nabla\eta \cdot \epsilon \nabla\eta \, dV.$$

The exact solution minimises the functional, and the gap measures the field error in an energy-weighted norm. If $\rho_f = 0$ the functional is the stored field energy. With embedded sources the linear term matters; the value of the functional is generally not just field energy. Restrict the trial fields to a finite space and minimize there. This is the variational origin of a potential-based finite-element method. A small change in the energy between two grids can coexist with a noticeably changing local peak field because the integral weights errors by volume.

A complete numerical comparison without a black box

Take a unit area filled by two dielectric slabs each of thickness $d = 1$ mm and relative permittivities 2 and 8. Set one electrode at 10 V, the other at zero, with no free charge inside. A trial straight line through the whole gap obeys both electrode voltages. Its energy per area is $\epsilon_0(2+8)d(5000)^2/2 = 1.107\ \mu\mathrm{J/m^2}$ after unit conversion. The exact interface problem requires constant normal displacement. It gives voltage drops of 8 and 2 V, fields of 8000 and 2000 V/m and energy per area $0.708\ \mu\mathrm{J/m^2}$. A single continuous slope produced too much energy by about 56%. The trial is admissible despite its incorrect interface flux, because stationarity, rather than a kinematic constraint, enforces that flux.

Recover the exact answer as a one-variable minimisation. Let u be the voltage at the interface measured relative to the grounded end, with the first material next to the 10 V electrode. The energy per area is $\epsilon_0[2(10-u)^2 + 8u^2]/(2d)$. Differentiation gives $-2(10-u) + 8u = 0$, hence $u = 2$ V. The derivative with respect to an interior trial voltage measures the flux imbalance between neighbouring elements. This makes the algebraic finite-element equation a local charge balance. Conversely a trial that fails to equal an electrode's prescribed voltage is inadmissible, even if its energy appears lower than the computed answer.

A maximum principle as a diagnostic independent of energy

In a charge-free region with uniform permittivity the potential at the centre of a sphere equals its mean over the sphere. To see this, differentiate the angular average with respect to its radius. The result is proportional to the total normal derivative, which is zero by Gauss's law for an empty sphere. Shrink the sphere to its centre to identify the constant average. Therefore a nonconstant harmonic function cannot have a strict interior maximum or minimum. If the centre assumes the maximum value, all sufficiently nearby directions must assume that same value to keep the average equal; continuing through the connected region forces constancy.

For source-free Poisson solvers an interior voltage above all fixed outer values indicates an issue with boundary data, source terms or discretisation. But the same observation is entirely possible with positive internal charge, as the one-dimensional grounded-plane parabola demonstrates. The maximum principle

concerns potentials; it does not say that a field magnitude, an individual component in an inhomogeneous medium, or the potential restricted to a line must remain between the corresponding boundary values on that line.

A thin dielectric coating turns a boundary voltage into a Robin condition

Suppose a grounded metal enclosure is lined with an insulating film of thickness d_f and permittivity ϵ_f. We want the electrostatic potential in an interior region large compared with the film thickness. Simply declaring the film's exposed face grounded neglects its voltage drop. If the tangential scale of the interior field and the radius of curvature of the surface are both much larger than d_f, the film behaves locally like a plane capacitor with capacitance per area $c_f = \epsilon_f / d_f$. Let $\mathbf{n}$ point from the interior into the film, let the backing metal be at V_b, and denote the interior-side surface potential by v. Without free charge at the contact, the outward displacement from the interior equals $c_f(v - V_b)$. Since $\mathbf{D} = -\epsilon \nabla V$ inside, the effective boundary condition is

$$\epsilon\, \partial_n V + c_f (V - V_b) = 0.$$

This is a Robin boundary condition: both the potential and its derivative enter. The coefficient c_f has units F/m², so both terms are surface charges. For $c_f \to \infty$ a bounded normal field forces V to the backing voltage. For $c_f \to 0$ a finite voltage difference can sustain almost no normal flux. The two familiar boundary ideals are limiting cases of one measurable material preparation. The derivation requires the film to contain no embedded free charge and to respond linearly; measured leakage over long times adds a current-balance problem.

The variational proof above extends naturally. Add $\frac{1}{2}\int_{S_f} c_f (V - V_b)^2 dA$ to the interior functional. Its first variation at the exposed face gives $\epsilon \partial_n V + c_f (V - V_b)$ times the arbitrary boundary variation. The added quadratic term is exactly the electrostatic energy stored in the eliminated thin layer under the one-dimensional approximation. For the difference of two solutions the energy identity becomes

$$\int \epsilon |\nabla w|^2 dV + \int c_f w^2 dA = 0.$$

Either a prescribed reference voltage or a positive-area Robin patch with $c_f > 0$ removes the constant null mode. This follows without pretending that the exposed potential itself was prescribed.

Consider a planar interior region of thickness 2.0 mm filled with $\epsilon_i = 4\epsilon_0$, separated from its 0 V backing by a 50 µm film with $\epsilon_f = 2\epsilon_0$. Set the opposite electrode to 10 V. The exact one-dimensional displacement is

$$D = 10 / [L/\epsilon_i + d_f/\epsilon_f].$$

The effective electric length in vacuum units is $0.50 + 0.025 = 0.525$ mm, hence $D = 169$ nC/m² and the film takes $10(0.025/0.525) = 0.476$ V. Imposing a direct 0 V boundary at the exposed film face would overpredict displacement by 5%. Solving with the Robin condition instead reproduces the series

result exactly in the flat one-dimensional model. For a patterned electrode with wavelength comparable to film thickness, tangential field in the film cannot be ignored and the effective boundary response depends on spatial frequency.

What a voltage error bound does and does not control

If two source-free solutions have slightly different Dirichlet data, their difference is harmonic, not necessarily zero. Let their boundary discrepancy have maximum magnitude δ. The maximum principle applied to the difference and its negative guarantees $|V_1 - V_2| \leq \delta$ throughout the region. This gives a stability estimate for voltage even where the exact solution is unknown. It requires an error bound on the whole boundary and identical sources inside. Collocation residuals evaluated only at a few points do not establish the premise between those points.

Does the same number bound the error in local electric field? Consider the upper half-space with boundary error $\delta\cos(kx)$. The harmonic difference at height h is $w = \delta e^{-kh}\cos(kx)$. Immediately at the boundary the field-error amplitude is $k\delta$, which can be arbitrarily large as the spatial wavelength shrinks even though the voltage error stays below δ. At nonzero h the field-error amplitude for this single mode is $k\delta e^{-kh}$. For fixed h it is maximal at $k = 1/h$, with value $\delta/(eh)$. Depth regularises the sensitivity to ever finer ripples. A global bound on arbitrary superpositions requires accounting for how their amplitudes combine; maximising one sinusoid does not prove that every boundary function attains the same bound.

Suppose a nominally grounded instrument panel has a sinusoidal ripple of peak voltage 5 mV and wavelength 1.0 mm. At the surface it creates an electric-field amplitude of 31.4 V/m. Just 1.0 mm away its amplitude is multiplied by $e^{-2\pi} = 0.00187$, leaving 0.0587 V/m. A sensor directly at the surface and one millimetre inside may therefore make very different accuracy demands on the boundary model, despite the same nominal voltage tolerance. A field solver claiming agreement of all electrode voltages to 5 mV still needs a spatial smoothness or resolution statement before claiming local field accuracy.

A useful related identity controls energy error when an approximate potential has an interior residual. Let V_h satisfy the exact boundary values, and define $r = \rho + \nabla\cdot(\epsilon\nabla V_h)$. With $e = V_* - V_h$ zero on the boundary,

$$-\nabla\cdot(\epsilon\nabla e) = r.$$

Multiplying by e gives $\int \epsilon|\nabla e|^2 dV = \int re\, dV$ for a smooth admissible approximation. If a piecewise field has jumps at internal element faces their residual contributions must be included. A tiny volume residual computed inside each piece can coexist with incorrect flux matching at every face. In the two-layer example, a straight-line trial has zero second derivative in both layers, yet its displacement mismatch at the interface is exactly what forces a different physical solution.

Why a conductor becomes equipotential when charge can move

So far conductor voltages or charges entered as boundary conditions. A related variational argument explains the equipotential condition itself. Imagine charges on one connected conductor that may redistribute while their total stays fixed. Treat the final material state as ideal and static, with no ongoing

currents or dissipative constraints. The change in electrostatic field energy for an infinitesimal change in free surface charge is $\delta U = \int_S V(\mathbf{x}) \delta\sigma(\mathbf{x})\, dA$. This follows either by slowly bringing in each incremental charge at its current potential or by varying the symmetric double integral $\frac{1}{2}\int\int \rho(\mathbf{x}) G(\mathbf{x},\mathbf{y}) \rho(\mathbf{y}) d^3x\, d^3y$. The half in the energy disappears upon variation because either source factor may vary.

Move a small positive charge dq from a patch at potential V_A to another at V_B, preserving total conductor charge. The change is $(V_B - V_A)dq$. If the two voltages differ, one direction of transfer lowers the energy. At equilibrium every such redistribution must have zero first-order energy change, hence the potential is constant over the connected conductor. For disconnected conductors whose individual totals are fixed the same reasoning gives a different allowed constant on each. If an ideal wire joins them, transfers across the wire become admissible and their two constants equalise. This is a statement about electrical connectivity and constraints, not merely the smoothness or shape of the conducting material.

The second-order change for a neutral redistribution is its own nonnegative field energy. For a fixed-charge isolated conductor it follows that the electrostatic equilibrium distribution minimises energy over all allowed placements of the same surface charge. This is a different trial principle from prescribing electrode voltages and varying a potential throughout the space. A trial charge that obeys a total-charge constraint need not produce an exactly equipotential conductor; its excess energy measures a failure of equilibrium. Confusing these two variational principles can switch the direction of an inferred capacitance bound.

As a measurable limit, take two small spheres far apart, with approximate capacitances $C_1 = 4\pi\epsilon_0 a_1$ and $C_2 = 4\pi\epsilon_0 a_2$ to infinity. Temporarily neglect mutual coupling. With total charge Q, write $U(q) = q^2/(2C_1) + (Q-q)^2/(2C_2)$. Differentiating gives $q/C_1 = (Q-q)/C_2$, the equipotential solution after wiring. For radii 10 and 20 mm and $Q = 30$ pC this gives shares 10 and 20 pC at a common voltage about 9.0 V. Putting all the charge initially on the smaller sphere would give energy $Q^2/(2C_1)$. After connection the energy is $Q^2/[2(C_1 + C_2)]$, one third as large. The missing field energy leaves during transient currents through radiation or dissipation; static uniqueness alone describes neither time history nor dissipation partition. As sphere spacing is reduced, mutual capacitance must be included and the simple radius ratio becomes an approximation to test rather than an exact rule.

Check a potential independently of its residual

Refine a grounded square with known boundary data. Compare centre voltage with the series solution as well as the discrete residual. The accompanying OneSimulation model solves the same field problem.

Open this experiment online

Try the calculation

Cells per side 12

Charge amplitude ρ₀ (nC/m³) 2

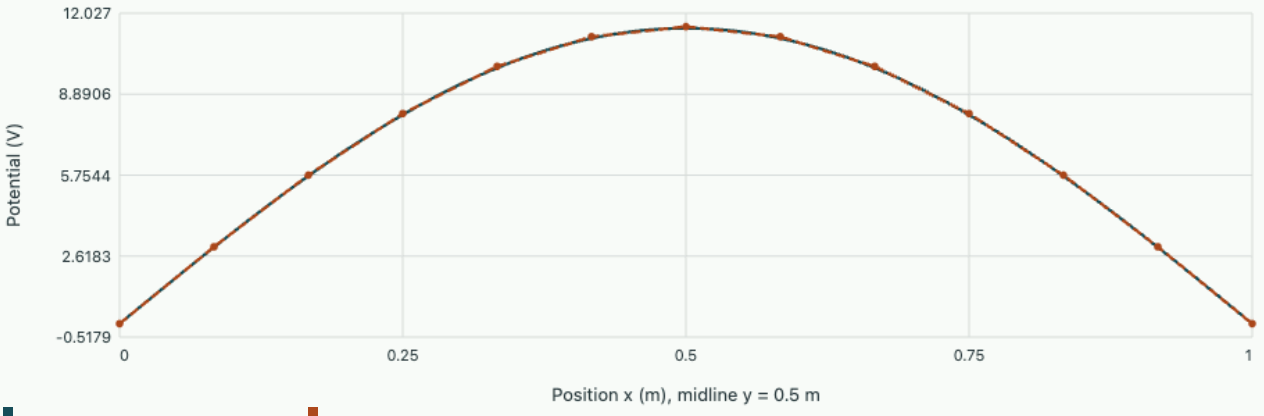

Continuous solution | Five-point grid solution

Centre potential 11.50889 V on the grid, 11.44331 V in the continuum. Nodal error 0.06558 V.

Download the OneSimulation model

In your OneSimulation environment, run the model with these inputs.

```
python grounded-square.py --cells 12 --charge 2
```

Tutorial · can the proposed computation represent this experiment?

Find a compatible flux and determine the remaining freedom

A slab $0 < x < L$ contains uniform positive free charge ρ. At $x = 0$ the outward displacement is measured as $D_n = -D_0$. Determine what flux must be prescribed at L, the electric field throughout, and one piece of information needed for the absolute potential.

▼ Work through the solution

Positive x displacement at the left is D_0 because that face's outward normal points towards negative x. Integrating $dD_x/dx = \rho$ gives

$$D_x = D_0 + \rho x.$$

Therefore the outward flux at L is $D_0 + \rho L$. Their sum per unit area equals ρL. In constant permittivity $E_x = (D_0 + \rho x)/\epsilon$ and $V(x) = V(0) - (D_0 x + \rho x^2/2)/\epsilon$. A reference voltage fixes $V(0)$; none can

fix an incompatible pair of flux measurements. A negative right-hand outward reading with very large positive enclosed charge would contradict Gauss's law before one even solves for V.

Bound a capacitance with an intentionally poor trial

In a charge-free parallel-plate vacuum gap of thickness L, use $V(x) = V_0(x/L)^2$ to bound the capacitance per area. Compare with the exact linear voltage. How does improving the potential shape turn into a monotonic bound?

▼ **Work through the solution**

The trial satisfies the endpoints. It gives energy per area $\epsilon_0 \int_0^L (2V_0 x/L^2)^2 dx/2 = 2\epsilon_0 V_0^2/(3L)$, hence a capacitance estimate $4\epsilon_0/(3L)$. The exact value is ϵ_0/L, lower by the predicted variational inequality. Expanding a trial space to include both the old functions and new ones cannot raise its optimal energy because the old minimiser remains available. This monotonic property requires nested trial spaces and consistent integration; changing quadrature or replacing the physical geometry changes the comparison.

Further reading

- Perturb a potential and measure the quadratic energy penalty
- Recover an interface charge using independent field measurements
- Griffiths, 5th ed., §§3.1.5–3.1.6 · uniqueness theorems

Electrostatic field theory and measurement · 4. Images in wedges, cylinders and dielectric interfaces

An image source is a construction for a particular physical domain and boundary condition. Three examples show how geometry determines the image position, how material response sets its amplitude, and why an apparent success on part of a boundary is insufficient.

Start with a domain in which the fictitious sources are excluded

Suppose we have a point charge in an open region bounded by conducting metal. Inside the vacuum we know where all real sources lie. Near each real point source the potential must have its prescribed Coulomb singularity. Elsewhere it must be harmonic. A method of images extends an expression for V beyond the physical region using additional sources chosen to enforce boundary values on the metal. The added singularities must lie outside the field domain. If all boundary data and the behaviour at infinity agree, the uniqueness theorem guarantees the solution there. The extension says nothing about the actual field inside the metal.

There are three separate checks. First locate the singularities. Next test every boundary value as a function over the entire surface, not at one point of symmetry. Finally check the decay or far-field background. Using a few image charges to make the voltage zero at a finite list of collocation points gives an approximation unless a separate argument enforces the boundary everywhere. It can still be an effective numerical method when one monitors the untested parts of the surface.

A family of wedges that permits a finite reflection construction

Take two grounded half-planes meeting along z, with vacuum opening angle $\alpha = \pi/m$ for positive integer m. A real point charge sits in the wedge at cylindrical coordinates (s_0, ϕ_0, z_0), $0 < \phi_0 < \alpha$. Reflection across either grounded plane reverses the charge sign. Two successive reflections amount to rotation by 2α with no sign reversal. Hence a useful set consists of m charges $+q$ at $\phi_0 + 2j\alpha$ and m charges $-q$ at $-\phi_0 + 2j\alpha$, $j = 0, \ldots, m-1$, all at the same s_0, z_0. Only the original lies in the physical wedge. Each metal face pairs equal-distance charges of opposite signs, so the summed potential vanishes on both faces.

For $\alpha = \pi/3$ there are five images in addition to the real charge. If the real charge is on the bisector $\phi_0 = \pi/6$, the total configuration is six alternating charges on a circle. All forces tangential to the bisector cancel by symmetry. Consider any other charge q_j displaced through azimuthal angle Δ from the real charge. Its separation is $2s_0|\sin(\Delta/2)|$, and the radial projection of the displacement vector from that image to the real source is $s_0(1-\cos\Delta)$. Its radial force on q is therefore $qq_j/[16\pi\epsilon_0 s_0^2|\sin(\Delta/2)|]$. Summing the five alternating terms gives

$$F_s = \frac{q^2}{16\pi\epsilon_0 s_0^2}\left(-5 + \frac{4}{\sqrt{3}}\right).$$

The sign points toward the wedge vertex. The nearest negative images at $\pm 60^\circ$ each contribute -2 in the bracket, the two positive ones at $\pm 120^\circ$ give $+2/\sqrt{3}$ each, and the opposite negative image gives -1. The radial scaling $1/s_0^2$ follows independently from the geometric similarity of the wedge. For arbitrary

opening angles the repeated images can fail to terminate, or introduce spurious singularities in the vacuum wedge. Separation in wedge coordinates then offers a better construction. A valid result for one rational angle cannot simply be extrapolated to a neighboring angle.

Try it · Change the opening and move the charge

Keep m integer, as required by this finite image construction. Move the source off the bisector and identify the nearer attracting face. Double the radial distance and check the inverse-square force scaling.

Open this boundary experiment

Try the calculation

Wedge denominator m	3
Radial source distance (m)	1
Selected fraction of opening	0.5

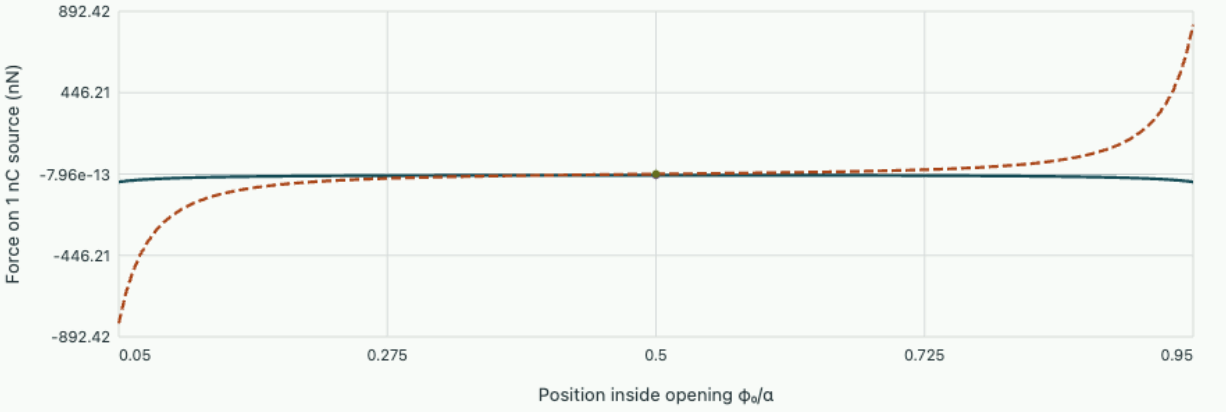

Opening 60°; 5 fictitious images. At ϕ₀/α=0.5, radial force -6.0455 nN and azimuthal force -2.6645e-15 nN. On the bisector the azimuthal component vanishes.

Notebook: reproduce the exact boundary constructions and the 3D collocation model

Find an image line from a constant distance ratio

An infinite metal cylinder of radius a is grounded. Outside it a parallel positive line charge λ is located a transverse distance $d > a$ from the centre, on the x-axis. Choose an interior image $-\lambda$ at $s = a^2/d$. For a surface point at polar angle ϕ, its distance from the real line is $R_q = \sqrt{a^2 + d^2 - 2ad\cos\phi}$. Its distance from the image satisfies

$$R_i = (a/d)R_q.$$

A line potential varies as a logarithm, so the ratio of distances, rather than a weighted sum of inverse distances, must be constant on the metal. With zero on the cylinder the exterior expression is

$$V = \frac{\lambda}{2\pi\epsilon_0}\ln\left(\frac{dR_i}{aR_q}\right).$$

At large transverse radius the logarithm approaches $\ln(d/a)$, yielding a constant nonzero distant voltage. This is consistent with the effectively two-dimensional infinite geometry and the chosen grounding convention. Insisting on zero potential both on the grounded cylinder and at infinity without an external return changes the problem. In the physical exterior the electric field nonetheless decays.

At the real line the image field attracts with magnitude per length $\lambda^2/[2\pi\epsilon_0(d - a^2/d)] = \lambda^2 d/[2\pi\epsilon_0(d^2 - a^2)]$. For $d = a + h$ and $h \ll a$, the image separation tends to $2h$, yielding the plane result for a line. For $a = 10$ mm, $d = 25$ mm and $\lambda = 1.0$ nC/m the attraction is 0.856 µN/m. A conducting sphere near a point charge uses the same geometric inversion $s = a^2/d$ but the image amplitude there is $-qa/d$ because its Green function is $1/R$. Dimensions of the source and its fundamental solution determine which rules transfer between the two calculations.

Try it · Compare grounded and isolated cylinders

Set a=10 mm, λ=1 nC/m and d/a=2.5 to recover the example above. Move farther away and compare the two asymptotic force laws. The two curves differ in the total conductor charge constraint.

Open this boundary experiment

Try the calculation

Cylinder radius a (mm)	10
Line charge (nC/m)	1
Selected d/a	2.5

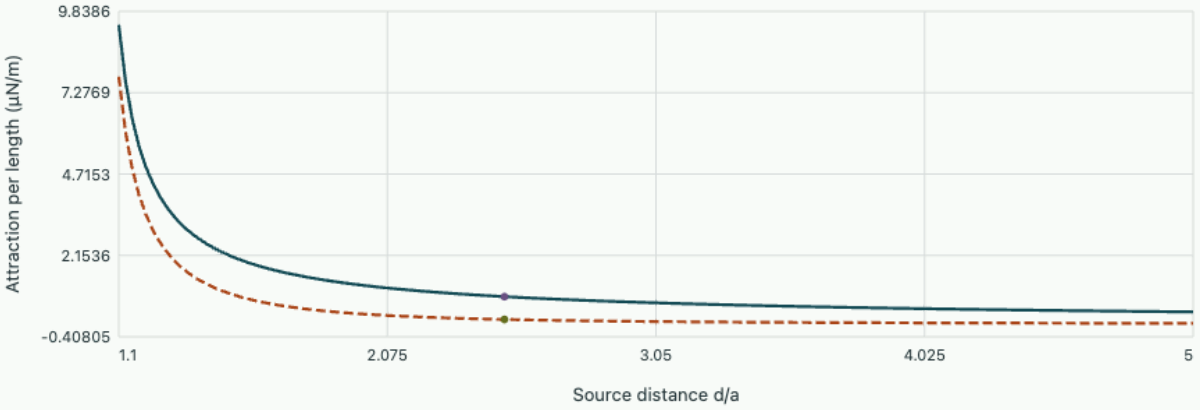

Grounded conductor · Neutral isolated conductor · Selected grounded force · Selected isolated force

At d=25 mm: grounded attraction 0.85596 μN/m, isolated attraction 0.13695 μN/m. The image lies 4 mm from the axis; electrical preparation changes the distant force law.

Notebook: reproduce the exact boundary constructions and the 3D collocation model

Try it · Compare grounded and isolated image spheres

Change the source position and compare the induced-charge constraints before trying the general collocation system below.

Open the exact sphere comparison

Try the calculation

Source distance d/a **2**

Isolated conductor charge Qc/q **0**

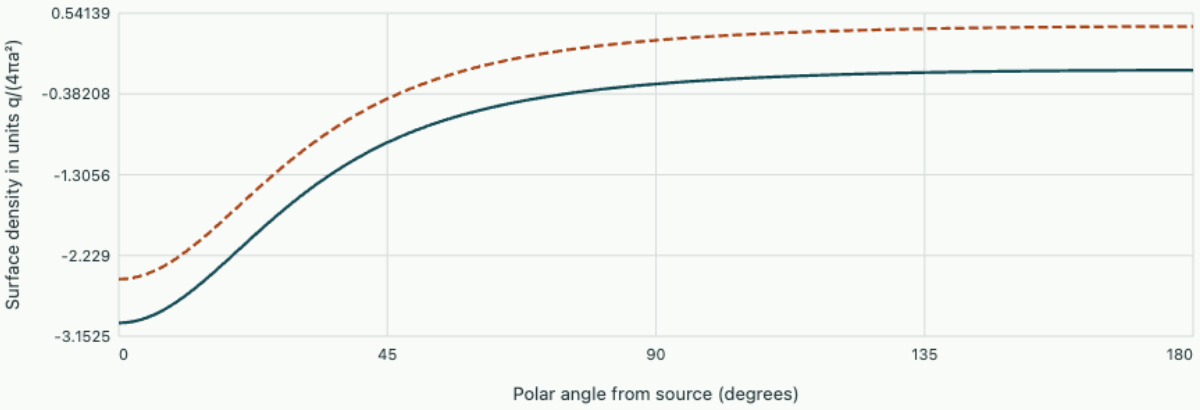

Grounding draws net charge -0.5 q. Forces in units q²/(4πε₀a²) are -0.2222 grounded and -0.09722 isolated; positive means away from the sphere.

An interface that supports bound charge but does not fix voltage

Let a point charge q occupy $z = d > 0$ in a medium of permittivity ϵ_1. The lower half-space has permittivity ϵ_2. Both extend to infinity and there is no free sheet on the interface. An ansatz for $z > 0$ contains the real charge plus an image q' at $z = -d$, using $1/(4\pi\epsilon_1)$ as its common prefactor. For $z < 0$, put an effective charge q'' at $z = d$ with prefactor $1/(4\pi\epsilon_2)$. That effective charge also lies outside its own solution domain. At the plane, the two distances are equal. Potential continuity gives

$$(q + q')/\epsilon_1 = q''/\epsilon_2.$$

Taking the oriented normal derivative gives $q - q' = q''$ because original and reflected source distances have opposite z-derivatives there. Solving,

$$q' = q\frac{\epsilon_1 - \epsilon_2}{\epsilon_1 + \epsilon_2},$$
$$q'' = \frac{2\epsilon_2 q}{\epsilon_1 + \epsilon_2}.$$

Check the equal-material limit: $q' = 0, q'' = q$. For an increasingly polarizable lower region $q' \to -q$, reproducing the grounded-plane exterior field, while the lower electric field becomes weak. For a lower-permittivity lower region the image has the same sign and the charge is repelled. Positive permittivity materials can therefore produce either direction of interface force; it is the comparison of the two constitutive laws that decides.

For $\epsilon_1 = 4\epsilon_0, \epsilon_2 = 2\epsilon_0$, the image is $q/3$. At $d = 1$ mm and $q = 10$ pC the repulsive force is $q^2/[4\pi(4\epsilon_0)12d^2] = 18.7$ nN. Moving the charge quasistatically from infinity to that position requires positive work. The interaction contribution to energy is

$$qV_{\text{image}}/2 = qq'/(16\pi\epsilon_1 d).$$

Minus its derivative with respect to d gives the same force as the real charge times the image field. The half accounts for inducing the bound charge. Treating the image as a second independently prescribed charge and differentiating its pair energy with both positions moving doubles the force.

Try it · Switch attraction into repulsion

Move $\varepsilon_2/\varepsilon_1$ through one. Check the equal-material limit and compare with the grounded-plane limit. The sign denotes force along increasing z; a negative value attracts the source toward the interface.

Open this boundary experiment

Try the calculation

Permittivity ratio $\varepsilon_2/\varepsilon_1$	0.5
Charge q (pC)	10
Selected height d (mm)	1

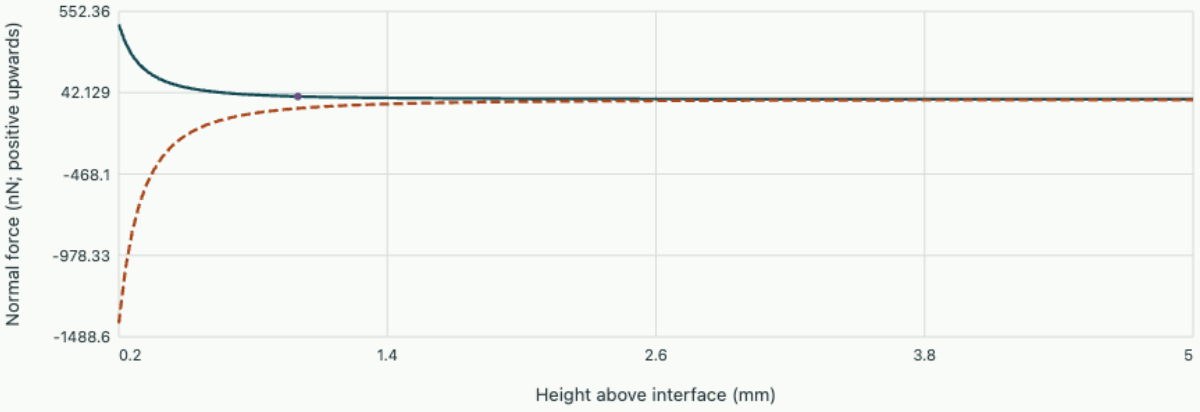

With $\varepsilon_1=4\varepsilon_0$, $q'/q=0.33333$ and $q''/q=0.66667$. Force at 1 mm is 18.724 nN: repulsive.

Notebook: reproduce the exact boundary constructions and the 3D collocation model

How to test a numerical image representation

For a smooth conducting enclosure of less convenient shape, place hypothetical source points inside the metal, impose the desired boundary voltages at accessible sample points, and solve linearly for strengths. The physical solution must remain smooth throughout the vacuum except at genuine specified sources. Choosing numerical source positions too close to the boundary may create narrow voltage oscillations between sampled surface points. Placing them too far can make influence columns almost indistinguishable, producing enormous opposite coefficients and poor numerical conditioning.

Test the candidate on surface points deliberately withheld from the fit. In a source-free region the difference between the approximation and the exact potential is harmonic if both use the same physical singularities. Its maximum voltage error cannot exceed the largest absolute boundary discrepancy when the far boundary is also controlled. This does not directly bound the normal-field error at the conductor, which can be sensitive to small short-wavelength ripples in voltage. Check flux and force separately, for

example by integrating the Maxwell stress over a vacuum surface displaced away from difficult corners. A voltage map, a force and a conductor's total charge impose complementary demands on accuracy.

OneSimulation in 3D · Test a fitted source system between its boundary points

A grounded sphere with a=1 m is placed beside q=1 nC at z=d. The exact image charge is −qa/d at z=a²/d. In the numerical construction, choose N fictitious points sj on an interior sphere of radius αa. Require zero potential at N points bi on the physical surface:

$$\sum_{j=1}^{N} \frac{w_j}{|\mathbf{b}_i - \mathbf{s}_j|} = -\frac{1}{|\mathbf{b}_i - d\mathbf{e}_z|},$$

$$V_h(\mathbf{x}) = \frac{q}{4\pi\epsilon_0}\left[\frac{1}{|\mathbf{x} - d\mathbf{e}_z|} + \sum_j \frac{w_j}{|\mathbf{x} - \mathbf{s}_j|}\right].$$

OneSimulation solves this dense collocation system in the downloadable notebook. The browser implements the same system with pivoted Gaussian elimination. All sources are inside the excluded metal; the field is evaluated outside. Its sum of numerical source strengths predicts total induced charge, independently checked against −qa/d. A tiny residual at fitted points can coexist with a substantial voltage error between them.

Refine N at fixed d and α. Then move the fictitious sources toward the boundary and observe the error between fitted points. Rotate the 3D field lines and notice that small azimuthal differences disappear with refinement. Field-line density here is chosen for readability and does not encode flux.

Open the 3D sphere experiment

Try the calculation

Number of source points	**48**
Charge distance d/a	**2**
Source radius / a	**0.65**

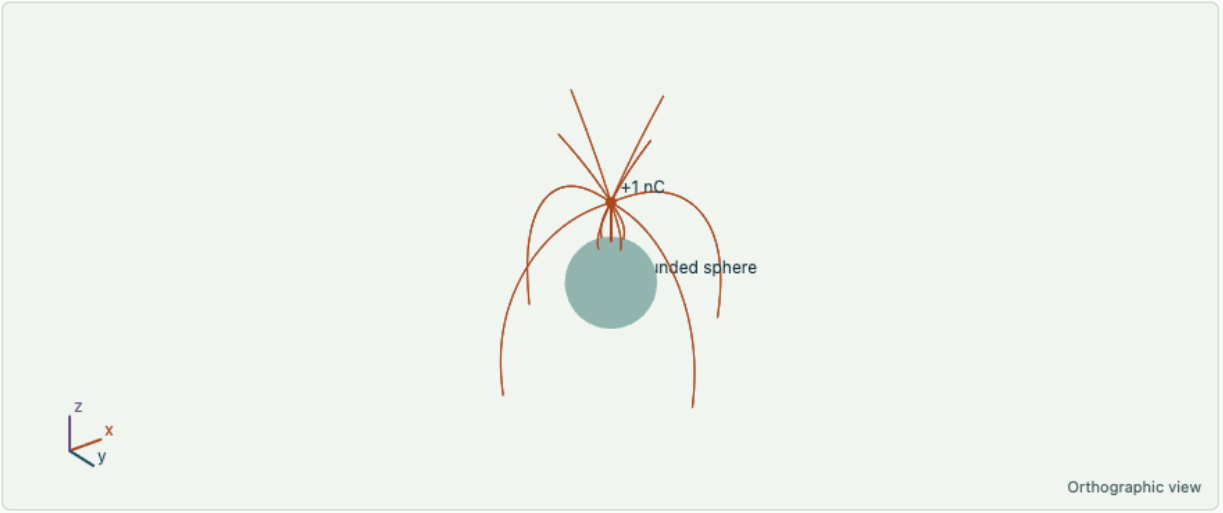

Numerically traced electric-field lines outside a grounded sphere (a=1 m). The computed field uses fitted interior sources; slight loss of axial symmetry is approximation error. The fictitious interior charges are not physical charges in the metal. Axes: x = x/a; y = y/a; z = z/a.

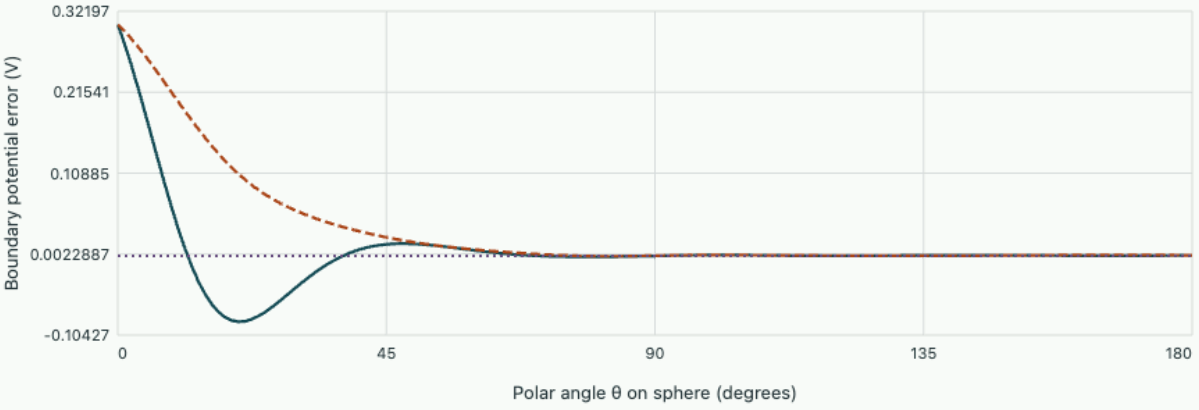

Computed surface, ϕ=0° Computed surface, ϕ=90° Exact image construction

Linear residual 5.55e-16; maximum error on 1201 withheld surface points 0.41847 V. Induced charge -0.49919 nC; exact -0.5 nC.

Download the OneSimulation model

In your OneSimulation environment, run the model with these inputs.

```
python complete-spatial-sphere.py --sources 48 --distance 2 --source-radius 0.65
```

Download the executed 3D OneSimulation notebook · Python model

```
"""Grounded sphere: a 3D source-collocation solve and an independent image solution."""
import argparse
import numpy as np
import matplotlib.pyplot as plt
from onesim.numerics.linear.matrices.dense_linear_algebra import solve_dense

parser = argparse.ArgumentParser(description=__doc__)
parser.add_argument('--sources', type=int, default=48)
parser.add_argument('--distance', type=float, default=2.0, help='Real-charge distance / sphere
radius')
parser.add_argument('--source-radius', type=float, default=.65, help='Fictitious-source radius /
sphere radius')
args = parser.parse_args()
if not 24 <= args.sources <= 96 or not 1.5 <= args.distance <= 3 or not .45 <= args.source_radius <=
.85:
    parser.error('Use 24–96 sources, distance 1.5–3, and source radius 0.45–0.85')

def fibonacci_sphere(n, offset=0.0):
    j = np.arange(n)
    z = 1 - 2*(j+.5)/n
    phi = j*np.pi*(3-np.sqrt(5))+offset
    return np.column_stack([np.sqrt(1-z*z)*np.cos(phi),np.sqrt(1-z*z)*np.sin(phi),z])

boundary = fibonacci_sphere(args.sources)
sources = args.source_radius*boundary
charge = np.array([0.,0.,args.distance])
influence = 1/np.linalg.norm(boundary[:,None,:]-sources[None,:,:],axis=2)
rhs = -1/np.linalg.norm(boundary-charge,axis=1)
weights = np.asarray(solve_dense(influence,rhs))
factor = 8.9875517923  # q/(4*pi*eps0), for q=1 nC and radius=1 m

def potential(points):
    points=np.atleast_2d(points)
    return factor*(1/np.linalg.norm(points-charge,axis=1)
                   + (1/np.linalg.norm(points[:,None,:]-sources[None,:,:],axis=2))@weights)

def exact(points):
    points=np.atleast_2d(points)
    image=np.array([0.,0.,1/args.distance])
    return factor*(1/np.linalg.norm(points-charge,axis=1)
                   -1/args.distance/np.linalg.norm(points-image,axis=1))

def field(point):
    real=point-charge
    delta=point-sources
    return real/np.linalg.norm(real)**3 + (weights[:,None]*delta/np.linalg.norm(delta,axis=1)
[:,None]**3).sum(axis=0)

check = fibonacci_sphere(1201,.37)
boundary_error=float(np.max(np.abs(potential(check))))
algebraic_error=float(np.max(np.abs(influence@weights-rhs)))
print(f'Sources: {args.sources}; d/a={args.distance:g}; source radius/a={args.source_radius:g}')
print(f'Linear residual: {algebraic_error:.3e}; withheld boundary error: {boundary_error:.6e} V')
print(f'Induced charge: {weights.sum():.8f} nC; exact: {-1/args.distance:.8f} nC')
assert algebraic_error < 1e-9

fig = plt.figure(figsize=(11,4.8),layout='constrained')
ax=fig.add_subplot(121,projection='3d')
theta=np.linspace(0,np.pi,25);phi=np.linspace(0,2*np.pi,49)
T,P=np.meshgrid(theta,phi)
ax.plot_surface(np.sin(T)*np.cos(P),np.sin(T)*np.sin(P),np.cos(T),color='#94b8af',alpha=.85,linewidth=
```

```
0)
for angle in [np.pi/6,np.pi/2,5*np.pi/6,np.pi]:
    for azimuth in [0,np.pi/2,np.pi,3*np.pi/2]:

p=charge+.08*np.array([np.sin(angle)*np.cos(azimuth),np.sin(angle)*np.sin(azimuth),np.cos(angle)])
        path=[p.copy()]
        for _ in range(160):
            e=field(p);p=p+.035*e/np.linalg.norm(e);path.append(p.copy())
            if np.linalg.norm(p)<1.015 or np.linalg.norm(p)>4.4:break
        curve=np.array(path);ax.plot(*curve.T,color='#ad491d',linewidth=.8)
ax.scatter(*charge,color='#ad491d',s=30)
ax.set(xlabel='x/a',ylabel='y/a',zlabel='z/a',title='Computed exterior field lines')
ax.set_box_aspect([1,1,1]);ax.set(xlim=(-2.5,2.5),ylim=(-2.5,2.5),zlim=(-2,4))
ax=fig.add_subplot(122)
angles=np.linspace(0,np.pi,181)
for azimuth in [0,np.pi/2]:

points=np.column_stack([np.sin(angles)*np.cos(azimuth),np.sin(angles)*np.sin(azimuth),np.cos(angles)])
    ax.plot(np.rad2deg(angles),potential(points),label=f'Collocation, ϕ={np.rad2deg(azimuth):g}°')
ax.axhline(0,color='black',linestyle='--',label='Exact image solution')
ax.set(xlabel='Polar angle θ (degrees)',ylabel='Boundary potential error (V)',title='Check locations
outside the fit')
ax.legend();ax.grid(alpha=.2)
fig.savefig('complete-spatial-sphere.png',dpi=170)
```

Actual output from the default OneSimulation solve:

```
Sources: 48; d/a=2; source radius/a=0.65
Linear residual: 2.220e-16; withheld boundary error: 4.184726e-01 V
Induced charge: -0.49918756 nC; exact: -0.50000000 nC
```

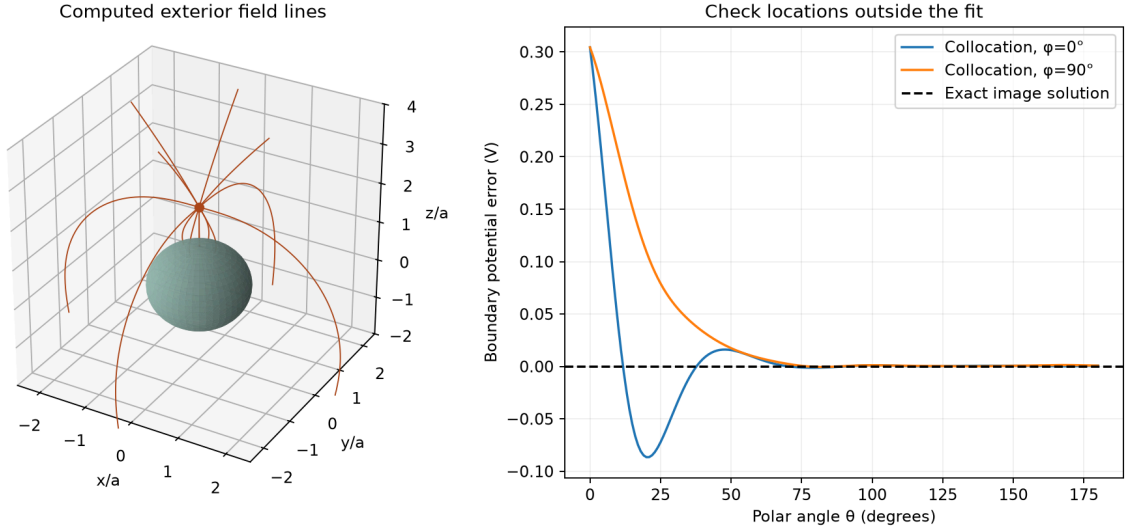

Full three-coordinate collocation model. The exact grounded-sphere solution has zero boundary potential; the plotted discrepancy measures approximation error.

Derive the external capacitance of a two-wire pair

Two long parallel metal cylinders of equal radius a have centre-to-centre separation $D > 2a$. They carry equal and opposite line charges and are maintained at opposite voltages. If the surface separation is

comparable to the wire radius, putting equivalent lines on the conductor axes fails to make each circumference equipotential. Instead exploit the geometry of a potential difference of two line sources. Place $+\lambda$ at $x = s$ and $-\lambda$ at $x = -s$, and write $R_{\pm}$ for their distances to a field point. The potential with distant zero reference is $\lambda \ln(R_-/R_+)/(2\pi\epsilon)$. Every contour with a constant distance ratio is a circle or a straight line.

For a positive conductor the ratio is

$$R_-/R_+ = e^{\eta} > 1.$$

Square the distances and complete the square in x, y. The resulting circle has centre $x_c = s\coth\eta$ and radius $s/\sinh\eta$. Its negative twin has centre $-x_c$. Requiring the physical radius and separation fixes $\cosh\eta = D/(2a)$ and $s = \sqrt{(D/2)^2 - a^2}$. Both effective lines lie inside their respective conductors. Since the cylinder voltages are $\pm\lambda\eta/(2\pi\epsilon)$, their voltage difference is $\lambda\eta/(\pi\epsilon)$. The pair capacitance per axial length is therefore

$$C' = \frac{\pi\epsilon}{\operatorname{arcosh}(D/(2a))}.$$

Here charge per length on one conductor is divided by the voltage difference between both. Dividing by the voltage of just the positive conductor relative to the symmetry plane would give twice this value, appropriate to a different terminal convention. Integrating field energy over the whole exterior also yields $\lambda^2/(2C')$, so the factor of two can be checked by comparing charge and energy definitions using the same two terminals.

For $a = 1.0$ mm and $D = 5.0$ mm in vacuum, $\eta = \operatorname{arcosh} 2.5 = 1.567$ and $C' = 17.8$ pF/m. In the far-separated limit $\operatorname{arcosh}(D/2a) \simeq \ln(D/a)$, explaining the familiar logarithmic dependence. In the opposite limit $D = 2a + g$ with $g \ll a$,

$$\operatorname{arcosh}(1 + g/2a) \simeq \sqrt{g/a}.$$

The capacitance then grows as $\pi\epsilon\sqrt{a/g}$, slower than the $1/g$ divergence of broad parallel plates. Why? Near the closest points the local gap increases approximately as $g + y^2/a$. Treating narrow strips as locally parallel gives

$$dC'/dy \simeq \epsilon/(g + y^2/a).$$

Integrating over all y produces $\pi\epsilon\sqrt{a/g}$, independently recovering the leading result. The active area shrinks laterally as the wires approach.

One can predict the mechanical consequence without integrating a surface force directly. For fixed $\pm\lambda$, energy per length is

$$U' = \lambda^2\eta/(2\pi\epsilon).$$

The force tending to increase separation is

$$-dU'/dD = -\lambda^2/[2\pi\epsilon\sqrt{D^2 - 4a^2}].$$

It is attractive. With fixed voltage the charges vary, but evaluating the appropriate coenergy derivative at the same $\lambda = C'\Delta V$ gives the same instantaneous force. This is a strong consistency check because a seemingly small geometric error in the image positions can preserve a reasonable far-field capacitance while badly mispredicting the near-gap force.

Try it · Resolve the two-wire capacitance

Reduce the gap and compare the exact result with its large-separation logarithm. Change permittivity and predict the scaling before moving the slider. C′ uses the voltage between both wires.

Open this boundary experiment

Try the calculation

Relative permittivity 1

Selected D/(2a) 2

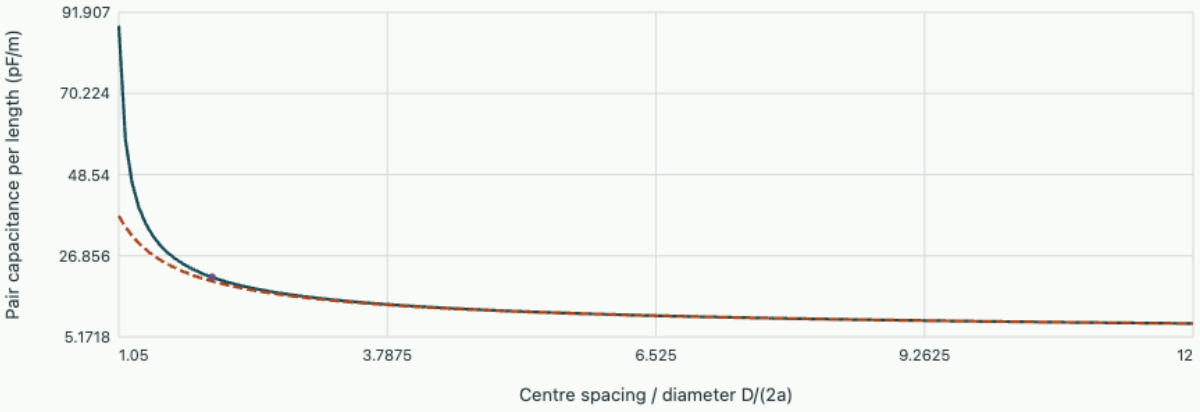

Exact bipolar-coordinate result | Widely separated approximation | Selected spacing

At D/(2a)=2, C′=21.122 pF/m. For a homogeneous nonmagnetic dielectric the corresponding TEM impedance is 157.93 Ω.

Notebook: reproduce the exact boundary constructions and the 3D collocation model

An infinite image series for two grounded planes

Put a charge q at $z = s$ between infinite grounded planes at $z = 0, L$. Reflecting in the bottom plane creates a charge $-q$ at $-s$; now the top plane no longer has zero voltage. Repeated reflections generate charges $+q$ at $z = 2nL + s$ and $-q$ at $z = 2nL - s$, for every integer n. At the bottom, equal-distance terms cancel pairwise by reflection across zero. At the top, reflection $z \mapsto 2L - z$ again exchanges the

two families. The original charge is the $n = 0$ positive one. Each other singularity lies outside the open strip $0 < z < L$.

For axial separation from the charge line $r_\perp$, the potential is the sum of $q/(4\pi\epsilon)$ times the differences of reciprocal distances to these pairs. Group each positive and negative image into a neutral pair before summing. Individual series of absolute monopole magnitudes diverge like a harmonic series, while the paired differences decay at least as fast as $1/n^2$ at fixed interior observation point. A numerical calculation should specify this paired convention and test voltage on both planes as more pairs are included. Summing a large collection of positives first and negatives afterward can produce large finite truncation offsets.

At $s = L/2$ the charge is equidistant from both grounded planes. Reflection about the midplane makes the field due to all images vanish at the source, so it feels no net axial force. Each conductor nevertheless receives induced charge $-q/2$. Reciprocity gives the split without summing any images: the weighting potential of the upper plane is z/L, so it receives $-qs/L$, with the rest on the lower plane. As s approaches zero the nearest negative image at $-s$ dominates the force, reproducing the single-plane attraction $q^2/(16\pi\epsilon s^2)$. A zero net central force therefore does not imply weak local conductor fields or no induced charge.

A useful numerical experiment places the source at several small offsets from the midpoint. The two conductors' integrated charge measurements change linearly with s by the exact reciprocity rule, while the force changes nonlinearly and diverges near either face. These independent analytic targets expose different errors. A coarse mesh may resolve smooth electrode weighting potentials and hence the charge split long before it resolves the closely spaced source-image pair needed for a trustworthy force. Replacing all images by the nearest one succeeds only near a chosen plate and fails both far-boundary conditions and midpoint force cancellation.

Try it · Test both grounded faces at once

Move the source around the midpoint and refine the image sum. Check antisymmetry of force and compare the nearest-image approximation. The induced electrode charges are also reported from reciprocity.

Open this boundary experiment

Try the calculation

Included image-pair order **12**

Selected charge position s/L **0.5**

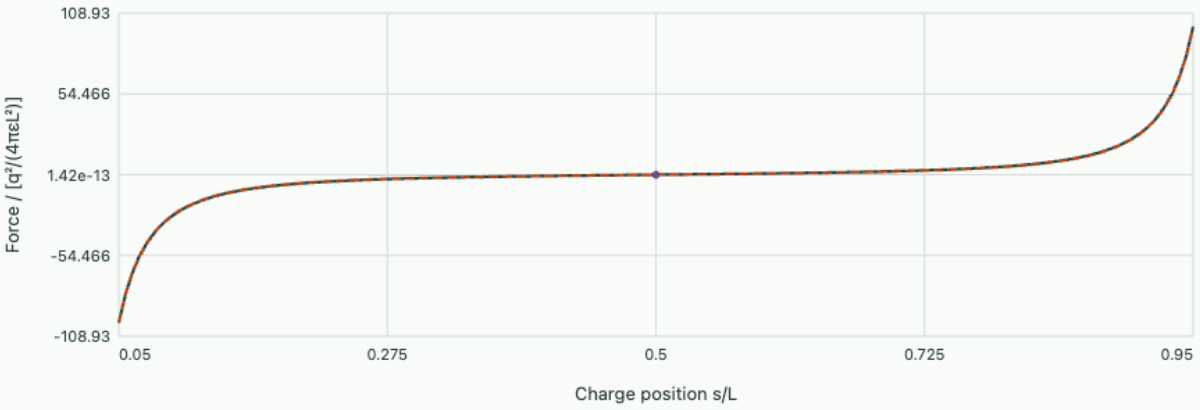

At s/L=0.5, normalised force=6.0715e-18. Induced charge fractions: lower plate -0.5, upper plate -0.5. At the midpoint force cancels, while both plates carry –q/2.

Notebook: reproduce the exact boundary constructions and the 3D collocation model

A buried grounded plane produces a scale-dependent image response

A charge is placed in medium 1 above a film of medium 2 with thickness t. The film spans $-t < z < 0$ and is backed by a grounded metal at $z = -t$. Both permittivities are positive and there is no free charge on the material interface. An intuitively appealing model uses one image representing the dielectric interface and another representing the metal. Their two boundary effects actually interact: the dielectric layer changes how strongly the field of the backing is seen at the upper surface. A sinusoidal lateral Fourier component exposes that interaction without constructing an infinite image series.

Let $k > 0$ be the magnitude of the wavevector parallel to the plane. In the portion of medium 1 below the source write the incident contribution near the interface as Ae^{kz} and the reflected contribution as Be^{-kz},

so their values there are A, B. In the film the grounded backing selects $C\sinh[k(z+t)]$. Potential continuity gives

$$A + B = C\sinh(kt).$$

Equality of oriented displacement at $z = 0$ gives

$$\epsilon_1 k(A - B) = \epsilon_2 kC\cosh(kt).$$

Dividing these two equations and solving for the ratio yields

$$r(k) = \frac{B}{A} = \frac{\epsilon_1 - \epsilon_2\coth(kt)}{\epsilon_1 + \epsilon_2\coth(kt)}.$$

At $kt \gg 1$ lateral variations decay within a small fraction of the film thickness, so the result tends to the familiar dielectric image factor. At $kt \ll 1$, $\coth(kt) \sim 1/(kt)$ and the ratio tends to -1: long-range variations see an effectively grounded boundary. When the two dielectric materials are identical the result is exactly $-e^{-2kt}$, the propagation factor to a grounded plane at depth t and back. These three limits independently test the sign convention for the decaying and growing terms in the local upper-region decomposition.

Take $\epsilon_1 = 4\epsilon_0, \epsilon_2 = 2\epsilon_0$. For a very short wavelength the real image coefficient tends to $+1/3$, while for very long wavelengths the reflected coefficient is negative. It crosses zero when $\coth(kt) = 2$, or $kt = \frac{1}{2}\ln 3 = 0.5493$. With a 1.0 mm film the crossover wavelength is

$$2\pi t/0.5493 = 11.4\,\mathrm{mm}.$$

A single image charge with a constant amplitude cannot represent all wavelengths. A point charge excites a broad spectrum; the force it experiences is an integral over those modes weighted by propagation between charge and interface. The sign change of one Fourier coefficient alone does not locate a force reversal at the same distance.

An experiment with a sinusoidal patterned source and a movable probe can estimate this reflection coefficient mode by mode, comparing to a calibration without the backing. Measuring at several wavelengths tests the film model more stringently than fitting one effective permittivity to one force reading. If the backing is ungrounded but maintained at one unknown uniform potential, nonzero k components can still use the same zero-variation boundary there while the $k = 0$ component must enforce the actual conductor charge. This subtle distinction is another reason to state both electrical reference and spatial mode whenever an image coefficient is used.

Try it · Find which wavelengths see the backing

Change film thickness and relative permittivity. Check the identical-material limit and locate the sign crossover when ε_2 is smaller than ε_1. This is a mode reflection coefficient; the force on a point charge requires integrating over its spectrum.

Open this boundary experiment

Try the calculation

Permittivity ratio $\varepsilon_2/\varepsilon_1$ **0.5**

Film thickness (mm) **1**

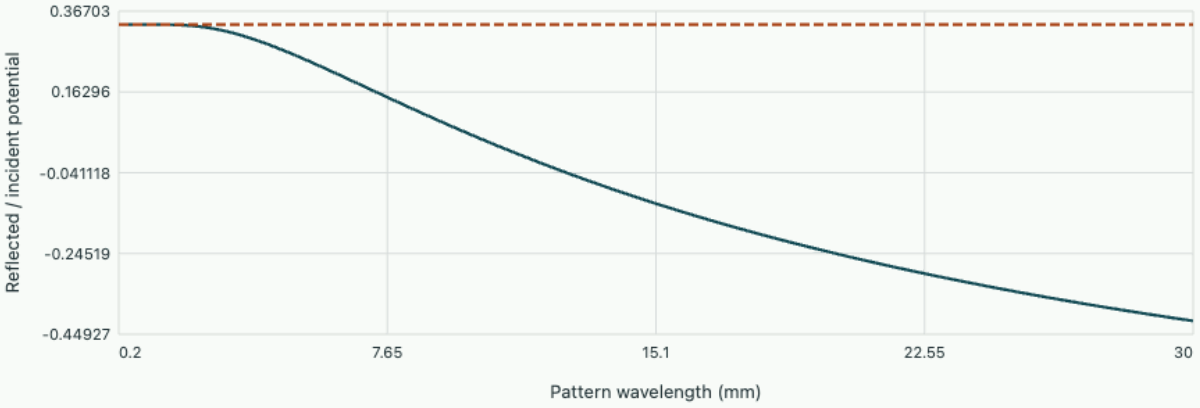

The reflection changes sign at wavelength 11.438 mm. Long wavelengths see the buried ground; short wavelengths see the dielectric interface.

Notebook: reproduce the exact boundary constructions and the 3D collocation model

Tutorial · apply and challenge an image system

What does an outside line induce on an isolated cylinder?

An initially neutral isolated conducting cylinder replaces the grounded one. Find the change needed in the image system, and calculate the leading far-separation force per length. State the observable that distinguishes the two preparations.

▼ **Work through the solution**

Retain the off-centre negative image to enforce equipotentiality, and add a central $+\lambda$. Its logarithmic potential has constant value on the cylinder. The equivalent enclosed charge per length is now zero. The radial force per length is

$$\lambda^2[1/d - d/(d^2 - a^2)]/(2\pi\epsilon_0) = -\lambda^2 a^2/[2\pi\epsilon_0 d(d^2 - a^2)].$$

At $d \gg a$ this varies as $-d^{-3}$, whereas the grounded-line problem gives a leading $-d^{-1}$ force. A total-charge measurement or a force-vs-distance measurement distinguishes the preparations. The total source including the real infinite line is no longer neutral, so potential differences must be referred to a finite reference or a specified return electrode.

Can a single medium describe the potential on both sides?

For the dielectric interface let $\epsilon_2 = 3\epsilon_1$. A voltmeter scanned along the plane finds a potential that looks like a charge of half the expected strength in medium 1. Predict the force direction, the transmitted field below, and why one apparent charge cannot describe the whole space.

▼ **Work through the solution**

Here $q' = -q/2$, so on the plane $q + q' = q/2$. The force is attractive toward the higher-permittivity medium. The lower-region effective charge is $q'' = 3q/2$, producing potential prefactor $q''/\epsilon_2 = (q/2)/\epsilon_1$, so the surface voltage agrees. Away from the plane the upper field contains two distances while the lower field contains only the continued source distance. Normal electric fields at the surface differ by the factor $\epsilon_2/\epsilon_1 = 3$ required by continuous displacement. Identical voltage along the interface does not imply equal three-dimensional fields near it.

Further reading

- Compare grounded and isolated image spheres numerically
- Integrate the induced charge on the two faces of a corner
- Griffiths, 5th ed., §§3.2, 4.4.2 · images and dielectric boundaries

Electrostatic field theory and measurement · 5. Green functions, the Poisson kernel and what a small electrode can influence

A Green function is the response of an entire boundary-value problem to a unit source. Once that response is known, a continuous charge distribution and a patterned boundary voltage can both be treated by integration. The two integrations require different kernels.

Define a point response with its boundary conditions

Let Ω be a vacuum domain with boundary on which the voltage is given. Use the convention $-\nabla^2_{\mathbf{y}} G(\mathbf{x},\mathbf{y}) = \delta^3(\mathbf{y}-\mathbf{x})$ and $G = 0$ on the boundary as a function of $\mathbf{y}$. In free space $G = 1/(4\pi|\mathbf{x}-\mathbf{y}|)$ if decay is required at infinity. This definition places no permittivity in G; physical charge enters as ρ/ϵ_0. A different frequent convention puts 4π in the defining equation, changing all subsequent prefactors. Comparing the near-source flux to unity is a straightforward way to fix which convention is being used.

Begin with two differentiable functions u, v. The difference $\nabla\cdot(u\nabla v - v\nabla u) = u\nabla^2 v - v\nabla^2 u$ has no mixed-gradient term. Integrate this identity with $u = V(\mathbf{y})$,

$$v = G(\mathbf{x},\mathbf{y}).$$

The source equation for G samples V at $\mathbf{x}$, while Poisson's equation for V supplies a volume density. With the outward normal taken from Ω,

$$V(\mathbf{x}) = \int_\Omega G(\mathbf{x},\mathbf{y})\frac{\rho(\mathbf{y})}{\epsilon_0}\,d^3y - \oint_{\partial\Omega} V(\mathbf{y})\partial_{n_\mathbf{y}} G(\mathbf{x},\mathbf{y})\,dA_\mathbf{y}.$$

The $G\partial_n V$ boundary term vanishes because $G = 0$ there. If the singularity causes concern, exclude a small sphere about $\mathbf{x}$, apply the ordinary identity, and shrink the sphere. The inward normal on the excised sphere produces the same $V(\mathbf{x})$ term. The representation separates charges in the volume from voltages maintained by electrode sources; it does not combine them into one fictitious material distribution.

Solve the half-space and differentiate with respect to source position

Consider $\mathbf{x} = (\mathbf{X}, h)$ with $h > 0$ above the plane $z = 0$. For an interior source $\mathbf{y} = (\mathbf{Y}, z)$, denote its reflection by $\mathbf{y}^* = (\mathbf{Y}, -z)$. The grounded half-space Green function is

$$G = \frac{1}{4\pi}\left[\frac{1}{\sqrt{|\mathbf{X}-\mathbf{Y}|^2 + (h-z)^2}} - \frac{1}{\sqrt{|\mathbf{X}-\mathbf{Y}|^2 + (h+z)^2}}\right].$$

It vanishes as the source coordinate approaches the plane. The outward domain normal there is $-\hat{\mathbf{z}}$; therefore the coefficient of a prescribed boundary voltage is

$$P_h = -\partial_n G = \partial_z G|_{z=0}.$$

Differentiating the two terms gives equal positive contributions:

$$P_h(\mathbf{X}-\mathbf{Y}) = \frac{h}{2\pi[|\mathbf{X}-\mathbf{Y}|^2+h^2]^{3/2}}.$$

Its units are inverse area, while G has inverse length in this three-dimensional convention. For no interior charge $V(\mathbf{X},h) = \int P_h(\mathbf{X}-\mathbf{Y})f(\mathbf{Y})\,d^2Y$. The kernel is positive. Integrate over the whole plane using $2\pi s\,ds$; the result is one. Hence a constant boundary voltage is reproduced, and an arbitrary voltage bounded between two numbers produces values between the same bounds inside. The integral solves the bounded half-space problem with the far-field condition appropriate to the data. Demanding decay for a nonzero constant boundary value would be inconsistent.

A detector at height h takes a weighted average over a neighbourhood of width comparable with h. The kernel has algebraic tails, so its support is not a sharp circular footprint. The contribution from radii smaller than b is $1 - h/\sqrt{b^2+h^2}$. Half the total weight lies within $b = \sqrt{3}h$. Ninety per cent requires

$$b = \sqrt{99}h \simeq 9.95h.$$

These quite different radii show why a full-width-at-half-maximum measurement of the kernel cannot by itself define the region that contains most of its influence.

A finite driven electrode and a reciprocity experiment

Fix a circular disk of radius b in the plane at voltage V_d while grounding the rest of the plane, with ideal thin insulating seams. Directly over its centre,

$$V(0,h) = V_d\left(1 - \frac{h}{\sqrt{h^2+b^2}}\right),$$

$$E_z(0,h) = V_d\frac{b^2}{(h^2+b^2)^{3/2}}.$$

At $h \to 0^+$ the electrode voltage is recovered at its centre. For $h \gg b$ the voltage scales as $V_d b^2/(2h^2)$. A small electrode surrounded by ground does not behave at long distance as an isolated charged electrode with a $1/h$ potential. Its surrounding return charge makes a combined disturbance whose far field has a different order. At the sharp ideal edge the boundary voltage jumps, and local fields there require an actual seam geometry if one wants a bounded peak or a breakdown prediction.

For $b = 5.0$ mm, $V_d = 4.0$ V and $h = 5.0$ mm the axial voltage is 1.17 V and field is 283 V/m. A separate experiment grounds every electrode and places a point charge q at that observation point. Green reciprocity relates the net charge on the disk to the previous weighting potential $w = V/V_d$: $Q_d = -q\,w$. With $q = 20$ pC the disk collects -5.86 pC. Direct integration of the image-plane surface charge $\sigma(s) = -qh/[2\pi(s^2+h^2)^{3/2}]$ gives the same result. It is precisely $-qP_h$. Thus the boundary kernel has both a voltage-producing interpretation and a charge-collection interpretation measurable with different instrumentation.

Recover the kernel of an electrode strip

A boundary pattern invariant in y should not require a two-dimensional source integral. Integrate P_h over the unused coordinate. With lateral separation $s = X - X'$, the result is

$$p_h(s) = h/[\pi(s^2 + h^2)].$$

It integrates to one over the real line. A strip between $-b, b$ at V_d gives on its central normal $V(0, h) = 2V_d \arctan(b/h)/\pi$. At $h = b$ the value is half the applied voltage, distinct from the circular electrode's $1 - 1/\sqrt{2}$. The strip extends in one more direction and occupies a larger angular range of boundary influence.

For sinusoidal boundary data $f(X) = \cos kX$ there is an independent way to determine the result without evaluating a difficult oscillatory integral. Translational symmetry and linearity preserve the sinusoid. Solving Laplace's equation with vertical factor $Z(h)$ gives

$$Z'' = k^2 Z.$$

The bounded decaying solution with unit boundary amplitude is $e^{-|k|h}$. Thus the Fourier transform of the strip kernel is $e^{-|k|h}$. Convolving twice with heights h_1, h_2 is equivalent to convolution once with height $h_1 + h_2$. This composition property checks a numerical propagation code without requiring separate analytic solutions for many different boundary patterns.

Which symmetries does an influence table possess?

Exchange source and detector in the defining equations for $G(\mathbf{x}, \cdot)$ and $G(\mathbf{z}, \cdot)$. Their difference identity gives $G(\mathbf{x}, \mathbf{z}) - G(\mathbf{z}, \mathbf{x}) = 0$, since both vanish on the same boundary. Symmetry extends to scalar or symmetric-tensor positive permittivity when the operator is defined as $-\nabla \cdot \epsilon \nabla$. It refers to exactly the same material, boundary preparation and domain in both experiments. Replacing one experiment's grounded conductor by a floating conductor changes the Green function.

On a nonuniform mesh it matters whether influence entries correspond to equal point charges or equal charge densities in unequal cells. If a finite-volume solver stores sources as densities, a column's total injected charge scales with its cell volume. An unweighted table of sampled voltages can look nonsymmetric even when the discrete physics is reciprocal. Form the matrix with unit total source and consistent detector averaging, or retain the correct volume-weighted inner product. Test positivity for positive sources as a second check. Symmetric influence entries by themselves cannot expose a common incorrect normalisation or a misplaced outer boundary.

A kernel that reproduces every harmonic around a circle

In a two-dimensional circular domain of radius a, prescribe a voltage $f(\phi')$ around the wall. For a detector at (r, ϕ) let $t = r/a < 1$. The angular Fourier component with order m is multiplied by $t^{|m|}$ on continuation into the disk. This follows directly from the regular radial power solution of Laplace's

equation. Substitute the Fourier coefficient integral into the series and interchange the integral and the absolutely convergent series at fixed $t < 1$. The boundary response per unit angle is then

$$P_t(\delta) = \frac{1}{2\pi} \sum_{m=-\infty}^{\infty} t^{|m|} e^{im\delta} = \frac{1 - t^2}{2\pi(1 - 2t\cos\delta + t^2)},$$

$$\delta = \phi - \phi'.$$

To obtain the rational form, separate the $m = 0$ term and sum the two conjugate geometric series $te^{\pm i\delta}/(1 - te^{\pm i\delta})$. The result is positive for every interior point. Integrating it over angle leaves only the constant Fourier mode, so it is normalised to unity. At the centre the kernel is simply $1/(2\pi)$, recovering the exact mean-value theorem for harmonic functions. Near the wall it becomes very sharply concentrated around the detector's azimuth while retaining a small nonlocal tail. Using prescribed boundary data as a flat average at every interior point would reproduce only the centre reading.

For a concrete experiment put a short arc of half-angle α centred on $\phi = 0$ at 1 V and ground the remaining circular boundary. Along $\phi = 0$ the potential equals the integral of P_t between $-\alpha, \alpha$. With $u = \tan(\phi'/2)$ one has $\cos\phi' = (1 - u^2)/(1 + u^2)$, $d\phi' = 2du/(1 + u^2)$. Substitution gives the weight

$$w(t) = \frac{2}{\pi} \arctan\left[\frac{1 + t}{1 - t} \tan(\alpha/2)\right].$$

At $t = 0$ it gives α/π, exactly the fraction of the circumference occupied by the arc. For a 60°-wide arc $\alpha = \pi/6$, hence the centre reads $1/6$ V. At $t = 0.6$ on the centreline it reads about 0.522 V. Placing a small positive line charge there while grounding the whole cylindrical wall induces -0.522 times the line charge on that arc by the same reciprocity argument used on the flat disk. The angular share depends on position inside the circle even though every point on the conductor has the same actual grounded voltage.

An independent check takes the limit of a very large circle with the probe only a distance $h = a - r$ from the nearest boundary point. For small angular displacement $\delta = s/a$, $1 - 2t\cos\delta + t^2 \simeq (h/a)^2 + (s/a)^2$ and $1 - t^2 \simeq 2h/a$. The angular probability element $P_t(\delta)d\delta$ therefore tends to $h\,ds/[\pi(h^2 + s^2)]$, precisely the translation-invariant strip kernel obtained by integrating the half-space formula over one coordinate. Curvature corrections can be estimated by increasing a/h at fixed physical arc width and comparing both predictions.

Why an insulated Green function needs a zero-mode subtraction

Consider the simpler interval $0 < x < L$ with prescribed zero flux at both ends. We would like a point response satisfying $-G'' = \delta(x - s)$, $G'(0) = G'(L) = 0$. Integrate this proposed equation over the interval: the left-hand side is $-G'(L) + G'(0) = 0$, whereas the right-hand side is 1. The attempted kernel violates compatibility. Physically a sealed insulating region cannot take a net free test charge without changing its prescribed outer flux. Adding an arbitrary constant to G cannot fix this contradiction.

A useful alternative removes the constant source mode and fixes the remaining voltage reference. Define $-G_N'' = \delta(x - s) - 1/L$, $G_N'(0) = G_N'(L) = 0$, and $\int_0^L G_N(x, s)\,dx = 0$. Away from the point the

curvature is $+1/L$. The left derivative must be x/L to vanish at zero, the right derivative $x/L-1$ to vanish at L. They jump by -1 at $x=s$. Integrating, imposing continuity and subtracting the mean gives the compact symmetric expression

$$G_N(x,s)=\frac{x^2+s^2}{2L}-\max(x,s)+\frac{L}{3}.$$

Differentiating verifies both end conditions and the jump. Integrating the quadratic part and the piecewise maximum over x verifies the mean condition. Its sign can be negative because the response includes an opposite uniform return source and uses a zero-mean reference. Unlike the positive grounded Dirichlet kernel, it is not a positive voltage weight to use for a maximum-principle test.

Apply a neutral pair of sheets $+\sigma$ at $s_1=0.2L$ and $-\sigma$ at $s_2=0.7L$. Their voltage is $\sigma[G_N(x,s_1)-G_N(x,s_2)]/\epsilon$. The two artificial uniform return sources cancel exactly. To the left of both sheets the field vanishes, between them it equals $+\sigma/\epsilon$, and to the right it vanishes again. The potential drops by $0.5L\sigma/\epsilon$ across the two sheets. This matches direct Gauss-law jumps, and the zero-mean potential fixes the constant that Gauss's law could not determine. For more complex closed domains numerical solvers implement the same idea by projecting out the constant eigenvector and checking the compatible total charge before inverting. An arbitrary tiny diagonal regularisation of a singular matrix can hide a physically impossible net-source input.

Construct a point response when the medium itself screens charge

A linear ionic or phenomenological screening model between two grounded parallel electrodes leads in one dimension to $[-\partial_x^2+\kappa^2]V=\rho_{\mathrm{imposed}}/\epsilon$, $0<x<L$. Here ρ_{imposed} excludes the mobile linear response already represented by κ^2V. We seek $G_\kappa(x,s)$ with zero voltage at both ends. Away from its unit source the equation has hyperbolic solutions. Use $A\sinh(\kappa x)$ on the left to vanish at zero and $B\sinh[\kappa(L-x)]$ on the right to vanish at L. Continuity at $x=s$ removes one constant. Integrating across the source gives $G'_\kappa(s^+)-G'_\kappa(s^-)=-1$; the finite mass term integrates to zero in a shrinking source interval.

To solve transparently use the functions $u(x)=\sinh(\kappa x)$,

$$v(x)=\sinh[\kappa(L-x)].$$

Their Wronskian $u'v-uv'$ is $\kappa\sinh(\kappa L)$, independent of x. Then continuity, the derivative jump, and symmetry under $s\leftrightarrow x$ are manifest in

$$G_\kappa(x,s)=\frac{\sinh(\kappa x_<)\sinh[\kappa(L-x_>)]}{\kappa\sinh(\kappa L)},$$

$$x_<=\min(x,s),$$

$$x_>=\max(x,s).$$

For $\kappa\to0$, expand each hyperbolic sine to first order. The result is $x_<(L-x_>)/L$, the grounded unscreened response. When both observation and source lie many screening lengths from every

boundary, the kernel tends to $e^{-\kappa|x-s|}/(2\kappa)$, the infinite-line screened solution. Thus one formula contains both geometric screening by grounded conductors and material screening by mobile charges.

At the midpoint source and detector coincide. The finite kernel reduces to $\tanh(\kappa L/2)/(2\kappa)$. Compared with the unscreened midpoint value $L/4$, its ratio is $2\tanh(\kappa L/2)/(\kappa L)$. At $\kappa L = 2$ a fixed inserted sheet therefore creates only 76.2% of its unscreened midpoint voltage. A naïve replacement of plate separation by the screening length would give a constant ratio and miss the smooth small-κ crossover. For long gaps the measured voltage saturates at fixed sheet charge, because the countercharge response near the sheet now sets the local scale.

Check the convolution using a uniform positive imposed charge density ρ_0. Without integrating the kernel directly, seek a constant particular solution plus a symmetric homogeneous correction. The result is

$$V(x) = [\rho_0/(\epsilon\kappa^2)]\{1 - \cosh[\kappa(x - L/2)]/\cosh(\kappa L/2)\}.$$

Twice differentiation reconstructs the source and zero endpoints. In the small-κL limit it tends to $\rho_0 x(L - x)/(2\epsilon)$. A numerical integration of the point response against a uniform source should match this independent closed solution throughout the interval, including the near-electrode regions. It is a stronger test than checking the point kernel at the centre alone.

Integrate the original equation across the gap. The sum of outward displacement fluxes equals imposed charge minus $\epsilon\kappa^2 \int V\,dx$, the magnitude of the compensating mobile charge. For the uniform source the fraction of imposed charge balanced by electrode rather than mobile charge is $2\tanh(\kappa L/2)/(\kappa L)$. For a long gap this fraction falls like twice the screening length divided by gap width, because only the two boundary regions communicate appreciably with the electrodes. A current meter attached to the electrodes and a chemical measurement of accumulated mobile ions can therefore close the same source budget independently.

Inspect the response to a localised source

Move the source while holding the boundaries fixed. Test the symmetry between source and observation point predicted by reciprocity.

Open this experiment online

Try the calculation

Sheet position s/L **0.3**

Sheet charge density (nC/m²) **3**

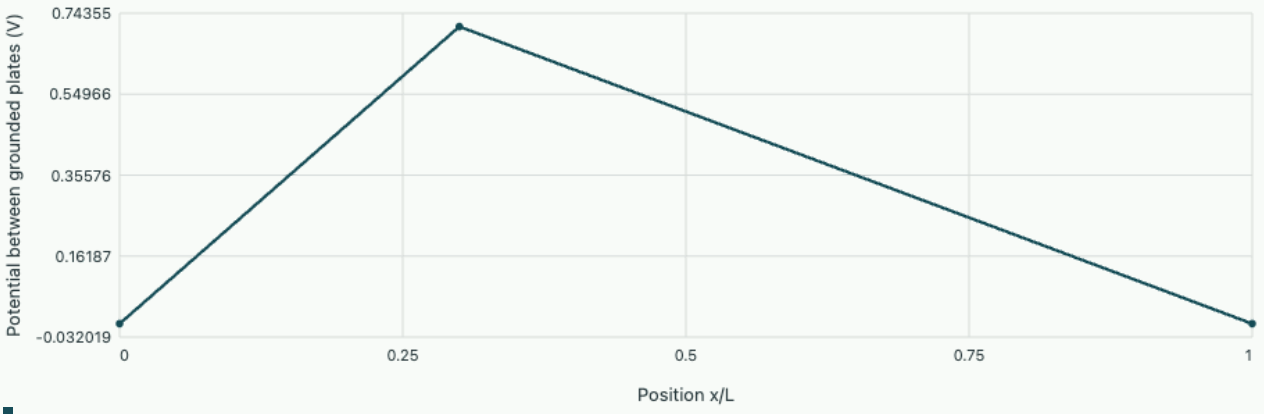

Grounded 10 mm gap

Induced densities are -2.1 nC/m² on the left and -0.9 nC/m² on the right. Potential at the sheet is 0.712 V.

Design a differential collecting electrode from its weighting functions

Two concentric electrodes supply one signed position signal

A grounded plane is divided into a central disk of radius a, a surrounding annulus from a to $2a$, and the remainder. A small charge moves along the central normal. Two charge amplifiers measure the disk and annulus. Construct an output that vanishes at $h = a$, then find its local height sensitivity. Why can that output alone not distinguish uncertain charge from height away from the null?

▼ Derive and check the result

Let $w_a = 1 - h/\sqrt{h^2 + a^2}$ and $w_{2a} = 1 - h/\sqrt{h^2 + 4a^2}$. The disk reads $Q_d = -qw_a$; the annulus reads $Q_r = -q(w_{2a} - w_a)$. An output $S = Q_d - \gamma Q_r$ vanishes at $h = a$ if $\gamma = (1 - 1/\sqrt{2})/(1/\sqrt{2} - 1/\sqrt{5}) = 1.127$ approximately. Both readings are negative for positive q, so it is their difference, not their sum, that rejects the reference position. The ideal zero does not depend on the magnitude of any nonzero q.

Differentiate with respect to height using $w_b' = -b^2/(h^2 + b^2)^{3/2}$. At the null $a\,w_a' = -1/(2\sqrt{2})$ and $a\,w_{2a}' = -4/(5\sqrt{5})$. Hence

$$a\,d(S/q)/dh = -(1 + \gamma)aw_a' + \gamma a w_{2a}' \simeq 0.349.$$

For $q = 10$ pC, $a = 2.0$ mm, a small upward displacement of 0.10 mm produces approximately $+0.175$ pC. Finite differences of the full two-disk formula at heights on both sides of a check the linear slope. For displacements that are no longer small compared with a, use the full expression rather than extrapolating that single sensitivity.

An additional sum channel $Q_d + Q_r = -qw_{2a}$ permits a dimensionless output $S/(Q_d + Q_r)$ that cancels the magnitude and sign of q while retaining height dependence. This ratio becomes noise sensitive far from the electrodes, where collected charge is small. A null by itself can also mean that there is no charge at all, so a usable position detector checks the sum channel at the same time. The exercise combines electrostatic reciprocity, electronic weighting and a finite signal-to-noise constraint while requiring only two precomputed boundary responses.

Tutorial · predict before numerically integrating the kernel

How much charge belongs to an annular collector?

An annular electrode with inner radius h and outer radius $3h$ lies in a grounded plane. A charge q sits at height h over its centre. Derive its induced charge. If a numerical integration omits all radii beyond $3h$, where does the missing charge go?

▼ Work through the solution

Subtract two circular weights. The annulus receives $Q/q = -[1/\sqrt{2} - 1/\sqrt{10}] = -0.3909$. The central disk receives $-(1 - 1/\sqrt{2})q = -0.2929q$. The whole plane should sum to $-q$, so the part beyond the outer edge supplies

$$-q/\sqrt{10} = -0.3162q.$$

Nothing has been lost by the physical system; a finite integration patch excludes a considerable piece of the long-tailed kernel. Radial extrapolation with the analytic far tail or an expanding integration domain distinguishes missing area from poor quadrature within the patch.

Use resistance to a modelling mistake

A student proposes G itself as the weight for setting electrode voltages on the plane. Another replaces it by $2P_h$, arguing that an image doubles the response. Predict two different tests that diagnose these errors.

▼ Work through the solution

The first proposal gives zero contribution since the Dirichlet Green function is zero at the boundary. It confuses volume source response with a boundary normal derivative. The second produces twice the prescribed constant voltage because the kernel would integrate to two. Independent electrostatic

reciprocity would assign $-2q$ to the whole grounded plane around a charge q, violating the charge sum derived from the real and image fields. For a numerical test, set successively a constant, a sinusoid, and a bounded disk on the same plane. Those cases examine normalisation, spectral attenuation, and spatial tails separately.

Further reading

- Move a source between two grounded electrodes
- Compare vertical attenuation for two boundary harmonics
- Fließbach, chapter 7 · electrostatic boundary problems

Electrostatic field theory and measurement · 6. Rectangular geometries, orthogonality and sources that drive individual modes

Fourier modes are solutions selected by their electrode walls. On a rectangle they turn a boundary-voltage problem into independent vertical equations. When a charge fills the rectangle the same eigenfunctions give a different denominator and a different physical response.

Determine which sign of a separation constant can fit the walls

Take a vacuum rectangle $0 < x < a,\ 0 < y < b$, invariant along z. Ground the left, right and bottom edges and impose $V(x, b) = f(x)$ at the top. If the boundary data disagree at a corner, the continuum problem can have large edge fields; we first choose smooth f vanishing at both endpoints. In the charge-free interior, a product solution $X(x)Y(y)$ gives $X''/X = -Y''/Y$, equal to a constant wherever the product is nonzero. If $X'' = k^2 X$, the only combination of hyperbolic functions zero at both $x = 0, a$ is zero. The same is true for the linear case $k = 0$. Thus $X'' = -k^2 X$. The left boundary picks a sine and the right boundary enforces $k = n\pi/a,\ n = 1, 2, \ldots$.

Then $Y'' = k^2 Y$, with the bottom condition choosing $\sinh ky$. Choosing its top value as unity gives the transfer function $Y_n = \sinh(k_n y)/\sinh(k_n b)$. Summing products,

$$V(x, y) = \sum_{n \geq 1} f_n \sin(k_n x) \frac{\sinh(k_n y)}{\sinh(k_n b)},$$

$$f_n = \frac{2}{a} \int_0^a f(x) \sin(k_n x)\, dx.$$

These coefficients follow by multiplying the top boundary by $\sin(k_m x)$ and integrating. For $n \neq m$ the product reduces to cosines with integer half-wave multiples and integral zero; for equal indices its integral is $a/2$. This orthogonality incorporates the edge boundary values. Periodically repeating a voltage function without regard to its endpoint conditions can give cosine or constant terms that violate the grounded side walls.

Track how geometry filters electrode detail

A mode's vertical derivative is $k_n \cosh(k_n y)/\sinh(k_n b)$, so the field normal to the electrode weights high modes differently from potential. At the top the magnitude multiplier is $k_n \coth(k_n b)$. For a half-space, high-frequency field content can be large very near a patterned electrode even if it disappears rapidly a short distance inside. For large $k_n b$, direct numerical evaluation of hyperbolic sines may overflow. The algebraically equivalent ratio $e^{-k_n(b-y)}[1 - e^{-2k_n y}]/[1 - e^{-2k_n b}]$ stays bounded; for very small arguments evaluate $1 - e^{-t}$ with a numerically stable exponential-difference routine.

Suppose the rectangle is square and the electrode has $f = 4\sin(\pi x/a) - 2\sin(3\pi x/a)$ V. At mid-height $y = a/2$, the fundamental transfer factor is $1/[2\cosh(\pi/2)] = 0.1993$, while the third is

$$1/[2\cosh(3\pi/2)] = 0.00898.$$

At $x = a/2$ the first sine is 1 and the third is -1, so the potential is 0.815 V approximately, compared with the 6 V drive at the same x on the electrode. Taking the simple arithmetic average of the top and bottom voltages at that x would predict 3 V and miss leakage to the grounded side walls.

If a second boundary carries a pattern, superpose the source-free solution produced by it with the other boundaries grounded. For example a nonzero bottom voltage pattern uses $\sinh[k_n(b-y)]/\sinh(k_n b)$. This works because the field equation and boundary conditions in fixed-voltage form are linear. A floating conductor imposes a different constraint coupling many modal coefficients, not the prescription of one extra arbitrary voltage profile.

Integrate a discontinuous electrode and distinguish two kinds of convergence

Let a short strip centred on the top boundary span $a/2 - w/2 < x < a/2 + w/2$ with voltage V_d, the remaining top grounded. Integrating the sine over that interval gives

$$f_n = 4V_d \sin(n\pi/2)\sin(n\pi w/(2a))/(n\pi).$$

Even modes vanish by mirror symmetry. Individual allowed coefficients decrease as $1/n$ at most because the boundary has jumps. On the boundary partial sums overshoot close to a jump. Adding terms narrows that region rather than removing its limiting fractional overshoot. At fixed interior distance the exponential transfer renders the series much better behaved.

For $w = a/3$, the first and third coefficients are $2V_d/\pi$ and $-4V_d/(3\pi)$. Along the centreline both contribute positively because their sine factors have opposite signs. A finite-width electrode cannot be captured exactly with a single spatial mode even when its interior signal far away is mainly fundamental. Recovering the electrode width from a distant scan by dividing attenuated high modes by their transfer factors will amplify measurement errors. Forward propagation and inverse reconstruction need different treatments of frequency content.

Let the volume rather than the electrode excite the modes

Ground all four edges and embed a known charge density $\rho(x, y)$. Choose double sines $\sin(m\pi x/a)\sin(n\pi y/b)$. They already vanish on all edges and are eigenfunctions of the negative Laplacian with eigenvalues $\lambda_{mn} = (m\pi/a)^2 + (n\pi/b)^2$. Project the charge using $\rho_{mn} = 4(ab)^{-1}\int_0^a \int_0^b \rho \sin(m\pi x/a)\sin(n\pi y/b)\,dy\,dx$. Applying Poisson's equation coefficient by coefficient yields

$$V_{mn} = \frac{\rho_{mn}}{\epsilon_0 \lambda_{mn}}.$$

High spatial frequencies of a volume charge produce weaker potentials by an inverse-square spectral factor. The corresponding normal field on a boundary involves an additional derivative. This polynomial filtering differs from the exponential decay of a boundary pattern measured away from its source. Both follow from the same PDE but answer different experiments.

For a manufactured test choose a square of side 10 mm with $\rho = \rho_0 \sin(\pi x/a)\sin(2\pi y/a)$. The voltage magnitude peaks at $\rho_0 a^2/(5\pi^2\epsilon_0)$. With $\rho_0 = 1.0\ \mu\mathrm{C/m^3}$ it is 0.229 V. The total charge integrates to zero, since the second sine is odd about the mid-height. The field and stored energy are nonzero. At $x = a/2, y = a/4$ the voltage is a positive maximum, consistent with a positive local source. At $x = a/2, y = 3a/4$ the same amplitude is negative.

Use an exact discrete eigenvalue for a rigorous code check

On a uniform square grid of spacing $h = a/N$, replace $-\partial_x^2$ by its centred three-point formula. Acting on the sampled sine gives eigenvalue $4h^{-2}\sin^2(m\pi h/(2a))$. The two-dimensional sum of the corresponding factors is therefore the exact discrete eigenvalue for this interior mode with zero edges. A computed solution can be compared first to $\rho_{mn}/(\epsilon_0\lambda_{mn,h})$, which tests the solver algebra, and then to the continuous $\rho_{mn}/(\epsilon_0\lambda_{mn})$, which tests spatial discretisation. Reducing the iterative residual alone cannot remove the difference between these two physical amplitudes.

At $N = 10$, modes $(1, 2)$ have $a^2\lambda_h = 4N^2[\sin^2(\pi/20) + \sin^2(\pi/10)] = 47.99$, versus $5\pi^2 = 49.35$. The discrete amplitude is about 2.8% high despite solving its linear equations exactly. For fixed mode under grid halving, expansion of the sine gives an eigenvalue error proportional to h^2. At wavelengths only a few cells wide this expansion is unreliable. Try a sequence of grids with the same physical mode and compare actual amplitude ratios. Holding instead a fixed number of cells per wavelength while changing the physical wavelength tests a different convergence question.

Two transverse dimensions select a different attenuation length

Extend the rectangle into a rectangular conducting shaft $0 < x < a,\ 0 < z < c$, running to $y > 0$. Ground all four side walls, require bounded potential far down the shaft and prescribe a voltage on its mouth at $y = 0$. Separation in the cross section now gives products $\sin(m\pi x/a)\sin(n\pi z/c)$ with both $m, n \geq 1$. The axial equation is

$$Y'' = [(m\pi/a)^2 + (n\pi/c)^2]Y.$$

Each boundary coefficient therefore propagates as $e^{-\gamma_{mn}y}$,

$$\gamma_{mn} = \pi\sqrt{m^2/a^2 + n^2/c^2}.$$

A narrow second dimension suppresses penetration even when the first dimension is very broad. Approximating the shaft by a two-dimensional strip removes an entire contribution to the decay constant.

If the aperture is driven uniformly at V_0, projecting gives $f_{mn} = 16V_0/(\pi^2 mn)$ for odd m, n, zero otherwise. The ideal mouth voltage jumps at the grounded rim. Deep inside, only the lowest odd pair survives and its amplitude exceeds V_0 before the exponential is applied; the higher terms restore the actual boundary value at $y = 0$. With $a = 20$ mm and $c = 10$ mm the slowest decay length is

$$1/\gamma_{11} = 2.85\,\mathrm{mm}.$$

A two-dimensional strip ignoring the 10 mm side would instead give

$$a/\pi = 6.37\,\mathrm{mm}.$$

After 10 mm penetration the first-mode attenuation factors are 0.0298 and 0.208, almost a factor of seven apart.

A simple numerical test samples the centreline voltage at several heights and calculates adjacent log slopes. Close to the mouth many odd modes matter, while deep inside the ratio between two positions Δy apart approaches $e^{-\gamma_{11}\Delta y}$. Compare with a second geometry that swaps a, c. The two lowest-order decay lengths must agree because the eigenvalue is symmetric in the two dimensions; an implementation that uses only the nominal 'width' may fail this check. A second observation path away from the centre can sense different mode weights, even though every mode's exponential is unchanged.

Suppose the mouth instead has opposite voltages on the left and right halves, antisymmetric about $x = a/2$. Its coefficients vanish for odd m, so the $(1, 1)$ mode is absent by symmetry. The leading allowed mode can be $(2, 1)$, shortening the decay length. A centreline probe would then read zero everywhere by antisymmetry and could not fit any length at all. Move the probe to $x = a/4$ while keeping it at mid-height of the cross section. This illustrates how an excited spectrum, a geometry's complete set of eigenvalues, and an instrument's observed spectrum may differ.

Why the energy of an ideal electrode voltage step depends on edge resolution

Return to a two-dimensional strip or half-plane. To focus on a single boundary Fourier mode take $V = A\sin(kx)e^{-ky}$ in $0 < x < a,\ y > 0$, with $ka = n\pi$. Its gradients in x and y have equal prefactor kAe^{-ky}. The sum of their squared sine and cosine factors is one, so the energy per perpendicular length is

$$U_n' = \epsilon a k A^2/4.$$

For many orthogonal sine modes cross terms vanish after integration. Thus the stored field energy involves the weighted sum $\sum_n n|f_n|^2$, while the mean-square boundary voltage itself involves simply $\sum_n |f_n|^2$. The extra factor of n comes from the steep near-electrode field of short-wavelength structure.

For a finite electrode patch abruptly stepping from 0 to V_d, the allowed Fourier amplitudes typically decay as $1/n$ along nonzero subsequences. The voltage series converges in mean square, but its energy sum can contain a logarithmically diverging $\sum 1/n$. This is the local singularity of the zero-width voltage discontinuity. It does not prevent a well-defined voltage at any interior distance, but it prevents assigning a finite total energy or a cut-off-independent peak electric field to that exact sharp-edge idealisation. Mesh refinement can produce progressively higher energy estimates even as interior voltage curves appear perfectly stable.

There is a local way to see the same conclusion without a Fourier series. Consider a small half-disk of vacuum around a junction where an otherwise flat boundary jumps between voltages zero and V_d. In polar coordinates about the junction, the leading harmonic solution depends only on angle: $V = V_d\phi/\pi$ with

angle origin chosen on the grounded side. Its field magnitude is $V_d/(\pi r)$. Integrating $\epsilon E^2/2$ over a half-annulus of inner radius δ and outer radius R gives

$$U' = \epsilon V_d^2 \ln(R/\delta)/(2\pi).$$

Halving the microscopic length changes this single-edge contribution by $\epsilon V_d^2 \ln 2/(2\pi)$. The independence of R in that change is a practical test of the logarithmic asymptotic regime.

A finite insulation seam between real electrodes supplies a different boundary problem. For a deliberately smoothed transition of width δ, the spectrum falls faster above $k \sim 1/\delta$; the local singularity is cut off. One can compare a family of specified physical seam widths while separately refining each numerical grid until it resolves its own seam. Shrinking seam width along with mesh spacing instead changes the physical geometry at each refinement. Report the interior voltage, near-edge energy within a named observation region and the physical seam model separately. Each can converge at a different rate even in a technically correct Laplace solver.

A discrete residual can fall quickly while the wrong spatial scale remains

The separated sine basis makes it possible to analyse the convergence of a concrete numerical Laplace solver as well as the continuum solution. On a square grid with equal spacing, the five-point discretisation in a charge-free cell says its voltage equals the mean of its four neighbours. A Jacobi sweep sets all new values to this mean of the old grid, preserving fixed boundary values meanwhile. Subtract the exact discrete solution from the current approximation: the error evolves by the same averaging step with zero boundary values, independently of the inhomogeneous source that generated the original solution.

Insert an error pattern $e_{ij} = \sin(m\pi i/N)\sin(n\pi j/N)$. Elementary sine addition on the two x-neighbours produces $2\cos(m\pi/N)e_{ij}$; the y-neighbours produce the analogous factor. Hence one sweep multiplies this error mode by $\mu_{mn} = [\cos(m\pi/N) + \cos(n\pi/N)]/2$. For the longest $(1,1)$ mode, $\mu \simeq 1 - \pi^2/(2N^2)$. Its amplitude takes roughly $2N^2/\pi^2$ sweeps to drop by $1/e$. Doubling resolution therefore makes this relaxation about four times slower per physical longest mode even before counting the four times as many cells per sweep.

Choose $N = 64$. Then $\mu_{11} = 0.99880$. After 100 sweeps about 88.6% of that initial smooth error still remains, although the update per cell has become small. At the opposite corner of the spectrum $(N-1, N-1)$ gives nearly -1, so a checkerboard mode also decays slowly while changing sign on successive sweeps. Weighted Jacobi replaces an old value by $(1-\omega)$ times itself plus ω times the neighbour mean. At $\omega = 2/3$ that checkerboard amplification becomes approximately $-1/3$, removing short-wavelength oscillations quickly. The long smooth mode still has amplification near one. An attractive smooth colour map after a few sweeps can thus be misleading.

A multigrid correction exploits these distinct errors. First relax high-frequency errors on the fine grid. Compute the residual of the original discrete equation and restrict it to a coarser grid. A long fine-grid mode becomes easier to change there. Solve the coarse error equation, prolong its correction back to the fine grid, and smooth again. The correction must solve for error with the appropriate homogeneous boundary constraints, not repeat the original boundary excitation a second time. The residual and

prolongation should respect the same physical units and grid volumes as the original source. Otherwise a visually plausible coarse correction can inject net charge at each level.

For a manufactured check initialise the fine-grid error to a known sine mode on top of an exact discrete solution. After one weighted sweep measure the inner product of the new error with the original mode and divide by its squared norm. The observed ratio must equal $1 - \omega + \omega\mu_{mn}$ before roundoff or boundary effects. Repeat with $(1, 1)$, a mixed $(1, N-1)$ mode, and the checkerboard-like $(N-1, N-1)$ mode. This directly tests the implementation's indexing, old-versus-new updates and boundary handling; it does not require the continuum equation to be discretisation exact.

Finally compare iterative and truncation errors in measurable volts. For a discrete mode, if the algebraic residual coefficient is r_{mn} in the form $-\nabla_h^2 e = r$, its error coefficient is $r_{mn}/\lambda_{mn,h}$. The same residual amplitude in a long-wavelength mode produces a larger voltage error than in a high-frequency mode. An absolute solver tolerance with no physical scaling is therefore insufficient to certify a voltage reading. Stop iterating when the solver error in the actual observable is small compared with discretisation and experimental uncertainty, then refine the spatial representation separately.

Resolve a short-wavelength electrode pattern

Increase the transverse mode number. Predict how far the pattern reaches into the strip before inspecting the voltage profile.

Open this experiment online

Try the calculation

Height y/a **0.18**

Third harmonic at the boundary (V) **3**

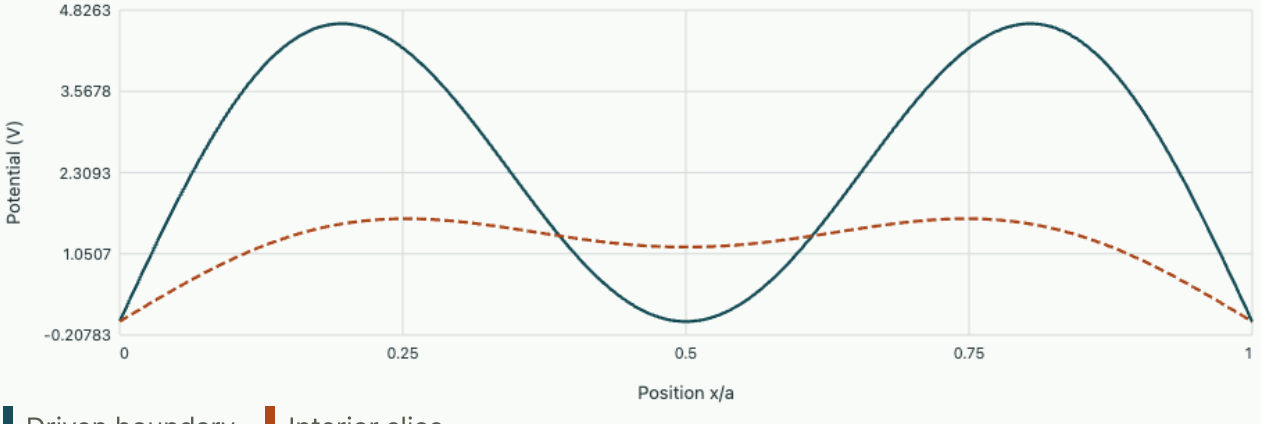

At the middle of the strip the potential is 1.15 V. The third harmonic retains 18.3% of its boundary amplitude.

Build a resistor-network analogue of the rectangular boundary problem

Use Kirchhoff measurements to check a field solver

A square lattice of nodes is connected by identical resistors R between nearest neighbours. Outer nodes are held at prescribed voltages. Derive the interior equation from charge conservation at a node. Which measured electrical quantity can test a normal field at the boundary? What changes on an anisotropic grid?

▼ **Derive and check the result**

For a steady interior node with no supplied current, the sum of currents $(V_{ij} - V_{\text{neighbour}})/R$ is zero. Rearrangement gives the same mean-of-four equation as the square-grid discrete Laplacian. Thus the resistor array reproduces the *discrete* Dirichlet solution for the same pinned boundary voltages. Its Joule dissipation $\sum_{\text{edges}} (V_i - V_j)^2/R$ is stationary against variations of the unfixed voltages, giving the same equations a second way. The numerical voltage maps can be compared node by node; the physical power and the electrostatic field energy are different dimensional quantities even though their quadratic forms are analogous.

To estimate the normal field near a flat boundary, measure the signed current from a boundary node along the edge connecting it to its nearest interior neighbour. This equals the observed voltage difference divided by R; multiplying by R/h converts it to the corresponding one-sided field magnitude in volts per metre. At sharp corners the one-sided difference has large discretisation error and the continuum physical field may be singular. Summing all currents supplied to a terminal edge gives a more robust integrated flux analogue. Account for any links between nodes at different prescribed boundary voltages if those links contribute separate current to the laboratory power supplies.

For horizontal spacing h_x and vertical spacing h_y, replacing every resistor by the same value no longer matches the isotropic Cartesian Laplacian. A finite-volume cell requires conductance proportional to face length divided by edge length: horizontal links have conductance proportional to h_y/h_x, vertical links to h_x/h_y. Their ratio is h_y^2/h_x^2. This restores a discrete conservation law with the correct physical area factors. A measured profile agreeing exactly with an equal-resistor lattice on a stretched geometry could therefore validate the wrong continuum material or geometry unless those weights were checked first.

Tutorial · design a boundary measurement and a solver benchmark

Identify a forbidden mode

A symmetric positive top electrode has its centre at $x = a/2$. A numerical sine transform reports a large $n = 2$ coefficient. Is it evidence of physical high-frequency content? Which controlled change could verify the sign of the defect?

▼ **Work through the solution**

Mirror substitution $x \mapsto a - x$ preserves the boundary voltage but changes $\sin(2\pi x/a)$ to its negative. Its exact projection is zero. Sharp electrode edges may require many odd modes; they cannot explain an even coefficient under exact symmetry. Check coordinate origin, edge alignment on the grid and measurement offsets. Shift the actual patterned patch by a small amount to one side, then the same amount to the opposite side. A genuine even coefficient changes sign under these mirrored displacements, while odd-mode amplitudes agree. The response at interior height has the same parity because the transfer factor depends on mode number alone.

Measure where electrode charge resides

For a single sinusoidal top voltage $V_d \sin(\pi x/a)$, derive the total free charge per perpendicular length on the upper electrode face. Why does it depend on the bottom distance even though the top voltage profile is the same?

▼ **Work through the solution**

At the upper metal the normal from metal into the dielectric is $-\hat{\mathbf{y}}$. With $E_y = -\partial_y V$, the metal charge density is

$$+\epsilon_0 \partial_y V = \epsilon_0 k V_d \coth(kb) \sin(kx),$$

$$k = \pi/a.$$

Integrating along $0 < x < a$ yields $2\epsilon_0 V_d \coth(\pi b/a)$ per length. Bringing the bottom closer increases $\coth(kb)$. For $kb \ll 1$ the expression tends to $\epsilon_0 b^{-1} \int_0^a f(x)dx$, the local parallel-plate limit. A segmented electrode supplies a nonuniform fixed profile; the result counts its integrated face charge and assumes the ideal voltage boundary remains prescribed in each segment.

Further reading

- Move the measurement plane above a patterned electrode
- Evaluate a grounded-enclosure boundary problem
- Griffiths, 5th ed., §3.3.1 · Cartesian separation

Electrostatic field theory and measurement · 7. Cylindrical geometry, coaxial boundaries and Bessel spectra

The radial coordinate of a cylinder leads to logarithms in one experiment and to Bessel functions in another. The difference is set by the variation along the axis and around the circumference. Recovering the radial weight from flux clarifies both.

A conducting annulus selects a logarithmic radial potential

Put a long cylindrical metal electrode of radius a inside a coaxial grounded tube of radius b, with homogeneous dielectric of permittivity ϵ in the gap. Long means that probes are far enough from both ends for axial variation to be negligible. With no free gap charge and no angular variation, Laplace's equation reduces to $\partial_r(r\partial_r V) = 0$. One integration gives $rV' = C$, a statement of conserved radial flux through cylinders; the second gives a logarithm. With inner electrode at V_0,

$$V(r) = V_0 \frac{\ln(b/r)}{\ln(b/a)},$$

$$E_r = \frac{V_0}{r \ln(b/a)},$$

$$C' = \frac{2\pi\epsilon}{\ln(b/a)}.$$

Here C' is capacitance per length. To obtain it, integrate D_r over the inner metal face per unit axial length and divide by V_0. Another route integrates the energy density $\epsilon E_r^2/2$ times $2\pi r\, dr$, giving $C'V_0^2/2$. For $a = 2$ mm, $b = 8$ mm and $\epsilon = 2\epsilon_0$, $C' = 80.3$ pF/m. At $r = \sqrt{ab} = 4$ mm the voltage is $V_0/2$; the half-voltage radius is the geometric mean. An equally spaced radial ruler does not sample equal voltage steps.

The logarithm is not allowed at the axis of a solid charge-free cylinder because it diverges and carries line-source flux. In the annular domain the singular axis is outside the field region. The same radial function can therefore be admissible or inadmissible in two problems with very similar geometry. Before discarding a mathematical solution, check which radii actually lie in the domain and whether singular sources were explicitly prescribed.

Nonuniform wall voltages in a two-dimensional disk

Next take a full disk of radius a with prescribed side voltage $f(\phi)$, invariant in z. Seek $R(r)e^{im\phi}$. Single-valuedness after $\phi \to \phi + 2\pi$ forces integer m. The radial equation $r^2R'' + rR' - m^2R = 0$ is solved by $r^{|m|}$ and $r^{-|m|}$ for $m \neq 0$; regularity at the centre chooses the growing power. The zero mode is constant, discarding its logarithmic partner. Thus an angular Fourier component on the wall penetrates as $(r/a)^{|m|}$. At $r = a/2$, a third harmonic retains one eighth while a sixth harmonic retains only one sixty-fourth. Both can coexist on the wall without being equally visible in the interior.

For $f(\phi) = 2 + 3\cos(2\phi)$ V, the interior is

$$2 + 3(r/a)^2 \cos(2\phi) = 2 + 3(x^2 - y^2)/a^2.$$

The potential has a saddle at the centre, with zero field there and opposite Cartesian curvatures. A scan along a single diameter could show a conspicuous maximum without detecting any charge. The two-dimensional Laplacian is zero because the curvatures cancel. This is also a useful finite-difference benchmark: a centred Cartesian Laplacian differentiates this quadratic exactly in the interior when the circular boundary has been represented correctly.

End effects produce a Sturm–Liouville problem

Now ground the side of a circular tube, excite its end at $z = 0$ and look for fields decaying into $z > 0$. For an axisymmetric source-free potential $V = R(r)Z(z)$, choose $Z = e^{-kz}$ for decay. Laplace's equation becomes

$$(rR')' + k^2 rR = 0.$$

The solutions are $J_0(kr)$ and $Y_0(kr)$. The former is regular with value one at zero; the latter diverges logarithmically. Grounding at $r = a$ requires $J_0(ka) = 0$, so $k_n = j_n/a$ with positive roots $j_1 = 2.40483,\ j_2 = 5.52008, \ldots$. Unlike sine wavenumbers they are not evenly spaced at low index.

Multiplying two such eigen-equations by the opposite radial function, subtracting and integrating gives $(k_m^2 - k_n^2)\int rR_m R_n\, dr$ equal to the endpoint term $r(R_n' R_m - R_m' R_n)$. It vanishes at a grounded wall and at a smooth axis. Hence modes at distinct eigenvalues are orthogonal with weight r. This weight arises physically from the circumference of a radial ring. Normalize dimensionless radius $x = r/a$. For a zero j_n, the squared modal norm is $J_1(j_n)^2/2$. An end profile $f(x)$ therefore gives

$$V(r,z) = \sum_n c_n J_0(j_n r/a) e^{-j_n z/a},$$

$$c_n = \frac{2}{J_1(j_n)^2}\int_0^1 x f(x) J_0(j_n x)\, dx.$$

For $f = V_0$ across the cap, $\int_0^1 xJ_0(jx)dx = J_1(j)/j$ by differentiating $xJ_1(jx)$. Then $c_n = 2V_0/[j_n J_1(j_n)]$, with alternating signs. The cap voltage jumps at the wall corner, making its near-rim reconstruction slow. A smooth end pattern that already vanishes at a yields faster coefficient decay. In either case a narrow radial strip at the axis should not be given as much integration weight as an equal width near the circumference.

Two ways to see which axial scale survives

Far enough from the cap the first excited nonzero coefficient dominates. Its length is

$$a/j_1 = 0.416a.$$

Ratios of distant on-axis voltages can then identify tube radius without absolute calibration of the cap voltage. For $a = 15.0$ mm, an added 5.0 mm of distance should give factor $e^{-2.40483/3} = 0.449$. Repeat this estimate at several starting positions. The ratio only approaches that value once competing modes

have decayed. A datum deep enough to suppress all higher modes may also be close to the instrument noise level, which biases a fitted decay length.

Instead impose an axial sinusoid e^{ikz} on a very long cylinder's side wall. The radial equation now has the opposite sign, $(rR')' - k^2 rR = 0$, whose regular solution is the modified Bessel function $I_0(kr)$. The potential is $V_0 I_0(kr)\cos(kz)/I_0(ka)$. The experiment selects a real oscillation along z, not an exponential attenuation away from an end. Near the axis $I_0(\xi) = 1 + \xi^2/4 + \cdots$; the field generated by a long-wavelength side modulation is nearly uniform across a narrow cross section. At large ka, $I_0(ka)$ grows exponentially and the axis scarcely senses a short-wavelength wall pattern. Calling every radial solution simply a Bessel mode without tracking the separation sign can exchange these two physical predictions.

Construct a grid that treats the axis as a regular point

A conservative radial discretisation starts from $\int_{r_-}^{r_+} r\,\nabla_r^2 V\,dr = [rV']_{r_-}^{r_+}$. Use annular cells and fluxes at shared ring faces. Near $r = 0$ the left face has zero circumference, requiring no unknown point beyond the axis. For a nodal grid with Taylor expansion $V(r) = V(0) + Ar^2 + O(r^4)$, the radial operator at zero is $4A$, so $\nabla_r^2 V(0) \simeq 4[V(h) - V(0)]/h^2$. Simply setting $1/r = 0$ and using the Cartesian one-dimensional second derivative misses a factor of two.

Compare a numerical response to the analytic J_0 mode at a fixed z/a. Test the wall value, axis derivative, radial energy norm and distant decay rate. These are independent observables. A discretisation can reproduce the slowest length while misrepresenting an edge profile composed of many faster modes. Conversely, matching a discontinuous cap perfectly at mesh nodes does not demonstrate that high-order interior amplitudes are accurate.

Can a coaxial dielectric be graded to produce a uniform field?

The homogeneous coaxial field grows as $1/r$ and reaches its highest magnitude at the inner wire. A designer proposes grading the dielectric radially so the full annular gap experiences one common radial field. Assume both metal faces are equipotentials, the scalar permittivity $\epsilon(r)$ may vary continuously, and there is no free volume charge. Cylindrical symmetry still gives $D_r = \lambda/(2\pi r)$, independent of how the material is graded. A constant electric-field magnitude E_g requires $\epsilon(r) = \lambda/(2\pi E_g r)$, that is, permittivity proportional to $1/r$. This construction replaces a uniform material by a known spatial distribution; applying $\epsilon(r)\nabla^2 V = 0$ would miss the material gradient and give the wrong field.

Write $\epsilon(r) = \epsilon_a a/r$. At applied voltage V_0, the constant field is $E_g = V_0/(b - a)$, and charge per length is

$$\lambda = 2\pi\epsilon_a a V_0/(b - a).$$

Thus $C' = 2\pi\epsilon_a a/(b - a)$. For $a = 2.0$ mm, $b = 6.0$ mm, $\epsilon_a = 6\epsilon_0$, the outer relative permittivity is 2, and $C' = 167$ pF/m. At 12 V every radius experiences 3000 V/m. For a homogeneous dielectric at the same voltage the inner surface field would be $12/[0.002\ln 3] = 5461$ V/m regardless of its constant

permittivity. The gradient reduces peak field at fixed voltage. Whether a real material benefits also depends on its local field limit, losses and interfaces.

Where is the polarisation charge that makes this possible? In the dielectric the true total charge satisfies

$$\rho_{\mathrm{tot}} = \epsilon_0 \nabla \cdot \mathbf{E} = \epsilon_0 E_g / r.$$

All of it is bound since $\rho_f = 0$. Direct evaluation from $\mathbf{P} = (\epsilon(r) - \epsilon_0) E_g \hat{\mathbf{r}}$ gives $-r^{-1}\partial_r(rP_r) = +\epsilon_0 E_g / r$, the same result. Material surfaces add bound charges $P_r(b)$ on the outer radial face and $-P_r(a)$ on the inner face. Integrating their surface contributions and the volume charge over a full annulus returns zero net bound charge, as required for a polarised neutral body. A constant radial electric magnitude can therefore coexist with zero free charge and nonzero total charge.

A manufactured graded material is often approximated by concentric homogeneous shells. For shell j from r_j to r_{j+1}, its voltage drop at fixed λ is $\lambda \ln(r_{j+1}/r_j)/(2\pi\epsilon_j)$. To reproduce the exact voltage drop of the continuously graded design over each shell, choose $\epsilon_j = \epsilon_a a \ln(r_{j+1}/r_j)/(r_{j+1} - r_j)$. This matches electrode capacitance even with relatively few shells. Yet the field inside each discrete shell still falls as $1/r$ and jumps at its interfaces. Matching terminal capacitance alone does not verify the target uniform-field profile. Compute the field just inside each shell edge and refine the radial layering against a local peak-field tolerance.

What a small displacement of the end electrode excites

An axisymmetric tube calculation retains only angular order $m = 0$. Now impose at the tube entrance a voltage profile proportional to $r\cos\phi$ near the axis and taper it to zero at the wall. This is a dipolar lateral pattern with positive voltage on one side and negative on the other. Separating $R(r)\cos(m\phi)e^{-kz}$ into Laplace's equation yields

$$(rR')' + \left(k^2 r - \frac{m^2}{r}\right) R = 0.$$

The regular solutions are $J_m(kr)$. Near the axis their leading powers are $r^{|m|}$, so an $m = 1$ potential vanishes on the centreline while its transverse gradient generally does not. The grounded wall selects zeros of J_m. The first zero of J_1 is 3.83171, larger than the first axisymmetric zero, so the slowest lateral disturbance decays faster than the slowest axisymmetric voltage. Probe design therefore changes which decay laws are experimentally accessible.

For a cap shaped exactly as $f = V_1 J_1(jr/a)\cos\phi$, $j = 3.83171$, the whole solution is a single mode. Near the axis $J_1(jr/a) \simeq jr/(2a)$; using $r\cos\phi = x$,

$$V \simeq V_1 j x e^{-jz/a}/(2a).$$

Hence $E_x(0, z) = -V_1 j e^{-jz/a}/(2a)$. With $V_1 = 2.0$ V and $a = 10$ mm, the lateral field starts at 383 V/m and falls to 8.30 V/m after an axial distance equal to one radius. A centreline voltmeter sees zero at both positions and gives no hint of the finite transverse force. A pair of voltmeters at small opposite x or a field probe oriented along x measures the relevant derivative.

For a realistic shifted electrode the input can contain both $m = 0$ and $m = 1$. Place detectors at $(r, 0, z)$ and (r, π, z). Their average selects even azimuthal orders; their difference selects odd ones. The ratio of the difference at two heights tests $m = 1$ decay after higher odd modes subside. The average also includes $m = 2, 4, \ldots$, so attributing it to $m = 0$ requires symmetry information or more angular sensors. Reversing the applied electrode displacement changes the sign of an odd response but leaves even corrections unchanged to leading order. This experiment links angular Fourier selection and radial eigenvalues to a measurable alignment tolerance without requiring an entire three-dimensional voltage map.

Project a ring source without calling an axis cell a point detector

Deposit a thin circular ring of total free charge q at radius s in the plane $z = z_0$ inside a long grounded cylindrical tube. Its volume density in an axisymmetric model is $q\,\delta(r - s)\delta(z - z_0)/(2\pi s)$, for $s > 0$. The $2\pi s$ removes the circumference introduced by the volume element. A radial code that deposits q directly as a density in one mesh bin, without dividing by annular volume, changes the total charge each time the radius or mesh spacing changes. In this calculation one can track that normalisation all the way to a voltage coefficient.

Take the tube infinite in both axial directions for simplicity. Expand $V = \sum_n v_n(z) J_0(j_n r/a)$ in the grounded radial eigenfunctions. Project Poisson's equation using weight $r\,dr$ and the norm $a^2 J_1(j_n)^2/2$. The ring produces

$$[-d_z^2 + (j_n/a)^2] v_n = \frac{q J_0(j_n s/a)}{\pi \epsilon a^2 J_1(j_n)^2}\,\delta(z - z_0).$$

The infinite-line Green response for $-d_z^2 + k^2$ is $e^{-k|z-z_0|}/(2k)$, as can be checked by integrating its derivative across z_0. Thus each modal voltage has a finite amplitude and two decaying tails, and the complete field is obtained by summing radial modes. At a detector separated axially from the ring the exponential factors ensure rapid convergence. Exactly on the mathematical ring the local potential diverges logarithmically like that of a thin filament; comparing finite-element peak voltages there requires a finite wire cross section or a specified detector average.

An unexpected and testable consequence concerns the source radius. The coupling to mode n is proportional to $J_0(j_n s/a)$. It becomes exactly zero when the source sits on a radial node of that mode. The second mode has an interior node at $s/a = j_1/j_2 \simeq 0.4357$. A ring there still carries charge and excites many other modes but contributes no second modal coefficient. As an experimental analogy, a weighting potential that changes sign across part of a sensor can receive cancelling contributions from an extended excitation. Here the cancellation is encoded exactly in orthogonality and the pointwise coupling value.

A check independent of the ring-charge normalisation uses reciprocity. Imagine two narrow coaxial source/detector rings of radii s, r, each with the same definition of total charge and voltage measured around its circumference. The modal response contains the symmetric product $J_0(j_n s/a) J_0(j_n r/a)$ multiplied by a factor that depends only on axial separation. Swapping radius and axial position therefore leaves voltage per total charge unchanged. If a numerical table instead looks symmetric per charge

density but not per total ring charge, check whether the radius-dependent integration weights were applied on both deposition and sampling.

Another useful test fixes total deposited charge but reduces a resolved annular thickness around s. First compare with an integral of the analytic ring solution across the same finite distribution. Then take the thin-ring limit at a detector away from the deposition region. Taking grid thickness and source thickness to zero together while comparing a self-voltage at the source conflates numerical refinement with a mathematically singular observable. Stating detector location, normalisation and order of limits turns a superficially straightforward ring source into a robust benchmark for cylindrical Poisson solvers.

Measure a radial cylindrical mode

Change the electrode mode and compare radial nodes with axial decay. A cylindrical boundary chooses a different eigenbasis from a rectangular one.

Open this experiment online

Try the calculation

Height z/a **0.25**

Retained modes **3**

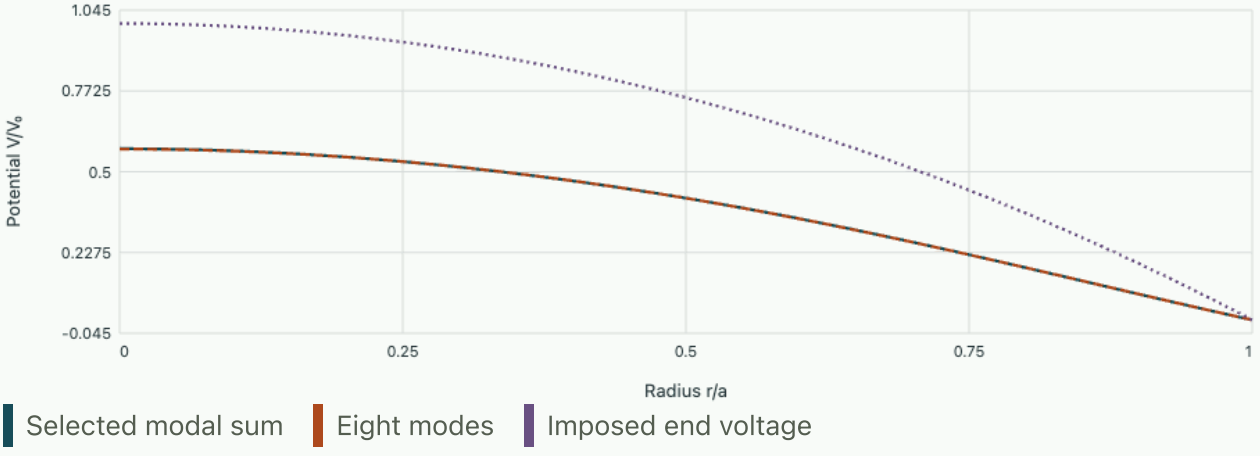

The on-axis potential is 0.5774 V_0 with the selected modes, versus 0.5765 V_0 using eight. The slowest mode has e-folding length 0.4158 a.

A cylindrical interface can carry induced bound charge with an entirely radial field

Separate the two charges detected at a coaxial material boundary

A long coaxial gap contains two homogeneous radial layers with interface at s, no free sheet there and fixed inner line charge $+\lambda$. Find the bound interface charge per length, verify it from the field jump, and determine the interface radius at which the layers take equal voltages. Evaluate the result for $a = 2$ mm, $b = 18$ mm and relative permittivities 2 and 4.

▼ **Derive and check the result**

For both regions $D_r = \lambda/(2\pi r)$. In material i the polarisation is $P_i = D_r(1 - \epsilon_0/\epsilon_i)$ along the radial direction. At the interface the outer face of material 1 has bound density $+P_1$, the inner face of material 2 has $-P_2$. Their sum times the circumference gives bound line charge $\lambda_b = \lambda(\epsilon_0/\epsilon_2 - \epsilon_0/\epsilon_1)$. It equals $-\lambda/4$ for the given ordering; the value per length is independent of s because the $1/s$ field cancels the interface circumference. A local density meter would see a different value at a different radius even though the integrated result stays the same.

Direct use of Gauss's law for the true electric field gives $\epsilon_0\, 2\pi s(E_{2r} - E_{1r}) = \lambda[\epsilon_0/\epsilon_2 - \epsilon_0/\epsilon_1]$, confirming the sign and magnitude. A check with displacement alone gives zero jump and thus correctly reports no *free* charge at that same surface. The two field laws answer different questions. Extending the shell calculation to include both exterior material faces returns zero total bound charge per material, so the internal negative interface charge never represents a net creation of charge.

The voltage drops are proportional to $\ln(s/a)/\epsilon_1$ and $\ln(b/s)/\epsilon_2$. Equality gives $s^{\epsilon_1+\epsilon_2} = a^{\epsilon_2} b^{\epsilon_1}$, or $s = a(b/a)^{\epsilon_1/(\epsilon_1+\epsilon_2)}$, a dimensionally transparent form. Numerically $s = 2(9)^{1/3} = 4.16$ mm. A half-voltage location at 4.16 mm is far from the arithmetic centre of this gap. It is also distinct from the 6.0 mm geometric mean for a homogeneous annulus, because the inner lower-permittivity layer needs less geometric thickness to take the same voltage.

Tutorial · radial modes with different physical boundaries

Replace the grounded wall by a reflecting boundary

A long tube has $\partial_r V = 0$ on its side instead of $V = 0$, and its end voltage profile is nonuniform. What happens to the radial eigenvalues and to the assertion that every end disturbance dies away?

▼ **Work through the solution**

The wall now requires

$$J_0'(ka) = -J_1(ka) = 0.$$

In addition a constant radial mode with $k = 0$ satisfies both side and axis conditions. Its axial equation is $Z'' = 0$, so boundedness allows a constant component. The end profile's weighted cross-sectional mean supplies that persistent offset. Only the components orthogonal to the constant decay. Requiring the potential to tend to zero at infinity while prescribing a nonzero mean cap voltage would be incompatible for this insulated side model unless other boundaries or sources are introduced.

Infer a radial charge density from a coaxial reading

Suppose the measured potential in a coaxial gap is $V = A\ln(b/r) + B(b^2 - r^2)$ with constant permittivity. Determine the volume charge and the signs of its contribution to the two face fluxes. Which part can be changed by externally altering the applied voltage at fixed charge density?

▼ **Work through the solution**

The logarithmic term is harmonic away from the excluded axis. For the quadratic term $\nabla_r^2[-Br^2] = -4B$, giving uniform $\rho = 4\epsilon B$. The radial field is $A/r + 2Br$. The net outward displacement flux through the gap per length is $2\pi\epsilon[bE(b) - aE(a)] = 4\pi\epsilon B(b^2 - a^2)$, exactly $\rho\pi(b^2 - a^2)$. At positive B the quadratic term contributes positive outer flux and negative inward-face flux, with the larger outer contribution from both area and field. Changing only the source-free boundary excitation adds a logarithmic term and, if the reference permits it, a constant. It alters both field readings without altering the inferred uniform volume density.

Further reading

- Reconstruct a radial electrode profile with one to eight Bessel modes
- Fließbach, chapter 10 · cylindrical problems

Electrostatic field theory and measurement · 8. Normalised spherical harmonics and the field of an arbitrary three-dimensional source

An axial voltage scan can determine Legendre coefficients only if the source is rotationally symmetric. A general spherical electrode or molecule needs angular modes with two indices. Their normalisation fixes the conversion from a measured multipole coefficient to a physical voltage.

Separate three coordinates without imposing axial symmetry

In spherical coordinates the source-free Laplace equation is $r^{-2}\partial_r(r^2\partial_r V) + r^{-2}\Delta_\Omega V = 0$, where $\Delta_\Omega = (\sin\theta)^{-1}\partial_\theta(\sin\theta\,\partial_\theta) + (\sin^2\theta)^{-1}\partial_\phi^2$. Assume $V = R(r)Y(\theta,\phi)$. Separation requires

$$-\Delta_\Omega Y = \lambda Y.$$

Multiply by Y^* and integrate over the unit sphere. Integration by parts has no actual surface boundary for globally smooth fields and gives

$$\lambda \int |Y|^2 d\Omega = \int |\nabla_\Omega Y|^2 d\Omega \geq 0.$$

The constant mode has eigenvalue zero.

Separate azimuth as $e^{im\phi}$. Continuity after a full rotation forces integer m. With $u = \cos\theta$, the remaining equation becomes

$$[(1-u^2)P']' + [\lambda - m^2/(1-u^2)]P = 0.$$

Requiring regular behaviour at both poles yields $\lambda = \ell(\ell+1)$ with integers $\ell \geq |m|$. The corresponding angular functions are the associated Legendre functions. For each ℓ there are $2\ell+1$ independent m's, all with identical radial behaviour. A rotation mixes coefficients within this subspace but cannot convert a dipole into a quadrupole.

Fix one convention and verify its first modes

Choose $P_\ell(1) = 1$ and for $m \geq 0$ include the Condon–Shortley phase in $P_\ell^m(u) = (-1)^m(1-u^2)^{m/2}d^m P_\ell/du^m$. Define

$$Y_{\ell m} = \sqrt{\frac{2\ell+1}{4\pi}\frac{(\ell-m)!}{(\ell+m)!}}\,P_\ell^m(\cos\theta)e^{im\phi},$$

$$Y_{\ell,-m} = (-1)^m Y_{\ell m}^*.$$

With this convention $\int Y_{\ell m}^* Y_{\ell' m'}\,d\Omega = \delta_{\ell\ell'}\delta_{mm'}$, using $d\Omega = \sin\theta\,d\theta\,d\phi$. In particular $Y_{00} = 1/\sqrt{4\pi}$,

$$Y_{10} = \sqrt{3/(4\pi)}\cos\theta,$$

$$Y_{11} = -\sqrt{3/(8\pi)}\sin\theta e^{i\phi}.$$

To check the dipole normalisation independently,

$$\int \cos^2\theta \, d\Omega = 4\pi/3.$$

For Y_{11},

$$\int \sin^2\theta \, d\Omega = 8\pi/3.$$

The complex basis is an accounting device. A real potential obeys $v_{\ell,-m} = (-1)^m v^*_{\ell m}$, leaving $2\ell+1$ real angular degrees of freedom at each order.

On a sphere of radius a suppose segmented electrodes prescribe $f(\theta,\phi)$. Its coefficients are $v_{\ell m} = \int Y^*_{\ell m} f \, d\Omega$. These have units of volts because the angular functions and solid angle are dimensionless. The radial equation $(r^2R')' - \ell(\ell+1)R = 0$ has solutions $r^\ell, r^{-\ell-1}$. For an empty interior, regularity selects $V_{\rm in} = \sum v_{\ell m}(r/a)^\ell Y_{\ell m}$. For empty exterior decaying at infinity,

$$V_{\rm out} = \sum v_{\ell m}(a/r)^{\ell+1} Y_{\ell m}.$$

Nonuniform prescribed surface voltage requires electrically distinct electrode patches or a specified ideal boundary; one continuous metal conductor could not sustain that static variation.

Represent a tilted dipole in the laboratory frame

Impose $f = V_0 \hat{\mathbf{p}}\cdot\hat{\mathbf{r}}$ with $\hat{\mathbf{p}} = (\sin\alpha, 0, \cos\alpha)$. In the rotated frame with polar axis along $\hat{\mathbf{p}}$ this is a pure $m=0, \ell=1$ pattern. In the laboratory it is $V_0[\cos\alpha\cos\theta + \sin\alpha\sin\theta\cos\phi]$. Using the explicit harmonics,

$$v_{10} = V_0\sqrt{4\pi/3}\cos\alpha,$$

$$v_{11} = -V_0\sqrt{2\pi/3}\sin\alpha,$$

$$v_{1,-1} = +V_0\sqrt{2\pi/3}\sin\alpha.$$

The sum of their squared magnitudes is $4\pi V_0^2/3$, independent of tilt. The interior solution simplifies to $V_0\hat{\mathbf{p}}\cdot\mathbf{r}/a$, giving uniform $\mathbf{E} = -V_0\hat{\mathbf{p}}/a$. At $a = 40$ mm, $V_0 = 2.0$ V and $\alpha = 30^\circ$, $E_x = -25.0$ V/m, $E_z = -43.3$ V/m. An axis-only fit would infer the correct axial component while losing the transverse one. A full vector field measurement at one interior point distinguishes the rotated dipole from a weaker aligned one.

Tie angular modes to an actual charge distribution

The addition theorem expresses $P_\ell(\hat{\mathbf{r}}\cdot\hat{\mathbf{s}}) = [4\pi/(2\ell+1)]\sum_m Y_{\ell m}(\hat{\mathbf{r}})Y^*_{\ell m}(\hat{\mathbf{s}})$. Rotational invariance explains its structure: the sum is unchanged by simultaneous rotation of both directions, so it depends only on their angle. Put $\hat{\mathbf{s}}$ at the north pole, where only $m=0$ survives, and the proportionality constant follows from $Y_{\ell 0}$ and $P_\ell(1)=1$. Checking $\ell=1$ recovers the dot product of the two unit vectors.

Use the generating series $1/|\mathbf{r}-\mathbf{s}| = \sum_{\ell\ge 0}(r_<^\ell/r_>^{\ell+1})P_\ell(\hat{\mathbf{r}}\cdot\hat{\mathbf{s}})$. For an observation radius outside every source point, define $q_{\ell m} = \int \rho(\mathbf{s}) s^\ell Y^*_{\ell m}(\hat{\mathbf{s}})\, d^3s$. Inserting the addition theorem into the Coulomb integral gives

$$V(\mathbf{r}) = \frac{1}{\epsilon_0}\sum_{\ell,m}\frac{q_{\ell m}}{(2\ell+1)r^{\ell+1}}Y_{\ell m}(\hat{\mathbf{r}}).$$

Unlike boundary voltage coefficients, $q_{\ell m}$ carries units C m$^\ell$. At $\ell=0$, $q_{00} = Q/\sqrt{4\pi}$ and multiplication by Y_{00} returns $Q/(4\pi\epsilon_0 r)$, fixing the prefactor. At $\ell=1, m=0$,

$$q_{10} = \sqrt{3/(4\pi)}\,p_z.$$

The two transverse coefficients reconstruct p_x, p_y. Measuring the voltage coefficient at two radii can distinguish a decaying exterior multipole from a regular potential imposed by distant equipment, whose local expansion instead grows as r^ℓ.

Design an angular quadrature that measures the claimed coefficient

Uniformly spaced latitude rings do not have equal area. In angular integrals substitute $u=\cos\theta$, giving $d\Omega = du\,d\phi$. Equal spacing in u and ϕ already avoids overweighting the polar caps. More accurate quadrature uses Gauss–Legendre nodes in u with their weights, combined with equispaced azimuthal samples for the Fourier factors. If a known angular pattern contains $|m|\le M$, at least $2M+1$ azimuthal samples are needed to distinguish these signed orders on a fixed ring. A higher order present in an unknown pattern can alias into the fitted low orders, so adding more sample angles and reserving independent test directions is informative.

A robust reconstruction checks the constant mode on $f=1$, the total power $\sum|v_{\ell m}|^2 = \int |f|^2 d\Omega$ for an exactly represented pattern, and the predicted angular field at withheld directions. With noisy overdetermined data use a weighted linear least-squares fit to the modes, including weights for sampling geometry or measurement uncertainty as appropriate. The two choices are physically different: one approximates an angular integral, the other quantifies independent noisy observations. State which objective your fit minimises. An angular reconstruction can predict a voltage while still having very poor sensitivity to high-order exterior source moments, whose signals decay rapidly with radius.

A displaced charge supplies an exact all-orders convergence experiment

Place a point charge q at $s\hat{\mathbf{z}}$ within an otherwise empty sphere used as a measurement surface. At radius $R > s$ the potential is $q/[4\pi\epsilon_0\sqrt{R^2 + s^2 - 2Rs\cos\theta}]$. The axial symmetry makes only $m = 0$ coefficients nonzero, giving the exact Legendre series $[q/(4\pi\epsilon_0 R)]\sum_{\ell\geq 0}(s/R)^\ell P_\ell(\cos\theta)$. This example exhibits the convergence parameter directly. It is the radius of the enclosing source relative to the measurement radius, not the magnitude of the charge or the number of sampled angles.

On the ray nearest the point charge, $\theta = 0$, every Legendre polynomial is unity. Truncation at order L there gives a geometric partial sum and a relative error exactly $(s/R)^{L+1}$ when compared with the exact voltage at that point. At $s/R = 0.40$, six retained orders $\ell = 0, \ldots, 5$ leave 0.410% relative error. At $s/R = 0.85$ the same approximation leaves 37.7%. Achieving 1% in the latter case requires $L + 1 > \ln(0.01)/\ln(0.85) = 28.3$, so at least 29 orders. A claim that retaining through quadrupole always suffices has no physical meaning without an observation radius and a desired error.

On the opposite ray $P_\ell(-1) = (-1)^\ell$, making the terms alternate. The absolute voltage error there has a smaller prefactor $1/(1 + s/R)$, in contrast to $1/(1 - s/R)$ on the near side. For this particular geometric series its relative error magnitude is still $(s/R)^{L+1}$, despite the alternating signs. At other angles the angular polynomial oscillations can produce much smaller error but not a uniformly improved bound. The simple inequality $|P_\ell(u)| \leq 1$ gives an absolute bound $|q|(s/R)^{L+1}/[4\pi\epsilon_0 R(1 - s/R)]$ for the entire angular surface. For an arbitrary signed source replace $|q|$ by integrated absolute charge and s by a radius enclosing all source points. A nearly neutral distribution can have a small exact voltage at some angles, making any comparable relative bound much less informative.

Now rotate the point charge through polar and azimuthal angles θ_s, ϕ_s without changing its radius. The coefficient is exactly $q_{\ell m} = q s^\ell Y^*_{\ell m}(\theta_s, \phi_s)$. Summing $|q_{\ell m}|^2$ over m gives $q^2 s^{2\ell}(2\ell + 1)/(4\pi)$, by setting the two angular arguments equal in the addition theorem. This rotational invariant is a strong test of a numerical angular projection: a rotation changes individual complex phases, but the total power at each angular order remains fixed. Rotating a sensor array rather than the source should produce the equivalent opposite rotation of the fitted description.

A spherical split electrode drives an interior field without net charge

Construct a spherical boundary of radius a whose northern half is held at $+V_0$ and southern half at $-V_0$, separated by a thin insulating equatorial seam. In the mathematical limit take $f(u) = V_0 \operatorname{sgn} u$, $u = \cos\theta$. The problem is axisymmetric and changes sign under reflection through the equator, so only odd ℓ occur. Using the Legendre (rather than unit-normalised harmonic) coefficients, the series inside is $V = \sum b_\ell (r/a)^\ell P_\ell(u)$, where $b_\ell = (2\ell + 1)V_0 \int_0^1 P_\ell(u)\, du$ for odd ℓ. There is no monopole, hence no change to the net charge when the two voltages are applied symmetrically in a symmetric environment.

The first two nonzero coefficients can be found without a general table. $P_1 = u$ gives

$$b_1 = 3V_0/2.$$

$P_3 = (5u^3 - 3u)/2$ integrates from zero to one to $-1/8$, so $b_3 = -7V_0/8$. At the centre all terms with $\ell \geq 2$ have vanishing gradient, leaving an exact central field $E_z(0) = -3V_0/(2a)$. Even though the electrode voltages jump abruptly at the equator, a single low-order coefficient determines this point measurement exactly. A finely resolved electrode charge density near the seam requires a very different number of modes and a model of the seam width.

Set $a = 30$ mm and $V_0 = 2.0$ V. The central field is -100 V/m. At $z = 0.20a$ on the northern axis, the $\ell = 1$ voltage contributes 0.600 V and $\ell = 3$ adds -0.0140 V. The first omitted odd term scales as $(0.2)^5$ times its angular coefficient. At $z = 0.9a$ the same rapidly convergent two-term approximation is no longer trustworthy. A student can compare the actual surface voltages estimated from a truncated expansion to predictions at selected interior radii. A converged central field and a conspicuously rounded numerical step can coexist in the same exact analytic model.

For a finite insulating angular seam suppose instead the boundary interpolates continuously and antisymmetrically near $u = 0$. Only a thin band changes relative to the sign function. The dipole coefficient depends on $\int f(u) u \, du$; the extra weight u suppresses the influence of perturbations concentrated around the equator. If the band spans $|u| < \delta$ and the change in potential is bounded by V_0, the dipole coefficient error is at most $3V_0\delta^2/2$. High-order edge charge can nevertheless change markedly. This estimate shows how a real imperfection can have a small impact on one observable and a large impact on another. It also provides a quantitative tolerance when using the ideal split boundary to predict a centre-field calibration.

Separate material inside a measurement sphere from fields imposed outside it

A laboratory sometimes measures voltages on two concentric source-free spherical surfaces, without knowing whether the disturbance comes from an object inside both surfaces or from distant electrodes outside both. A single angular map determines the coefficient of each measured harmonic at that radius but cannot in general distinguish these two origins. In an annulus lacking sources, each angular component takes the radial form $v_{\ell m}(r) = A_{\ell m} r^{\ell} + B_{\ell m} r^{-\ell-1}$. The regular term is compatible with external forcing, and the decaying term with sources inside the inner radius. Both are harmonic in the measurement shell.

For a single $\ell = 1$ component, denote its coefficient of an ordinary $\cos\theta$ pattern by $v(r) = a_1 (r/R_1) + b_1 (R_1/r)^2$, so a_1, b_1 are voltages at the first radius. If two scans give $v(R_1) = 2.00$ V and $v(2R_1) = 1.30$ V, the equations are

$$a_1 + b_1 = 2.00, \; 2a_1 + b_1/4 = 1.30.$$

Multiply the first by one quarter and subtract, giving $a_1 = 0.4571$ V and $b_1 = 1.5429$ V. At a third radius $1.5R_1$ the predicted value is 1.371 V. A pure internal dipole would have returned 0.50 V on the second sphere, while a pure uniform external field would have returned 4.00 V. Fitting a single dipole to the first reading alone would grossly misdescribe the second.

For general order the determinant of the two normalised equations is $t^{-\ell-1} - t^{\ell}$ with $t = R_2/R_1$. As the two radii approach each other, this determinant tends to zero and the coefficients cannot be separated

reliably. Increasing separation improves discrimination of the two radial powers up to the point where one component falls below the measurement noise or additional sources enter the annulus. The monopole case deserves separate attention: its growing branch is just a constant voltage offset, while its decaying branch reveals total charge. A voltage reference common to both scans is therefore indispensable when using their difference to infer monopole charge.

Suppose the field was measured rather than voltage. Radial field coefficients are $-\ell A_{\ell m} r^{\ell-1} + (\ell+1) B_{\ell m} r^{-\ell-2}$. Measuring both radial field and voltage on one sphere can, in principle, supply the two independent equations needed to separate regular and decaying parts. For $\ell = 0$ the constant reference disappears from the radial field. An independently calibrated force probe then constrains total internal charge even when the voltmeter has a common offset. Numerically estimated radial derivatives from two very close voltage scans, however, share measurement errors with those voltages; treating them as two independent precise observations overstates the information gained.

A final issue is the coordinate origin. Moving it can create higher moments from lower ones for a nonneutral distribution. If the actual source is a displaced point charge and the coordinate origin shifts toward it, the series converges faster at a given observation sphere. If the charge distribution is unknown, choosing the origin solely to minimise apparent high-order coefficients can hide genuine structure or amplify noise. Record the physical origin of the measuring geometry, report withheld predictions, and compare the integrated monopole flux, which is independent of the choice of origin as long as the source remains enclosed. This separates a useful coordinate convention from an inferred physical symmetry.

Propagate measured boundary harmonics

Choose angular boundary data and examine its attenuation away from the spherical surface. Relate the relative loss of detail to harmonic degree.

Open this experiment online

Try the calculation

Observation radius r/a **0.5**

Quadrupole on the sphere (V) **2**

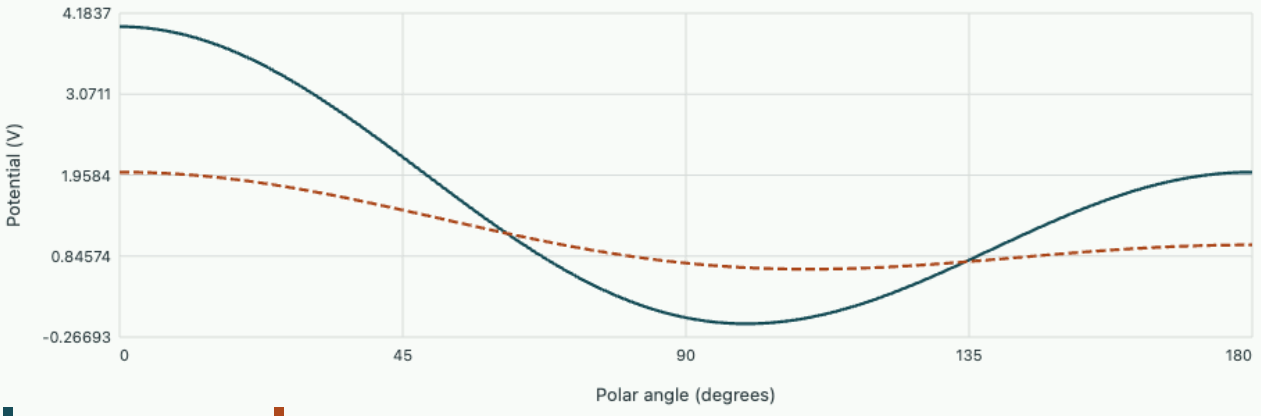

The north pole and equator read 2 V and 0.75 V at this radius. Both branches coincide on the boundary.

Predict an angular sampling requirement before buying more probes

How many angular measurements are needed for a declared band limit?

A real boundary pattern is known, independently of the current measurement, to contain only harmonics with $\ell \le 3$. Count its real degrees of freedom. Design a separable quadrature that exactly projects such a pattern onto the same harmonics in exact arithmetic. Explain what can still go wrong when the true band limit was assumed incorrectly.

▼ **Derive and check the result**

There are $\sum_{\ell=0}^{3}(2\ell+1) = 16$ independent real degrees of freedom. Sixteen arbitrary readings need not determine them: their locations must give a full-rank observation matrix. Equatorial-only data, for example, miss every axisymmetric odd pattern there. A straightforward overdetermined grid uses uniform azimuths and Gauss–Legendre nodes in $u = \cos\theta$. For $L = 3$ use at least $2L + 1 = 7$ equally spaced azimuths so that differences $m - m'$ up to 6 cannot alias a nonzero azimuthal difference into the constant component of a projection.

After that exact azimuthal sum, only equal m terms survive. Their products in u are proportional to $P_\ell^m(u)P_{\ell'}^m(u)$. Each contains $(1-u^2)^{|m|}$ times a polynomial and is itself a polynomial of degree at most $\ell + \ell' \le 6$. A four-point Gauss–Legendre rule integrates polynomials through degree 7 exactly. Thus four latitudes times seven azimuths, 28 weighted samples, suffice to reconstruct all 16 coefficients for the

declared band limit. Both polar caps are represented by quadrature weights; no point must lie precisely on either pole.

If the true field contains order $m = 7$, then $e^{i7\phi} = 1$ at the seven uniformly spaced azimuths starting at zero. Its azimuthal variation can masquerade as a constant on each sampled circle. A second scan shifted by half an azimuthal spacing flips the sign of this harmonic but preserves a true constant, exposing the alias. Unmodelled high latitudinal orders can similarly corrupt low coefficients through the finite radial quadrature. With noisy measurements evaluate withheld off-grid directions and report both the sensitivity to additional modes and the precision assumed in the protected low orders. An exactly integrating grid under a band-limit hypothesis is not a proof that the physical source obeyed that hypothesis.

Tutorial · derive a surface charge and test identifiability

Two spheres agree on their voltage patterns

The same prescribed $v_{\ell m}$ is realised on an infinitesimally thin spherical electrode array between identical dielectric media of permittivity ϵ. Find the coefficient of its free charge density. Which integrated measurement isolates the monopole?

▼ **Work through the solution**

The interior and exterior radial derivatives on $r = a$ are $\ell v_{\ell m} Y_{\ell m}/a$ and $-(\ell+1) v_{\ell m} Y_{\ell m}/a$. With outward normal pointing from interior to exterior, $\sigma_f = \epsilon(E_{\mathrm{out},r} - E_{\mathrm{in},r})$, giving coefficient $\epsilon(2\ell+1)v_{\ell m}/a$. A whole-surface integral of $\sigma_f a^2 d\Omega$ retains only the monopole since all nonconstant harmonics are orthogonal to Y_{00}. For uniform boundary voltage V_0, $v_{00} = \sqrt{4\pi} V_0$ and total charge $4\pi\epsilon a V_0$, the capacitance of an isolated sphere times voltage. High-order voltage components can instead demand strong local charge densities despite zero net added charge.

A ring of detectors misses an entire pattern

Twelve probes placed uniformly on the equator read zero voltage. Can this exclude a substantial $\ell = 1$ component? Give an explicit counterexample and a second configuration still invisible after adding a north-pole probe.

▼ **Work through the solution**

A pure Y_{10} vanishes all along the equator, whatever its amplitude. A north-pole reading would detect it. But the real quadrupole proportional to $\sin\theta\cos\theta\cos\phi$, corresponding to xz/r^2, vanishes on both the equator and at either pole. An intermediate ring or a set of oblique directions is needed. Increasing the number of equatorial samples alone cannot resolve a lack of checks at other latitudes. Under a declared band limit compute the rank and singular values of the probe-by-harmonic matrix before interpreting a null reading as an absent multipole.

Further reading

- Compare interior and exterior harmonics with a polar scan
- Infer a tilted quadrupole from six independent probe readings
- Fließbach, chapter 11 · spherical harmonics
- Griffiths, 5th ed., §§3.3–3.4 · spherical separation and multipoles

Electrostatic field theory and measurement · 9. Capacitance matrices, floating nodes and controlled approximation bounds

A multi-electrode device generally has no single capacitance until the other terminals have been connected or isolated. An energy identity determines the matrix that relates voltages to charges, and a complementary flux identity can certify estimates even when the exact field is unknown.

Build the matrix from unit-voltage experiments

Consider n isolated conductor surfaces embedded in a connected linear dielectric, plus a grounded reference conductor or decay relative to a reference at infinity. There is no free charge in the dielectric. Define the weighting function $w_j(\mathbf{x})$ by putting conductor j at 1 V, all other conductors and the reference at zero, then dividing by 1 V. For arbitrary voltages V_j, linearity and uniqueness give

$$\phi(\mathbf{x}) = \sum_j V_j w_j(\mathbf{x}).$$

The charge on conductor i is an integral of displacement leaving its metal into the dielectric. Using a normal $\mathbf{n}$ pointing out of the dielectric into the metal gives

$$Q_i = \int_{S_i} \epsilon \partial_n \phi \, dA.$$

Therefore

$$Q_i = \sum_j C_{ij} V_j,$$

$$C_{ij} = \int_{S_i} \epsilon \, \partial_n w_j \, dA = \int_\Omega \nabla w_i \cdot \epsilon \nabla w_j \, dV.$$

The last equality follows by multiplying the charge-free field equation for w_j by w_i and integrating by parts. The boundary integral selects just conductor i because its weighting function is unity there and zero on every other conductor. The volume expression proves reciprocity $C_{ij} = C_{ji}$ for a symmetric dielectric tensor. The diagonal terms are positive, since they integrate the squared fields of each independent one-volt experiment. In an ordinary connected isotropic configuration a positive voltage on j with $i \neq j$ grounded puts negative induced charge on i; the corresponding mutual coefficient C_{ij} is nonpositive.

The stored energy is

$$U = \tfrac{1}{2} \sum_{ij} V_i C_{ij} V_j.$$

Positive material response makes the reduced matrix with an effective reference positive definite under usual connected boundary conditions. If all conductors including the external closing conductor are retained without fixing a reference, changing all voltages by a common constant produces no field. The

full matrix then has a zero common-voltage mode and each row sums to zero. Removing the grounded reference from the matrix removes this gauge null direction; its remaining rows need not sum to zero. Treating both statements as universal would create a spurious constraint on measured terminal data.

Convert a field matrix to a circuit measurement

A two-port device might have reduced matrix in picofarads $C = \begin{pmatrix} 12 & -3 \\ -3 & 8 \end{pmatrix}$ relative to its grounded enclosure. With conductor 1 at 2 V and conductor 2 at 0 V, charges are 24 pC and -6 pC. The grounded enclosure takes the compensating -18 pC. Reciprocity predicts that holding conductor 1 at 0 V and conductor 2 at 2 V puts -6 pC on conductor 1. The diagonal 12 pF includes both the coupling to conductor 2 and the path to the enclosure. In an equivalent lumped model the positive pair capacitance between 1 and 2 is 3 pF, while the two separate couplings to ground are 9 and 5 pF. The sign of a Maxwell matrix off-diagonal is opposite to a positive capacitor drawn between two nodes.

Now disconnect conductor 2 after neutralising it. Its total charge stays zero while its voltage becomes an unknown. The second matrix row demands $-3V_1 + 8V_2 = 0$. Thus $V_2 = 3V_1/8$, giving apparent capacitance seen at terminal 1 equal to $12 - 9/8 = 10.875$ pF. Grounding conductor 2 would instead yield 12 pF. The change is a measurable effect of the prepared state, not a change in the dielectric constant of the material. If conductor 2 already carries charge Q_2^0, its voltage acquires a constant offset Q_2^0/C_{22} in addition to the response to V_1.

For several floating nodes write their block equation as $Q_f = C_{fa}V_a + C_{ff}V_f$. If the reference fixes the potential freedom, solve $V_f = C_{ff}^{-1}(Q_f - C_{fa}V_a)$ and substitute into the active-node block. The differential active capacitance is the Schur complement $C_{aa} - C_{af}C_{ff}^{-1}C_{fa}$. It is symmetric and positive for a positive full reduced matrix. With fixed floating charges the constant term shifts active charges but leaves this differential matrix unchanged in a linear medium. An actual cable measurement that results from leaving a neighbouring shield unconnected should be compared to this elimination, not to the original diagonal.

Obtain an upper capacitance bound by trying a voltage

For a two-terminal charge-free dielectric at prescribed voltage difference V, every admissible continuous trial potential satisfying the electrode voltages gives an energy at least as large as the exact electrostatic energy. This follows by writing the trial as exact plus a perturbation vanishing on fixed-voltage electrodes and expanding the energy. The mixed term integrates to zero because the exact displacement is divergence free. If exterior walls are insulated, the exact normal displacement vanishes there and the trial need not be assigned a fixed potential on them. Thus $C \le 2U_{\mathrm{trial}}/V^2$. The fields must genuinely arise as a gradient of one trial voltage. Guessing unrelated components of an electric field does not provide this upper bound.

For a capacitor of plate area A, separation d, and scalar permittivity varying in the gap, choose a linear voltage along the plate normal. The trial energy gives

$$C/A \le \langle \epsilon \rangle / d,$$

where the average is over the gap volume divided by Ad. For dielectric columns that run parallel to the applied field with no change of material along the field direction, the linear potential can be exact. For layers stacked normal to the field it usually overestimates capacitance. The same arithmetic average thus serves as the actual result or a strict upper bound depending on geometry, even when the material fractions are identical.

A complementary trial with a divergence-free displacement

Fix total plate charges $\pm Q$ instead, taking no volume free charge. An admissible displacement trial must have the prescribed flux into each electrode, no flux through insulating side walls, continuous normal component across free-charge-free interfaces, and zero divergence inside. It need not correspond to an exact potential-gradient electric field. Consider $U_D[\mathbf{D}] = \frac{1}{2}\int \mathbf{D}\cdot\epsilon^{-1}\mathbf{D}\,dV$. Write a trial as $\mathbf{D}_* + \delta\mathbf{D}$. The cross term is $\int(-\nabla\phi_*)\cdot\delta\mathbf{D}\,dV = 0$: integration by parts gives zero bulk divergence and each conductor has constant voltage multiplying zero net flux change. Thus $U_D \geq Q^2/(2C)$ and

$$\frac{Q^2}{2U_D^{\mathrm{trial}}} \leq C \leq \frac{2U_V^{\mathrm{trial}}}{V^2}.$$

Unlike two competing estimates, these inequalities identify which side contains the exact answer. For the same parallel-plate geometry choose constant displacement $D_z = Q/A$. It yields $C/A \geq 1/[d\langle 1/\epsilon\rangle]$, the harmonic-mean lower bound. For layers stacked normal to the plates that trial is exact. For columns parallel to the field the upper bound is exact. An arbitrarily shaped two-phase composite satisfies both under the stated plate and insulating-side conditions. This gives a strong physical check before solving detailed microstructure on a mesh.

Use measured numbers to rule out a material model

Take equal volume fractions of relative permittivities 2 and 8 in a cell of area 100 mm² and thickness 1.0 mm. The harmonic mean is 3.2, arithmetic mean 5.0. Since $\epsilon_0 A/d = 0.8854$ pF, the admissible capacitance interval is 2.83–4.43 pF. A measured 3.3 pF is consistent with many internal geometries and does not determine how the two materials are arranged. A calibrated value of 5.2 pF would require examining fringing, area and thickness, parallel cable capacitance, dispersive or conducting response, and the assumed constituent data. Merely refining an interior mesh cannot produce a static value outside the proven interval if it faithfully solves the same ideal model.

For a field computation use the matrix reciprocity relation as one diagnostic and the two variational bounds as another. An electrostatic finite-element potential may produce a reliable energy estimate while numerical differentiation at a sharp electrode edge produces poor charge density. Integrating boundary fluxes gives each terminal charge, but reconstructing C_{ij} by the mixed energy integral often has a different error sensitivity. Comparing both over a grid sequence can indicate whether the error is concentrated at edges or in the field volume. Symmetrising a noisy measured matrix by averaging its transpose removes an antisymmetric discrepancy but cannot establish positivity or explain an inaccurate common scale.

Construct a complete measurable matrix without numerical differentiation

Three thin spherical conductors have radii $a < b < c$. The outer one is tied to the reference potential. Homogeneous material of permittivity ϵ_1 fills the inner annulus $a < r < b$ and another material ϵ_2 fills $b < r < c$. Spherical symmetry gives each annulus its own independent radial displacement field fixed by its electrode voltage difference. Define the ordinary two-sphere gap capacitances $K_1 = 4\pi\epsilon_1 ab/(b-a)$,

$$K_2 = 4\pi\epsilon_2 bc/(c-b).$$

The inner conductor takes $K_1(V_1 - V_2)$. The middle one has two faces, carrying the opposite inner gap charge and an outer gap charge $K_2 V_2$. Thus $Q_1 = K_1 V_1 - K_1 V_2$ and $Q_2 = -K_1 V_1 + (K_1 + K_2)V_2$. Every sign and every term can be read from a physical face.

In vacuum choose $a = 10$ mm, $b = 20$ mm, $c = 40$ mm. Then $K_1 = 2.225$ pF and $K_2 = 4.451$ pF. Driven at 3.0 V with the middle conductor grounded, the inner sphere carries 6.68 pC and the outer gap has zero field. With the middle conductor floating and neutral, $V_2 = K_1 V_1/(K_1 + K_2) = 1.0$ V. The inner sphere now carries 4.45 pC. The inner and outer faces of the floating sphere carry exactly opposite charges, although the conductor has a nonzero voltage. Integrating a current meter attached to the conductor during charging need not tell you each face's charge separately.

Now electrically connect the inner two conductors. Their common voltage sets the inner field to zero. The combined conductor has capacitance K_2 to the exterior, independent of a. This third preparation is distinct from grounding or floating the middle shell. Before calculating an experimental 'device capacitance', draw the electrical connections as well as the geometric cross section. In a larger matrix a driven conductor and a driven guard at the same voltage should have their charges combined only if the experimental ammeter actually measures their total current.

One can also recover the two constituent permittivities from just two carefully selected scalar measurements. Ground the middle shell to determine K_1 directly. Then float it neutral and measure $K_{\mathrm{ser}} = K_1 K_2/(K_1 + K_2)$, giving $K_2 = K_{\mathrm{ser}} K_1/(K_1 - K_{\mathrm{ser}})$. If K_2 is very large, the floating and grounded readings nearly coincide and their difference becomes noise sensitive. An alternative is to drive inner and middle together and measure the outer-gap current directly. The algebra selects a better experimental protocol instead of hiding ill-conditioning in a formula.

Tighten a variational bound without solving the entire field

Take the stacked two-layer capacitor with no space charge, equal layer thickness and isotropic permittivities $\epsilon_1 = 2\epsilon_0, \epsilon_2 = 8\epsilon_0$. A single linear trial produces the arithmetic-mean upper bound. Insert one interior voltage degree of freedom at a point that coincides with the material interface. The resulting piecewise-linear trial space contains the exact solution. Minimising its energy makes the normal displacements equal, reproducing the harmonic-mean capacitance exactly. A global quadratic trial with the same number of extra parameters will usually perform worse because its derivative is continuous while the exact normal field jumps.

To see this quantitatively write $x = z/d$ on the unit interval and $V(x) = V_0[x + \eta x(1-x)]$, with the lower half at relative permittivity 2 and upper half at 8. This trial fixes both endpoints. Its dimensionless capacitance upper estimate is

$$c(\eta) = \int_0^1 \epsilon_r(x)[1 + \eta(1-2x)]^2 dx.$$

Integrating gives

$$c(\eta) = 5 - 3\eta + (5/3)\eta^2.$$

The best quadratic trial has $\eta = 0.9$ and $c = 3.65$, compared with 5.00 for the straight line and 3.20 for the exact layered solution. The unrefined constant-displacement lower trial already supplies 3.20, so the two-field comparison certifies an interval before any field-map visualisation.

Why did the smooth trial still overestimate by 14%? At its endpoints it predicts slopes 1.9 and 0.1 times the mean field magnitude, whereas the exact field has slopes 1.6 and 0.4 in the two halves. Optimising a volume energy distributes a global smooth approximation across both layers. It has no mechanism to jump at the known interface, so an error persists even with its one coefficient optimised perfectly. The example explains why fitting material interfaces in a mesh, or using basis functions that admit correct normal derivative jumps, can matter more than merely increasing polynomial degree.

In an irregular two-dimensional composite an exactly divergence-free complementary trial can be constructed from a stream function Ψ: take $\mathbf{D} = (\partial_y \Psi, -\partial_x \Psi)$ in Cartesian coordinates. Its divergence vanishes identically. Total flux through an oriented path is a difference of Ψ at its endpoints, so carefully chosen boundary values enforce required electrode charges and zero leakage on insulating sides. Optimising $\int \mathbf{D} \cdot \epsilon^{-1}\mathbf{D}/2$ over such trial functions tightens the lower capacitance bound. Optimising the independent voltage trial tightens the upper one. The difference between their resulting bounds quantifies what the chosen approximation spaces still fail to resolve.

What an AC bridge measures when a nominally floating terminal leaks

A real high-impedance lead is neither perfectly floating nor an ideal ground at every frequency. Add a leakage resistance R from conductor 2 of the two-port example to its grounded enclosure. Keep the reduced static capacitance matrix C fixed, linear and quasistatic at the frequencies of interest. Let terminal 1 be driven sinusoidally and terminal 2 have no other external drive. Using $e^{i\omega t}$ here for circuit phasors, charge continuity at terminal 2 gives

$$i\omega(C_{21}V_1 + C_{22}V_2) + V_2/R = 0.$$

The outward conductive current plus the rate of charge stored in the electrode must vanish. Solving for the active terminal admittance gives

$$Y_{\mathrm{in}} = i\omega C_{11} + \frac{\omega^2 C_{12}C_{21}}{1/R + i\omega C_{22}}.$$

At low frequency the leakage holds terminal 2 close to ground, so the leading measured capacitance is C_{11}. At high frequency the floating condition is recovered and $Y_{\mathrm{in}}/(i\omega) \to C_{11} - C_{12}C_{21}/C_{22}$. The effective admittance also has a positive real part, since the driven voltage on terminal 2 supplies Joule heat in the leakage resistance. This term persists even if the dielectric itself is lossless. An AC capacitance meter reporting a frequency-dependent loss tangent might therefore be detecting a boundary preparation rather than intrinsic material loss.

Take $C_{22} = 8$ pF and $R = 100$ MΩ. The crossover $1/(2\pi R C_{22})$ is 199 Hz. At this frequency the quadrature capacitance is halfway between 12.0 and 10.875 pF, namely 11.4375 pF. The corresponding loss conductance divided by ω is 0.5625 pF. An independent verification uses the port voltage ratio at crossover,

$$|V_2/V_1| = |C_{21}|/(\sqrt{2}C_{22}) = 0.265.$$

Compute dissipated power as $|V_2|^2/(2R)$ for peak phasor amplitudes and compare it with $\mathrm{Re}\, Y_{\mathrm{in}} |V_1|^2/2$; the two results must coincide.

The crossover shifts inversely with the leakage resistance while its two limiting capacitances stay fixed in this simple model. Measuring several shunt resistances or adding a known external one provides a direct way to test this interpretation. If a neighbouring shield is connected to a voltage follower instead, its response includes the follower's own gain and phase; static floating-node elimination is insufficient. Extending the field-derived capacitance matrix by experimentally known terminal circuits makes it possible to distinguish changes in electrostatic geometry from changes in what the surrounding measurement wiring enforces.

Close the charge balance at a floating conductor

Compare voltages obtained by fixing a conductor potential and by prescribing its net charge. Check the sign of the off-diagonal capacitance terms.

Open this experiment online

Try the calculation

Mutual capacitance (pF) 4

Drive voltage V_1 (V) 2

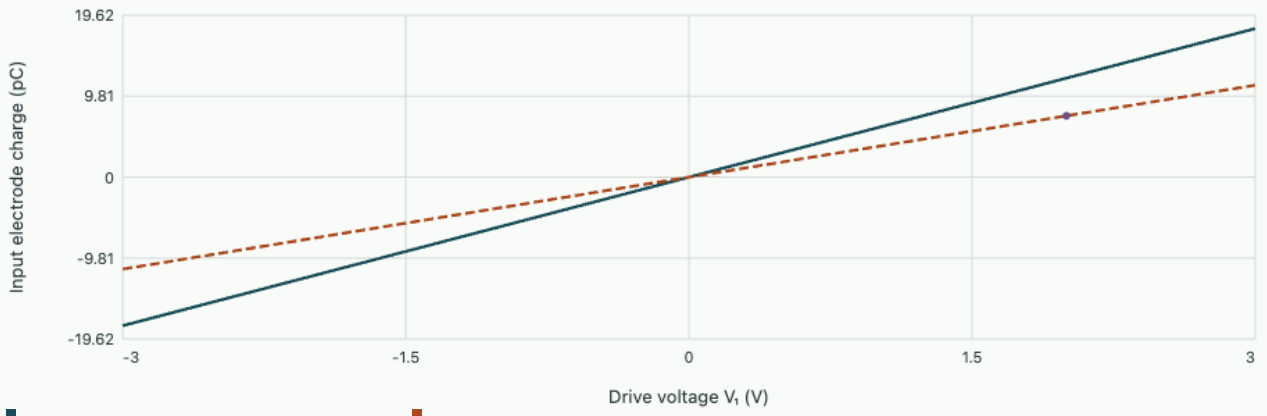

Second electrode grounded
Second electrode neutral and floating
Selected floating charge on electrode 1

Neutral electrode 2 floats to 1.143 V. Grounded input capacitance 6 pF, floating input capacitance 3.714 pF. Floating-case field energy 7.429 pJ.

Tutorial · distinguish a floating port and an inadmissible trial

What changes after disconnecting a biased guard?

Using the 12, 8 and –3 pF coefficients, start with terminal 1 at 0 V and terminal 2 at 1 V. Disconnect terminal 2, then raise terminal 1 to 2 V. Find the new floating voltage, both charges and the change of active charge.

▼ **Work through the solution**

Initially $Q_2 = 8$ pC, which stays fixed. The new condition is $8 = -3(2) + 8V_2$, giving $V_2 = 1.75$ V. Terminal 1 initially held -3 pC; finally it holds $12(2) - 3(1.75) = 18.75$ pC. Its change is 21.75 pC, or 10.875 pF times the 2 V increment. This reproduces the neutral-floating differential result but a different absolute charge. A charge amplifier reset at the initial state observes the change, whereas a device measuring absolute node potential distinguishes the stored preparation.

Can a lower voltage-trial estimate be trusted?

A potential approximation for the two-phase cell returns 2.70 pF while a constant-displacement trial gives 2.83 pF. The implementer reports the smaller number because its potential looked smoother. Diagnose the inconsistent pair.

▼ **Work through the solution**

For admissible fields on the same problem the flux trial gives a lower capacitance bound and the potential trial an upper one. The reversed interval cannot result from arbitrary coarseness alone. Check that the voltage trial satisfies the exact terminal difference and that all physical material volumes and energy factors are included. Check that the displacement trial has the correct area-normalised total charge and satisfies flux continuity. Finally examine numerical quadrature and unit conversion. Comparing the plots of the two fields does not fix an inadmissible constraint. If both are corrected, their gap gives an actual a posteriori uncertainty interval even without an analytic solution.

Further reading

- Measure a variational energy gap
- Change the geometry and permittivity of a layered capacitor
- Griffiths, 5th ed., §§2.4–2.5 and 4.4 · capacitance and field energy

Electrostatic field theory and measurement · 10. Anisotropic and nonlinear dielectrics from local measurements to global fields

A single dielectric constant cannot describe a crystal whose displacement tilts away from its electric field, or a reversible material whose incremental response changes with bias. Starting with the constitutive measurement clarifies which parts of ordinary electrostatics survive.

Measure a tensor rather than assuming collinearity

In a homogeneous linear anisotropic material,

$$\mathbf{D} = \boldsymbol{\epsilon}\mathbf{E}.$$

The entry ϵ_{ij} measures displacement component i in response to electric-field component j. A reversible reciprocal dielectric has a symmetric positive-definite tensor. Its principal axes are orthogonal and its positive eigenvalues are the principal permittivities. Field-energy density $u = \mathbf{E}\cdot\boldsymbol{\epsilon}\mathbf{E}/2$ is then positive for a nonzero field. Positive definiteness concerns all directions; having three positive diagonal entries in one basis alone is insufficient.

Choose principal relative permittivities $2, 4, 6$ along x, y, z. With a field $(1000, 0, 1000)$ V/m the displacement is $\epsilon_0(2000, 0, 6000)$. The field makes 45° to z, the displacement only 18.4°; their directions differ. Energy density is 3.54×10^{-5} J/m³. A flat free-charge sensor normal to z responds to D_z; an electrostatic force probe constrained along x measures E_x. Their readings cannot be interpreted as two component measurements of one vector differing by a single scalar.

Derive the field of a point charge in an anisotropic bulk

For a constant symmetric tensor write $\boldsymbol{\epsilon} = \epsilon_0 K$, with positive dimensionless matrix K. Poisson's equation is

$$-\epsilon_0 \nabla_{\mathbf{x}} \cdot K \nabla_{\mathbf{x}} V = q\delta^3(\mathbf{x}).$$

Change coordinates to $\mathbf{y} = K^{-1/2}\mathbf{x}$. The gradient transforms by the same symmetric matrix and the operator becomes the ordinary isotropic Laplacian in $\mathbf{y}$. The source transforms too: physical volume is $d^3x = \sqrt{\det K}\, d^3y$, so

$$\delta^3(\mathbf{x}) = \delta^3(\mathbf{y})/\sqrt{\det K}.$$

The decaying solution is

$$V(\mathbf{x}) = \frac{q}{4\pi\epsilon_0\sqrt{\det K}}\,\frac{1}{\sqrt{\mathbf{x}^T K^{-1}\mathbf{x}}},$$

$$\mathbf{E} = \frac{q}{4\pi\epsilon_0\sqrt{\det K}}\,\frac{K^{-1}\mathbf{x}}{(\mathbf{x}^T K^{-1}\mathbf{x})^{3/2}}.$$

A check is the scalar case $K = kI$. The determinant contributes $k^{3/2}$ and the distance contributes $1/\sqrt{k}$, returning $q/(4\pi\epsilon_0 kr)$. The equipotentials in laboratory coordinates are ellipsoids, while $\mathbf{D} = \epsilon_0 K\mathbf{E}$ happens to point along $\mathbf{x}$ for this infinite homogeneous point-source problem. Its magnitude varies with direction on a physical sphere. Gauss's law still gives total free flux q; equating that flux to $4\pi r^2$ times a constant magnitude would be invalid. Conducting or material boundaries also transform under this coordinate map and generally cease to be simple physical spheres.

Along any principal axis i, at distance r, the potential is proportional to $\sqrt{K_i}/\sqrt{\det K}$. With principal values $2, 4, 6$, two probes equally far away on the z, x axes measure a voltage ratio $\sqrt{6/2} = \sqrt{3}$. One might have expected the largest permittivity to reduce the voltage most strongly along that axis. The observed result reflects how the full anisotropic medium distributes the displacement of a point source; it cannot be derived by inserting a direction-specific permittivity into the isotropic radial formula.

Which permittivity does a slab capacitance measure?

Place broad metal plates normal to a unit vector $\mathbf{n}$ and neglect edge effects. Constant electrode potentials force a purely normal electric field $V\mathbf{n}/d$, independent of the off-diagonal dielectric entries. The displacement generally has a tangential component, but the metal's free-charge reading is D_n. Thus the measured normal capacitance per area is

$$C/A = (\mathbf{n}^T \boldsymbol{\epsilon} \mathbf{n})/d.$$

For axes with relative values 2 and 6, cut the normal at 45° between them. The relative plate permittivity is 4.

A different preparation constrains displacement to be purely normal, for instance in an effectively uniform bulk state with known flux vector. Then $\mathbf{E} = \boldsymbol{\epsilon}^{-1} D_n \mathbf{n}$, so

$$D_n/E_n = 1/(\mathbf{n}^T \boldsymbol{\epsilon}^{-1} \mathbf{n}).$$

For the same cut the result is $1/[(1/2 + 1/6)/2] = 3$ in relative units. Both are correct for their own field constraints. Flat equipotential plates do not generally enforce tangential displacement equal to zero. A boundary-value calculation using that extra condition could report the wrong dielectric constant from an otherwise perfect experiment.

With an interface between two tensors, integrate Faraday's law around a small static rectangular loop to enforce continuous tangential E and Gauss's law over a pillbox to enforce the specified normal D jump. Write the first material's measured tangential field into the second's constitutive law and solve for its normal electric field from D_n. No scalar Snell-like rule involving only a ratio of two relative permittivities can represent arbitrary crystal orientations. Some field components may vanish by symmetry in one experiment and reappear after rotating the sample.

Reversible response distinguishes stored energy and coenergy

For a slowly and reversibly assembled homogeneous dielectric, increment of stored electrical energy per volume is $du = \mathbf{E} \cdot d\mathbf{D}$. A complementary density $w(\mathbf{E}) = \mathbf{E} \cdot \mathbf{D} - u$ has $dw = \mathbf{D} \cdot d\mathbf{E}$. In a scalar nonlinear law $D(E) = \epsilon E + \alpha E^3$ with $\epsilon, \alpha > 0$, integration gives

$$w(E) = \tfrac{1}{2}\epsilon E^2 + \tfrac{1}{4}\alpha E^4,$$

$$u(E) = ED(E) - w(E) = \tfrac{1}{2}\epsilon E^2 + \tfrac{3}{4}\alpha E^4.$$

The familiar $ED/2$ holds only in the linear case. For a small perturbation superposed on bias E_b, $dD/dE = \epsilon + 3\alpha E_b^2$ is the differential permittivity. A dc charge-to-voltage ratio measures the secant value $\epsilon + \alpha E_b^2$. At $\alpha E_b^2 = 0.20\epsilon$ these are 1.60ϵ and 1.20ϵ, a substantial difference even though the constitutive curve remains smooth.

The field equation becomes $\nabla \cdot \mathbf{D}(-\nabla V) = \rho_f$ and superposition generally fails. For a differentiable energy-based vector law, $\partial D_i/\partial E_j = \partial^2 w/\partial E_i \partial E_j$ is symmetric. A positive-definite differential tensor gives local stability and helps preserve ellipticity of the electrostatic boundary problem. A hysteretic material can depend on its prior history and need extra state variables; an area in a closed constitutive cycle then measures dissipated work, not reversible recoverable energy.

A nonlinear field calculation that needs only a scalar root

Place a sphere with charge q in an infinite isotropic nonlinear medium of the preceding type. Spherical symmetry and Gauss's law still determine $D_r = q/(4\pi r^2)$ outside. Invert $\epsilon E_r + \alpha E_r^3 = D_r$ point by point. For $\alpha > 0$ the derivative is positive everywhere, ensuring one physical real root for each D_r. A bisection bracket for $q > 0$ is $0 \le E_r \le D_r/\epsilon$; evaluating the residual at the upper endpoint gives positive cubic surplus. Compute voltage relative to infinity by integrating this field, rather than replacing D/E by an arbitrary constant taken at the surface.

For weak nonlinearity set $E = D/\epsilon + \delta$ and keep the leading cubic correction. One obtains

$$E \simeq D/\epsilon - \alpha D^3/\epsilon^4.$$

At large radii a $1/r^2$ displacement therefore acquires a negative $1/r^6$ correction in the electric field, giving a $1/r^5$ potential correction. A probe can misinterpret that extra radial scale as a change of source shape if material nonlinearity is not independently controlled. Double the source charge and compare the field after division by q. In a linear medium those curves coincide; the perturbative deviation here scales as q^2.

Resolve an oblique crystal interface component by component

A lateral detail or an oblique electrode can produce a field with both normal and tangential components at an interface. Consider a locally planar interface with tangent $\hat{\mathbf{x}}$ and normal $\hat{\mathbf{z}}$ from isotropic medium 1 into a crystal. In the xz plane let the crystal's relative tensor be $\begin{pmatrix} 4 & 1 \\ 1 & 3 \end{pmatrix}$, with entries in the order x, z.

Medium 1 has relative permittivity 2 and measured field $E_{1x} = 120$ V/m, $E_{1z} = 240$ V/m. There is no free sheet at the interface. Neither input field is assumed normal to the boundary.

From a very short rectangular loop crossing the interface, the tangential electrostatic field is continuous, so $E_{2x} = 120$ V/m. The normal displacement on side 1 is $D_{1z}/\epsilon_0 = 2(240) = 480$ V/m. Equating it to $E_{2x} + 3E_{2z}$ yields $E_{2z} = 120$ V/m. The tangential displacement can jump. In the crystal it is $D_{2x}/\epsilon_0 = 4(120) + 120 = 600$ V/m, compared with $D_{1x}/\epsilon_0 = 240$ V/m. Neither tangent D nor normal E is required to be continuous. A field solver that enforces continuity of all components can silently erase the very anisotropy the experiment was intended to measure.

Find the bound surface charge using two routes. The true charge jump is $\epsilon_0(E_{2z} - E_{1z}) = -120\epsilon_0 = -1.06$ nC/m². With no free sheet this must be bound. Directly, $P_{1z}/\epsilon_0 = D_{1z}/\epsilon_0 - E_{1z} = 240$ V/m and $P_{2z}/\epsilon_0 = 480 - 120 = 360$ V/m. The net bound charge from the two facing polarisation surfaces is $P_{1z} - P_{2z} = -120\epsilon_0$, giving the same result. At a rotated interface it can be safer to perform these component checks than to infer charge from one visual change in field-line angle.

A controlled reversal can expose the off-diagonal tensor entry. Keep E_{1z} fixed and reverse E_{1x} using independent side electrodes. Then $E_{2x} = -120$ V/m and $E_{2z} = (480 + 120)/3 = 200$ V/m. The normal response therefore changes by 80 V/m even though the imposed normal displacement is unchanged. A scalar model, or a crystal whose tensor had zero xz entry in this coordinate system, would predict no such change. In practice the side electrodes must be far enough from the chosen interface patch for their intended approximately uniform fields to be realised locally.

Derive pressure for a reversible nonlinear capacitor under both electrical controls

Take a parallel-plate gap d, area A, completely filled by a reversible material with specified constitutive law $D(E)$. For this idealised calculation assume that changing d changes only the volume occupied by otherwise identical material at fixed thermodynamic properties. Exclude any additional mechanical elastic stress, electrostriction or chemical work needed to preserve that preparation. Keep the field homogeneous and neglect fringing. Under charge control the displacement $D = Q/A$ is fixed, so the stored electric energy is $U = Ad\,u(D)$ with $u = \int_0^D E(D')\,dD'$. The force tending to increase the gap is

$$F = -\partial_d U|_Q = -Au(D).$$

Thus the attractive field contribution has magnitude Au.

Now hold voltage fixed. The electric field is $E = V/d$; decreasing the gap also changes the charge the source must supply. Legendre transforming the energy by subtracting VQ gives the appropriate potential $\mathcal{G} = U - VQ = -Ad\,w(E)$. Its derivative at fixed V is $-Aw(E) + AE\,dw/dE = -Aw + AED = Au$. Hence $F = -\partial_d \mathcal{G}|_V = -Au$, agreeing for the same instantaneous state. Differentiating U at fixed voltage without the source term would produce a different answer. The calculation identifies the source work excluded by that incorrect derivative.

For $D = \epsilon E + \alpha E^3$ with $\alpha E_b^2 = 0.20\epsilon$,

$$u(E_b) = 0.65\epsilon E_b^2.$$

The often-used linear formula $E_b D_b/2$ would give $0.60\epsilon E_b^2$, underestimating the stated ideal field contribution. With $\epsilon = 4\epsilon_0,\ E_b = 1.0 \times 10^5$ V/m, the predicted magnitude per area is 0.230 Pa. This number follows from a particular reversible constitutive model and mechanical variation. A real force between electrodes compressing a solid sample also contains material mechanical stresses, and the permittivity itself can change with density. The correct experiment must specify which matter moves when the gap changes.

An independent numerical test computes $U(d \pm \delta d, Q)$ at fixed charge or $\mathcal{G}(d \pm \delta d, V)$ at fixed voltage, forms centred derivatives and chooses the charges or voltages that describe the same midpoint state. If the two forces converge to opposite signs, check the mechanical displacement convention and the source-work term. Agreement of the pressures at a single bias does not prove the constitutive approximation is valid at other fields. A separate differential capacitance scan can verify the slope required by the energy model across the displacement range.

Solve a layered nonlinear capacitor by displacement continuation

A useful intermediate problem between a uniform nonlinear slab and a full finite-element solve is a pair of different nonlinear layers stacked normal to large plates. With no free interface charge, the same normal displacement D passes through both. Each has a reversible monotone law $D_i(E_i) = \epsilon_i E_i + \alpha_i E_i^3$, $\epsilon_i > 0, \alpha_i \geq 0$. At fixed terminal charge $D = Q/A$ is known. Invert each material separately and add the voltages,

$$V(D) = d_1 E_1(D) + d_2 E_2(D).$$

At fixed voltage solve this last scalar equation for D. Its derivative is positive:

$$\frac{dV}{dD} = \frac{d_1}{\epsilon_1 + 3\alpha_1 E_1^2} + \frac{d_2}{\epsilon_2 + 3\alpha_2 E_2^2},$$

$$\frac{C_{\text{diff}}}{A} = \left(\frac{dV}{dD}\right)^{-1}.$$

Thus it is the differential permittivities, evaluated at the two actual and generally different local fields, that combine as a series small-signal capacitance. Using a differential response measured at the overall average field can give an inconsistent result even when the series formula itself is correct. The secant ratio D/V has another interpretation and should be compared only with a dc charge reading.

Choose a field scale $E_* = 1000$ V/m and $D_* = \epsilon_0 E_*$. In the first material let $D/D_* = 2e_1 + e_1^3$, $e_1 = E_1/E_*$, while the second is linear $D/D_* = 6e_2$. Give both layers thickness 1 mm. At $D = 3D_*$, the first equation is solved by $e_1 = 1$; the second gives $e_2 = 0.50$. The total voltage is 1.50 V, and $D = 26.56$ nC/m². The dc capacitance per area is 17.71 nF/m². At this same operating point the differential relative permittivities are 5 and 6, giving $C_{\text{diff}}/A = \epsilon_0/[0.001/5 + 0.001/6] = 24.15$ nF/m². A small voltage ripple measures a capacitance about 36% larger than the secant value.

Check the bias state from energy without using terminal current. The stored energy per volume in layer 1 is $\epsilon_0 E_*^2[e_1^2 + 3e_1^4/4]$ and in layer 2 is $3\epsilon_0 E_*^2 e_2^2$. Multiplying by the respective thicknesses at the chosen state gives total energy per area $0.00250\epsilon_0 E_*^2 = 22.14$ nJ/m². Integrating the voltage as a function of displacement from zero to $3D_*$ must give the same result, since $d(U/A) = V\,dD$. The shortcut $VD/2$ would instead give 19.92 nJ/m². It lies between neither two guaranteed bounds nor two voltage controls; it is simply unjustified for this nonlinear path.

For voltage-controlled computation use a continuation in applied voltage. Start at low bias with the known linear two-layer solution and reuse its displacement as a first guess for the next monotone scalar solve. A bracketing method with increasing positive endpoints always finds the root for positive applied voltage in these specific laws. Once converged, evaluate both layers' displacement residuals, their voltage sum and the independent energy integral. A lower iteration error alone cannot correct a model that accidentally multiplied the cubic coefficient by field rather than field cubed, or used a common E across both materials. Direct field checks at a selected bias make the numerical experiment physically interpretable.

Rotate the field relative to a microstructure

Study a layered material with calculable normal and tangential responses. Change its composition before deciding whether one scalar permittivity can describe both measurements.

Open this experiment online

Try the calculation

Fraction of low-permittivity phase **0.5**

Measurement angle (degrees) **45**

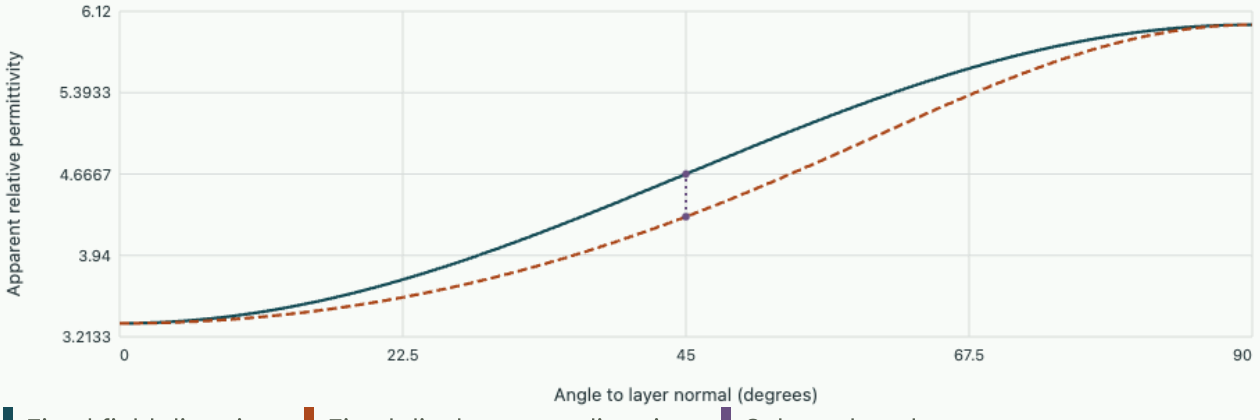

Principal relative permittivities: normal 3.3333, tangential 6. At 45° the two responses are 4.6667 and 4.2857.

Recover dielectric alignment torque from electrode work

Will positive or negative rotation increase capacitance?

A slab completely filling an ideal parallel-plate cell can rotate its uniaxial permittivity tensor reversibly without changing plate geometry. The angle θ between plate normal and the larger principal-permittivity axis is adjustable. Derive the torque on this ideal material coordinate, compare voltage and charge control, and calculate the maximum for a stated geometry.

▼ **Derive and check the result**

With area A, separation d, principal absolute permittivities $\epsilon_{\parallel} > \epsilon_{\perp}$, the normal capacitance is $C(\theta) = (A/d)(\epsilon_{\parallel}\cos^2\theta + \epsilon_{\perp}\sin^2\theta)$. For fixed voltage electrical coenergy is $CV^2/2$. The torque doing work in the direction of increasing θ is its derivative,

$$T = (A/d)(\epsilon_{\perp} - \epsilon_{\parallel})V^2\sin(2\theta)/2.$$

For $0 < \theta < \pi/2$ it drives the larger-permittivity principal axis towards the plate normal, increasing capacitance. The configurations at 0° and 90° both have zero torque but only the former minimises the fixed-voltage mechanical potential $-CV^2/2$.

Under fixed charge the stored energy is $Q^2/(2C)$, so the torque is $-\partial_\theta U = Q^2C'/(2C^2)$. At the same instantaneous voltage Q/C it agrees with the voltage-controlled result. Following two entire rotation curves with different preparations generally yields different magnitudes because the isolated cell voltage varies with angle. This equality at the same state is an independent sign check and distinguishes the field torque from the external holding torque of opposite sign.

Take $A = 1.0$ cm², $d = 1.0$ mm, principal relative permittivities 6 and 2, and $V = 20$ V. At 45°, the magnitude is $0.5(A/d)4\epsilon_0V^2 = 7.08\times10^{-10}$ N m. A small-angle torque measurement close to the aligned state would also reveal a positive angular restoring stiffness. In a real sample the crystal lattice, liquid-crystal elasticity or mount supplies additional energy and boundary conditions for rotation. The electrostatic contribution just calculated can be isolated by varying V^2 and checking the $\sin 2\theta$ angular dependence at sufficiently slow drive.

Tutorial · diagnose a tensor and a bias dependence

Recover a rotated tensor from three plate measurements

In a material plane, cuts with normals $x, y, (x+y)/\sqrt{2}$ yield relative plate permittivities $3, 5, 5$, respectively. Reconstruct the 2×2 tensor, check positivity and predict the result for the other bisector.

▼ **Work through the solution**

The first two values are

$$K_{xx} = 3, K_{yy} = 5.$$

The third is $(3 + 5)/2 + K_{xy} = 5$, so $K_{xy} = 1$. The symmetric matrix has determinant 14 and positive first diagonal entry, hence is positive definite. Its principal values are $4 \pm \sqrt{2}$. The other bisector gives $4 - 1 = 3$. This extra reading can test the assumed orientation and symmetry independently. All four inferences assume the plate experiment imposes electric field normal to each cut and fringing is negligible.

Distinguish charge measurements before integrating electrical work

At a bias E_b, a sample following the cubic constitutive law gives secant permittivity $1.30\epsilon_*$ and differential permittivity $1.70\epsilon_*$, where ϵ_* is a calibration permittivity. Infer its linear coefficient, cubic contribution at bias and true stored energy density.

▼ **Work through the solution**

Subtract the two measurements. The difference is $2\alpha E_b^2 = 0.40\epsilon_*$, so $\alpha E_b^2 = 0.20\epsilon_*$,

$$\epsilon = 1.10\epsilon_*.$$

The energy at bias is

$$[0.55 + 0.15]\epsilon_* E_b^2 = 0.70\epsilon_* E_b^2.$$

Using $ED/2$ would give $0.65\epsilon_* E_b^2$. To test the law rather than just fit two parameters, obtain a second set of secant and differential readings at a different bias and check the predicted quadratic change with bias field.

Further reading

- Inspect normal displacement across a dielectric interface
- Follow the optical consequences of a permittivity tensor
- Griffiths, 5th ed., §§4.3–4.4 · constitutive laws and dielectric work

Electrostatic field theory and measurement · 11. From mobile ions to screening lengths and differential double-layer capacitance

A charged planar wall in an electrolyte can be studied without assuming a capacitance in advance. Diffusion and electrostatic drift first establish an ion cloud. The charge–voltage slope of that cloud is an experimental output of the model.

An electric field competes with entropy of mixing

Take a bulk reservoir containing mobile ions with charges $+e$, $-e$, each at number density n_b. The solvent is a uniform continuum of permittivity ϵ, the bath holds absolute temperature T, and no reactions or Faradaic currents occur at the wall. At thermal equilibrium the electrochemical potential of each species is spatially constant. For an ideal dilute gas of particles it contains $k_B T \ln(n_\pm / n_b)$ from mixing plus electrostatic energy $\pm eV$. Set the bulk potential to zero. Equating the local and bulk electrochemical potentials yields

$$n_\pm = n_b e^{\mp eV/k_B T}.$$

At positive V the negative counterions concentrate and the positive coions are depleted. Total mobile charge is

$$\rho = e(n_+ - n_-) = -2en_b \sinh(eV/k_B T).$$

Substituting into Poisson's equation and defining dimensionless $\psi = eV/(k_B T)$ gives

$$\nabla^2 \psi = \kappa^2 \sinh \psi,$$

$$\kappa^2 = \frac{2e^2 n_b}{\epsilon k_B T}.$$

The parameter n_b is a density of one species, not both together. For a 1:1 salt specified in mol/litre convert to formula units per cubic metre using $1000 N_A$ before substitution. For a mixture the linear screening coefficient generalises to $e^2 \sum_i z_i^2 n_i / (\epsilon k_B T)$, whereas the full nonlinear right-hand side remains a sum of exponentials. An externally maintained reservoir fixes chemical potentials; a sealed very small cell can instead require separate number conservation for every species.

What the small-potential limit predicts and what it neglects

For $|\psi| \ll 1$, replace $\sinh \psi$ by ψ. Above a planar wall at $z = 0$ with prescribed potential V_s and $V \to 0$ far away, the bounded solution is

$$V(z) = V_s e^{-\kappa z}.$$

With the normal into liquid $+\hat{\mathbf{z}}$, the wall displacement is

$$D_z(0^+) = -\epsilon V'(0) = \epsilon \kappa V_s.$$

For a conducting wall with no interior field this equals its free surface charge. Therefore $C_{\mathrm{diff}}/A = d\sigma/dV_s = \epsilon\kappa$, dimensionally a dielectric layer of thickness κ^{-1}. The ionic concentration actually varies continuously; it is not a plate of opposite charge located at that distance.

Integrating charge density $-\epsilon\kappa^2 V(z)$ over $z > 0$ gives

$$-\epsilon\kappa V_s = -\sigma.$$

The screening cloud and wall together are neutral per area. The fraction of compensating charge within distance h is $1 - e^{-\kappa h}$. At one screening length the potential has fallen to $1/e$ and 63.2% of the countercharge has accumulated. For a spherical bead curvature changes this simple relationship between potential ratio and enclosed charge. The ionic constitutive relation is the same, but the spatial Laplacian and collecting area differ.

With $\epsilon_r = 78.5,\ T = 298$ K and 1.00 mM of a fully dissociated symmetric monovalent salt, $n_b \simeq 6.02 \times 10^{23}$ m⁻³ and $\kappa^{-1} \simeq 9.62$ nm. The linear diffuse capacitance is about 0.072 F/m². Increasing concentration fourfold halves the screening length and doubles this capacitance at fixed solvent response. Close to molecular length scales the continuum assumptions and concentration-independent permittivity become progressively questionable, so the square-root law should be tested in the intended concentration range.

Background · How small is a small electrostatic potential?

In a symmetric electrolyte the mean charge term is proportional to $\sinh u$, with $u = ze\psi/(k_B T)$ measured relative to the neutral reservoir. A potential being small in volts gives no absolute criterion: the valence and temperature set the relevant scale. Taylor expansion yields the fractional error in replacing the ionic source by its linearised value,

$$\frac{\sinh u - u}{u} = \frac{u^2}{6} + O(u^4).$$

For roughly 1% local source accuracy this estimate asks for $|u| \lesssim 0.245$. At 298 K it gives about 6.3 mV for monovalent ions and 3.1 mV for divalent ions. This is a criterion on the local differential equation. An integrated charge or differential capacitance can have a different relative error and merits its own check.

Solve the nonlinear planar boundary problem

With planar symmetry $\psi'' = \kappa^2 \sinh\psi$. Multiply both sides by ψ' and integrate from the remote bulk where $\psi, \psi' \to 0$. This gives

$$\tfrac{1}{2}(\psi')^2 = \kappa^2(\cosh\psi - 1) = 2\kappa^2 \sinh^2(\psi/2).$$

Choose the branch $\psi' = -2\kappa \sinh(\psi/2)$, which decays to zero for either sign of surface potential. The identity $d \ln|\tanh(\psi/4)|/d\psi = [2\sinh(\psi/2)]^{-1}$ turns the separated equation into

$$\tanh\frac{\psi(z)}{4} = \tanh\frac{\psi_s}{4}\, e^{-\kappa z}.$$

The physical potential itself is not a simple exponential at finite bias. Its distant tail has the same decay length but extrapolates back to a different amplitude $4\tanh(\psi_s/4)$ in dimensionless units. A far-field slope can therefore recover κ, while a linear extrapolation of its intercept underestimates large surface potentials. The nonlinear solution reduces continuously to the linear one because $\tanh x \sim x$.

At $z = 0$, using $D_z = -\epsilon k_B T \psi'/e$ gives

$$\sigma(V_s) = \frac{2\epsilon\kappa k_B T}{e}\sinh\left(\frac{eV_s}{2k_B T}\right),$$

$$\frac{C_{\mathrm{diff}}}{A} = \epsilon\kappa\cosh\left(\frac{eV_s}{2k_B T}\right).$$

The first relation is odd in surface voltage and the differential capacitance is even for this symmetric salt model. Increasing voltage concentrates counterions and allows more charge per further voltage increment. For $V_s = 50$ mV at 298 K, $V_s/(2k_BT/e) \simeq 0.973$. The differential capacitance is about 1.51 times its zero-bias value, while the secant ratio σ/V_s is only about 1.17 times that value. A small AC perturbation superposed slowly about a DC bias measures the differential slope if ionic transport remains equilibrated.

An independent mechanical check of the nonlinear field

The ideal mobile ions have an osmotic pressure excess relative to the reservoir $\Delta p = k_B T(n_+ + n_- - 2n_b) = 2n_b k_B T(\cosh\psi - 1)$. From the first integral the electrical normal stress magnitude $\epsilon E^2/2$ equals this excess. Thus $\Delta p - \epsilon E^2/2$ is spatially constant and vanishes in the bulk of the isolated-wall problem. One can derive the same result by differentiating the pressure: $d\Delta p/dz = \rho E$ at equilibrium. The cancellation provides a sensitive joint test of the ion distribution and the potential gradient.

Confine electrolyte between two equal positively biased parallel walls instead. By symmetry $E = 0$ at the midplane but ψ_m generally remains positive. The constant excess normal pressure is then $2n_b k_B T(\cosh\psi_m - 1) > 0$. Overlap of the diffuse layers produces a repulsive osmotic force per area in this mean-field model. With large separation the midplane potential tends to zero and so does that force. A solution built by naively superposing two high-voltage nonlinear wall profiles will generally violate the constant-pressure test.

Separate a near-wall compact layer from the diffuse response

A finite exclusion distance for ion centres near a real electrode can be modelled at first by a compact dielectric layer of capacitance per area c_s. Its voltage drop is σ/c_s; the diffuse layer starts at potential V_d. For applied bias measured relative to the bulk and a chosen neutral reference,

$$V_{\mathrm{app}} = V_d + \sigma(V_d)/c_s.$$

Differentiate with respect to surface charge:

$$\frac{1}{c_{\mathrm{meas}}} = \frac{1}{c_s} + \frac{1}{c_d(V_d)}.$$

The diffuse constitutive relation must use V_d, not the entire applied voltage. For $c_s = 0.20$ F/m² and low-bias $c_d = 0.072$ F/m², the measured capacitance is about 0.053 F/m². Even as c_d grows, this simple series model cannot exceed c_s. It offers a physically distinct explanation for a measured saturation, alongside finite ion size, adsorption, dielectric variation and other model extensions. A static capacitance measurement alone cannot uniquely distinguish all of them.

Use layer overlap to infer a mechanical force independently of capacitance

Consider identical parallel electrodes at $z = \pm H$, held at the same small positive potential V_s relative to a salt reservoir in chemical equilibrium with the gap. Neither electrode is an ordinary reference for the other: a voltage meter connected only between them reads zero while each diffuse layer experiences a nonzero potential relative to the reservoir. Under the linear screening approximation the potential obeys $V'' = \kappa^2 V$. Reflection symmetry enforces $V'(0) = 0$. Matching both wall potentials gives $V(z) = V_s \cosh(\kappa z)/\cosh(\kappa H)$, so the midplane voltage is

$$V_m = V_s/\cosh(\kappa H).$$

The magnitude of free charge per area on each inner electrode face is $\epsilon\kappa V_s \tanh(\kappa H)$. At large H each plate recovers its isolated-wall charge. At small H the whole gap is nearly at V_s, so very little normal field is required to maintain it and each facing surface carries less charge. This behaviour differs from two oppositely biased plates, whose nearly uniform internal field grows as their separation decreases. The reservoir reference and voltage symmetry decide which experiment is being performed.

To leading nonzero order in V_s, the osmotic excess force per area between these identical walls can be found at the field-free midplane. There it is $2n_b k_B T(\cosh\psi_m - 1) \simeq n_b k_B T \psi_m^2 = \epsilon\kappa^2 V_s^2/[2\cosh^2(\kappa H)]$. Why use a term quadratic in V_s when the potential was found linearly? The pressure's zeroth-order excess vanishes and the first-order ionic density changes cancel between opposite species. Its first measurable correction is quadratic. The cubic error in the linear potential changes the computed pressure only at fourth order in V_s, making the mixed expansion consistent.

For $\kappa^{-1} = 10$ nm, $\epsilon = 78.5\epsilon_0$ and $V_s = 5.0$ mV, at half-gap $H = 10$ nm the predicted repulsive pressure is about 36.5 Pa. At $H = 20$ nm it drops to roughly 6.14 Pa. The potential rose by only a few millivolts yet its ionic osmotic consequence extends across the entire overlap region. As H becomes large, $\cosh^{-2}(\kappa H) \simeq 4e^{-2\kappa H}$, giving exponential decay with the full separation $2H$. This is a force measurement of the same screening scale measured independently by a voltage probe. Surface

roughness, salt exclusion and adsorption can influence a real nanometre-scale force curve and should be distinguished from deviations in the bulk screening length.

If the electrode charges rather than their potentials are fixed, the wall derivative is prescribed. The even solution then has $V_m = \sigma/[\epsilon\kappa \sinh(\kappa H)]$ in the linear regime, and pressure $\sigma^2/[2\epsilon \sinh^2(\kappa H)]$. As H shrinks the linear approximation will eventually fail for fixed nonzero σ, because V_m grows. Comparing the constant-potential and constant-charge formulas without adjusting their boundary conditions could suggest contradictory predictions where each applies to a different experiment.

Estimate how quickly the ion cloud can follow a capacitance measurement

Static Poisson–Boltzmann theory assumes ions are in equilibrium at each measured voltage. A time-dependent measurement can test that assumption. For dilute symmetric monovalent ions with equal diffusivity D_i, small density perturbations obey the linearised number fluxes $\mathbf{j}_\pm = -D_i[\nabla \delta n_\pm \pm e n_b \nabla V/(k_B T)]$, combining diffusion with electric drift. Assume no bulk reactions. Subtract the two continuity equations and multiply by e, yielding a charge-current density $\mathbf{J} = -D_i[\nabla \rho + 2e^2 n_b \nabla V/(k_B T)]$. Use $\nabla^2 V = -\rho/\epsilon$ in the bulk to obtain

$$\partial_t \rho = D_i(\nabla^2 \rho - \kappa^2 \rho).$$

A spatial harmonic of wavenumber k decays at rate $D_i(k^2 + \kappa^2)$ in the unbounded linear bulk model. The long-wavelength Debye charge-relaxation time is $\tau_D = 1/(D_i \kappa^2)$, also recovered by dividing permittivity by the dilute ionic conductivity $\sigma_{\text{ion}} = 2e^2 n_b D_i/(k_B T)$. The total salt-density perturbation instead obeys ordinary diffusion because the leading positive and negative drift terms cancel. Fast local charge relaxation and slower redistribution of neutral salt are different observables.

For $D_i = 1.0 \times 10^{-9}$ m²/s and $\kappa^{-1} = 10$ nm, this local time is 100 ns, corresponding to an angular rollover scale $1/\tau_D = 10^7$ s⁻¹ or ordinary frequency about 1.6 MHz. Blocking electrodes in a cell of thickness $L \gg \kappa^{-1}$ can display a slower charging time. Estimate its series resistance $R = L/(\sigma_{\text{ion}} A)$ and diffuse capacitance $C \sim \epsilon\kappa A$ for one interface. Their product is of order $L/(D_i \kappa)$. For $L = 100$ µm with the preceding parameters this is about 1 ms, orders of magnitude above the local bulk time. Two identical interfaces in series supply an extra numerical factor; finite reservoirs and unequal mobilities can introduce further scales.

A low-frequency impedance experiment interpreted as the equilibrium $d\sigma/dV$ must therefore allow the actual circuit and cell to charge, not merely wait several local Debye times. Varying cell spacing helps distinguish a geometry-dependent charging time from an intrinsic screening-length change. This diffusion calculation and the static pressure calculation share the same κ, giving independent checks on a physical fit to voltage, force and time-resolved measurements.

Check reservoir and continuum assumptions using actual particle numbers

The grand-canonical ion profiles implicitly allow the diffuse layers to draw particles from a large reservoir without changing the reservoir's chemical potentials. Whether this is reasonable can be checked with a dimensioned inventory. For a 1 mM monovalent salt, each species has about 6.02×10^{23} particles per cubic metre. A cell of area 1 mm² and depth 100 µm therefore starts with 6.02×10^{13} ions of each species. A surface charge density of 1.0 mC/m² on one plate amounts to 6.24×10^{9} elementary charges on that area. Even a conservative estimate in which each net countercharge requires one ion from the bulk uses only about 10^{-4} of the available counterions.

Keep the same area and salt concentration but reduce the gap to 20 nm. Now only 1.20×10^{10} ions of each species occupy the cell initially. The same surface charge is comparable with half the inventory of one species. The remote-neutral-reservoir approximation is no longer automatically credible, especially if both walls attract counterions of the same sign. One must specify how ions and compensating charge can enter or leave, what the electrodes' chemical or electrical preparations enforce, and how much fluid actually belongs to the reservoir. An applied electrostatic boundary voltage fixes no ionic chemical potential by itself.

For a sealed cell write the equilibrium densities instead as $n_{\pm}(z) = A_{\pm} \exp[\mp eV(z)/(k_B T)]$. The constants $A_{\pm}$ must be chosen so that integrals of $n_{\pm}$ over the physical volume equal the known numbers of each species. Substitution into Poisson's equation gives a coupled boundary problem with two additional global constraints. Adding a constant to V and appropriately rescaling $A_{\pm}$ leaves the densities unchanged; electrical reference and chemical normalisation must be chosen consistently. A calculation holding both fixed bulk densities and exact sealed inventories can be overconstrained if diffuse layers hold appreciable salt.

The continuum approximation also makes a statement about scale. A cube of side one screening length near 10 nm at 1 mM holds roughly 0.60 ions of either species on average. This does not by itself invalidate a mean density for a large planar electrode, which averages over many lateral regions and thermal configurations. It does warn against interpreting the smooth one-dimensional density as a snapshot of a single nanometre-sized volume with a deterministic fractional particle. Force or voltage measurements with different lateral averaging areas can show quite different fluctuations even when their mean profiles follow the same equation.

As another self-check compare the predicted contact concentration with available molecular packing. The ideal theory gives

$$n_{\mathrm{counter}}(0) = n_b e^{|\psi_s|}.$$

Starting from 1 mM, a surface potential near 0.25 V at 298 K would multiply concentration by roughly 1.7×10^{4}, corresponding to tens of molar even before allowing room for solvent. A molecular model or a measured finite-size constitutive relation is then more appropriate for quantitative contact density. The failure is in extrapolating the dilute ideal entropy, not in Gauss's law or the electrostatic boundary condition. Source, solvent, reservoir and detector scales determine where the otherwise elegant analytic solution becomes an approximation to test.

Resolve a screening length

Compare the linear screened profile with a grid solution as the ratio of thickness to screening length grows. Separate failure to resolve the layer from failure of the linear material law.

Open this experiment online

Try the calculation

Cells across slab **16**

Gap / screening length **4**

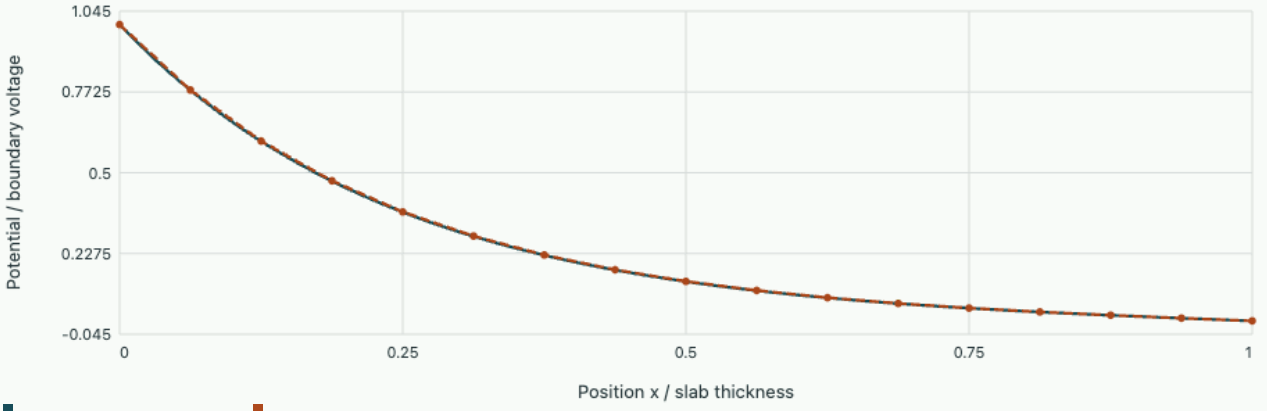

Continuum slab Solved grid values

Midpoint 0.13357, exact 0.1329. Discrete decay constant × thickness = 3.9897.

Download the OneSimulation model

In your OneSimulation environment, run the model with these inputs.

```
python field-laboratory.py screen --cells 16 --contrast 4
```

How many excess ions, not just how much net charge?

Count the salt adsorbed in a planar diffuse layer

The total countercharge per area equals the negative surface charge. Separately calculate the excess number of ions of both signs over the neutral bulk value for a symmetric electrolyte at prescribed surface potential. Which quantity changes sign if the wall voltage reverses?

▼ **Derive and check the result**

Define $\Gamma = \int_0^\infty [n_+(z) + n_-(z) - 2n_b]\, dz = 2n_b \int_0^\infty (\cosh\psi - 1) dz$. The integrand is nonnegative for either sign of wall voltage. For $\psi_s > 0$, substitute $dz = -d\psi/[2\kappa \sinh(\psi/2)]$ from the first integral. Then $\cosh\psi - 1 = 2\sinh^2(\psi/2)$ makes the resulting integral elementary. The result, also valid at negative

bias by symmetry, is $\Gamma = (4n_b/\kappa)[\cosh(\psi_s/2) - 1]$. It has units particles per area. The signed excess charge divided by elementary charge, in contrast, is

$$-\sigma/e = -(4n_b/\kappa)\sinh(\psi_s/2).$$

For positive surface charge the negative counterion excess and positive coion depletion follow by taking half the sum and difference of these two measurements. At small ψ_s, the net charge excess is linear in voltage while Γ is quadratic: the two ion species redistribute in opposite directions before appreciable neutral salt adsorption appears. Reversing the bias swaps which species is enriched but leaves the total ion-number excess unchanged. Thus a mass-sensitive and a charge-sensitive measurement give complementary responses even in the same equilibrium model.

At $\psi_s = 2$,

$$\Gamma/[|\sigma|/e] = [\cosh 1 - 1]/\sinh 1 = \tanh(1/2) = 0.462.$$

The total excess count can be smaller than the magnitude of countercharge measured in elementary charges because some compensation occurs through removing coions rather than adding counterions. An optical concentration measurement that tracks only total dissolved ion count cannot be converted into net countercharge by multiplying by e. Sampling both quantities, or calibrating the signal against the appropriate species, is needed to test the adsorption prediction. The derivation assumes the same dilute reservoir as the planar Poisson–Boltzmann solution and should not be applied unmodified to a cell with fixed small ion inventories.

Tutorial · infer a screening length and check the model

Use two potential measurements at finite bias

In a 298 K symmetric electrolyte, $\tanh[eV(z)/(4k_BT)]$ decreases from 0.30 to 0.15 over 8.0 nm. Infer the screening length, and reconstruct the two physical voltages. Why is taking a raw voltage ratio slightly different?

▼ Work through the solution

The transformed profile decays exponentially, so

$$\kappa^{-1} = 8.0/\ln 2 = 11.54\,\text{nm}.$$

Since $4k_BT/e \simeq 102.7$ mV, the voltages are $102.7\,\text{artanh}(0.30) = 31.8$ mV and $102.7\,\text{artanh}(0.15) = 15.5$ mV. Their physical ratio is about 0.488 rather than 0.500. Inferring a linear-log decay using only these points gives a biased length. Repeating at smaller voltages would test convergence towards the same result without assuming the nonlinear transformation.

Which capacitance was measured?

At low bias a diffuse model independently predicts 0.080 F/m² but a low-frequency measurement gives 0.050 F/m². Infer the compact capacitance of the ideal series model. What would make this inversion impossible with positive capacitances?

▼ **Work through the solution**

From the reciprocal difference $1/c_s = 20 - 12.5 = 7.5$ m²/F we obtain $c_s = 0.133$ F/m². A measured capacitance larger than the predicted diffuse one would imply a negative reciprocal compact capacitance in this two-positive-series model. Check the normalisation area, frequency response, adsorption or additional parallel charging processes before assigning a negative parameter. To distinguish the two capacitances experimentally, vary reservoir concentration at fixed temperature and compare the predicted $\sqrt{n_b}$ trend of the diffuse contribution with the remaining offset in reciprocal capacitance.

Further reading

- Compare planar screening to a spherical bead
- Cambridge Electromagnetism, chapter 6 · screening and electrostatics of mobile charge

Electrostatic field theory and measurement · 12. Reconstructing a source from noisy voltage measurements

A forward electrostatic calculation can be unique and stable while the inverse problem constructed from it is unstable or nonunique. A scanned electrode, a finite collecting area and an explicitly chosen noise level make these statements experimentally testable.

Write down what the instrument actually measures

Pattern a long electrode at $z = 0$ with an unknown voltage $f(x)$, periodic over length L for this model. The region above is homogeneous, charge free, and contains a sufficiently weak probe at height h. For a Fourier component $f_m e^{ik_m x}$, $k_m = 2\pi m/L$, the bounded harmonic solution at height h is $f_m e^{-|k_m|h} e^{ik_m x}$. Treat the constant component according to the actual reference. Suppose the probe reports an average over a rectangular window of width w centred at x_j, plus noise e_j. For uniform probe sensitivity the forward relation is

$$y_j = \sum_m H_m f_m e^{ik_m x_j} + e_j,$$

$$H_m = e^{-|k_m|h}\,\mathrm{sinc}(k_m w/2),$$

$$\mathrm{sinc}\, t = \frac{\sin t}{t}.$$

The exponential is physical propagation from boundary to probe; the sinc factor is averaging by the detector. The latter has exact zeros in this idealised model. For modes at those zeros no noise-free reading at the same width and height can recover the lost amplitude. More closely spaced scan positions increase the sampling bandwidth but cannot undo either such instrumental nulls or the exponential decrease of the true high-frequency signal.

A nonuniform probe shape replaces the sinc by its Fourier transform. Unknown height adds an additional calibration problem: increasing h and increasing high-frequency boundary amplitudes can yield the same readings if the amplitudes are unrestricted. Before inferring boundary detail, calibrate the probe width and decide whether height is known, measured with uncertainty or jointly estimated using an independent constraint.

A direct inverse amplifies uncertainty in predictable bands

In an ideal complete periodic scan the discrete Fourier transform separates resolvable modes. Let $\hat{y}_m = H_m f_m + \eta_m$. Inverting one coefficient gives $f_m^{\mathrm{dir}} = \hat{y}_m / H_m$ whenever $H_m \neq 0$. A perturbation $\delta\hat{y}_m$ becomes

$$\delta f_m = \delta\hat{y}_m / H_m.$$

With $H_m = e^{-|k|h}$, the amplification grows exponentially with spatial frequency. The mode values can be uniquely determined in ideal noiseless data of infinite precision, yet the inverse is unbounded as increasingly fine modes are admitted. Finite data can additionally produce exact nonuniqueness.

For $h = 2.0$ mm and negligible aperture, boundary wavelengths 20, 10 and 4 mm have transfers $0.533, 0.285, 0.0432$, respectively. With 1 mV noise in the measured amplitude of each Fourier component, inverse noise levels are $1.87, 3.51, 23.1$ mV. A genuine 10 mV boundary ripple at wavelength 4 mm contributes only 0.432 mV at the probe, smaller than that noise. Plotting its raw inverted coefficient with a smooth line does not improve its information content. Reducing height to 1 mm raises that ripple's signal to 2.08 mV and changes the experiment's resolving power before any reconstruction choice is made.

Derive a regularised inverse and expose its bias

Assume coefficients are inferred separately and use a quadratic penalty. For each m, minimise $J_m = |H_m f - \hat{y}_m|^2 + \alpha^2 w_m^2 |f|^2$ with positive weights w_m and positive regularisation parameter α. Splitting real and imaginary parts, or differentiating with respect to f^*, gives

$$\widehat{f}_m = \frac{H_m^* \hat{y}_m}{|H_m|^2 + \alpha^2 w_m^2},$$

$$W_m = \frac{|H_m|^2}{|H_m|^2 + \alpha^2 w_m^2},$$

$$\mathbb{E}[\widehat{f}_m] = W_m f_m$$

for zero-mean measurement noise. The reconstruction suppresses noise near a small transfer by introducing deterministic bias $(W_m - 1) f_m$. Its variance for known mode-noise variance s_m^2 is $|H_m|^2 s_m^2 / (|H_m|^2 + \alpha^2 w_m^2)^2$. Neither low variance alone nor a small data residual is evidence that a spatial ripple was recovered. Setting α very large produces a smooth, nearly zero estimate regardless of the data. Setting it very small can reproduce noise almost exactly.

For $w_m = 1, \alpha = 0.10$ and wavelength 4 mm in the example above, $W_m \simeq 0.157$. A true 10 mV ripple is estimated at only 1.57 mV on average. The inversion gain is about 3.64 rather than 23.1. At 20 mm, the same penalty retains 96.6% of the true amplitude. If the purpose is to quantify a short ripple, improving the experiment can be preferable to changing the penalty. A derivative penalty $w_m \propto |k_m|$ encodes a stronger preference against fine structure; a constant mode must be handled separately if the voltage reference or the derivative penalty leaves it unconstrained.

What survives away from a uniform grid or simple geometry?

For arbitrary electrode shapes and detector positions, represent source or boundary data in a chosen basis $f = \sum_j a_j b_j$. Solve the forward field problem for each unit coefficient and sample it exactly as the real probe would, giving matrix entries A_{ij}. A noise covariance Σ weights the misfit through $\|\Sigma^{-1/2}(A\mathbf{a} - \mathbf{y})\|^2$. For an identity penalty apply the singular-value decomposition to the whitened matrix,

$$\Sigma^{-1/2} A = U S V^*.$$

Each right singular vector is a source pattern; its singular value tells how strongly it appears in the whitened measurement space. Multiplication by U^* diagonalises the data misfit and reduces the problem to the scalar filters above.

A zero singular value means the chosen sensors are insensitive to an entire source combination. No choice of numerical precision or regularisation changes that observational fact. A small nonzero value means one needs sufficiently small noise and modelling errors to identify the corresponding component. A practical resolution matrix $R = (A^*\Sigma^{-1}A + \alpha^2 I)^{-1}A^*\Sigma^{-1}A$ maps a noiseless true coefficient vector to the regularised estimate. A column of R shows which neighbouring coefficients respond when one ideal source coefficient is present. Testing such impulse responses describes the reconstruction's spatial smoothing more honestly than quoting the spacing of its output grid.

Use withheld measurements and identifiable physical quantities

Reserve some independently measured positions, heights or probe widths. Fit the rest and use the recovered candidates to predict the withheld measurements by applying the forward operator. The test is more informative when the withheld observations have different sensitivity patterns. A second distant scan can verify low modes while remaining insensitive to every high-frequency ambiguity. A second close scan or a different probe width can fill modes attenuated or nulled by the first. Correlated calibration errors, such as one common voltage offset, should be modelled as such, rather than being counted as many independent observations.

A distinct nonuniqueness occurs when trying to infer an arbitrary three-dimensional charge density solely from exterior voltages. Take any smooth compactly supported potential $g(\mathbf{x})$ inside the source region whose value and derivatives vanish outside. Add $\delta\rho = -\epsilon_0\nabla^2 g$ to a candidate charge distribution. Its induced potential is g and therefore vanishes at every external detector. Unless additional sign, support or constitutive assumptions constrain the source, infinitely many internal distributions remain consistent with exact exterior data. This is stronger than amplification of measurement noise. Total charge from a closed-surface flux or low multipole moments can still be identifiable when the internal density is not.

See an ill-conditioned inverse in a two-source instrument

Two possible source patches sit symmetrically beneath two voltage probes. A calibrated forward response, in volts of probe signal per chosen source unit, is $A = \begin{pmatrix} 1 & 0.98 \\ 0.98 & 1 \end{pmatrix}$. Each patch affects both probes almost equally. The sum pattern $(1, 1)/\sqrt{2}$ and difference pattern $(1, -1)/\sqrt{2}$ are orthonormal eigenvectors as well as singular vectors, with gains 1.98 and 0.02. The condition number is 99. The instrument localises total source strength much more reliably than it locates its division between the two patches.

Suppose the actual source vector is $(1, 0)$. The predictions are $(1.00, 0.98)$ V. A measurement perturbation $(+0.01, -0.01)$ V, though small compared with the signal, lies in the weak difference mode. The exact inverse interprets it as source error $(+0.50, -0.50)$, giving a reconstructed distribution $(1.50, -0.50)$. A common perturbation $(+0.01, +0.01)$ instead produces almost negligible source

changes $+0.00505$ each. A single rms error statistic for the voltage readings misses how their spatial correlation changes uncertainty in the reconstruction.

Use an identity Tikhonov penalty $\alpha = 0.10$. The response factors for the two true source directions become

$$W_{+} = 1.98^2/(1.98^2 + 0.10^2) = 0.9975,$$
$$W_{-} = 0.02^2/(0.02^2 + 0.10^2) = 0.0385.$$

In the absence of noise the estimated source from $(1, 0)$ is approximately $(0.518, 0.480)$. Both patches light up almost equally. This is the resolution matrix in action: the model predicts the observed voltages well yet cannot confidently identify which of the two patches generated them. Under the same opposite noise perturbation the additional reconstructed difference is only 0.0192 on each patch in opposite directions. A visually smooth result is reproducible but biased towards nearly equal strengths.

Add a third probe designed to respond as $(0.6, -0.6)$. This linear combination may be implemented physically by a differential electrode, so negative coefficients are meaningful. The squared singular gain of the old difference direction increases from 0.0004 to $0.0004 + 2(0.6)^2 = 0.7204$, while the common gain is unchanged. The new difference singular value is 0.849, reducing the ratio of the largest to smallest singular values to about 2.33 if the three channels have comparable independent noise in the specified units. Adding another copy of the first common-sensitive probe would have been much less effective. Designing measurements against the weak singular vector can improve source resolution far more than collecting many redundant readings.

Separate numerical error from height uncertainty and unknown backgrounds

Return to a sinusoidal source with negligible aperture. If its true height is h but one divides by an assumed transfer computed at $h + \delta h$, then even exact noiseless data return $\widehat{f}/f = e^{|k|\delta h}$. For a 4 mm wavelength and positive height error 0.10 mm, the fractional amplitude bias is

$$e^{0.157} - 1 = 17.0\%.$$

Unlike random noise this bias does not shrink by averaging repeated scans at the same miscalibrated height. A 20 mm calibration pattern at that same error suffers only about 3.2% bias, so testing one long-wavelength standard need not guarantee short-wavelength accuracy.

For an unknown but stable boundary pattern recorded at two known relative probe heights, $\hat{y}_m(h_2)/\hat{y}_m(h_1) = e^{-|k_m|(h_2 - h_1)}$ for modes above noise when the aperture is unchanged. The source amplitude and common aperture factor cancel. This measures a relative vertical displacement but not the absolute height if the true boundary amplitudes are unknown. Add a calibration electrode of known voltage and wavelength, or an independently measured mechanical height, to determine the absolute scale. Near a sensor's aperture zero the ratio is exceptionally noise sensitive and should not be used for the height fit.

Consider also a slowly varying stray background produced by distant conductors. In a source-free layer of finite thickness a Fourier mode can contain both $Ae^{-|k|z}$ and $Be^{+|k|z}$. The growing term is excluded in a bounded half-space continued to infinity, but can represent a field launched from the upper boundary of a finite domain. For a single spatial mode measured at two heights one can solve a 2×2 system for A, B. Its determinant is $2\sinh[|k|(h_2 - h_1)]$, up to a sign fixed by the column order. As the two heights coalesce their rows become nearly dependent. A measurement showing unexpected height scaling may thus indicate the wrong outer boundary in the forward model rather than a faulty inverse algorithm.

A reproducible inverse analysis can be audited along three independent axes. First manufacture noise-free readings from a source whose exact forward voltage is known, then refine only the forward discretisation. Second add noise with a specified amplitude and covariance and repeat enough draws to estimate recovered variation in identified modes. Third perturb physical nuisance parameters such as probe width, height and background independently of the noise draws. For each stage state what quantity is being recovered: total charge, a few spatial coefficients, or a real-space image biased by a chosen penalty. These stages expose different error mechanisms even when they yield similar changes in a plotted voltage trace.

Build an exactly invisible internal charge perturbation

The general construction of a silent source can be made explicit for a spherical support of radius a. Pick a smooth interior potential perturbation $g(r) = V_g[1 - (r/a)^2]^3$ for $0 \le r < a$, and set $g = 0$ outside. At $r = a$ both the potential and its first radial derivative vanish; its second radial derivative also approaches zero, avoiding unmodelled surface sheets. It is regular at the origin. Therefore g itself is the potential relative to infinity of the compact charge distribution $\delta\rho = -\epsilon_0 r^{-2} d(r^2 g')/dr$. With $x = r/a$, expansion gives

$$\delta\rho = \frac{\epsilon_0 V_g}{a^2}(18 - 60x^2 + 42x^4), \qquad 0 \le x < 1.$$

The perturbation is positive near the centre and negative in an outer band if $V_g > 0$. Its enclosed charge is

$$-4\pi\epsilon_0 r^2 g' = 24\pi\epsilon_0 V_g a\, x^3(1 - x^2)^2.$$

It vanishes at both ends of the radius interval and is positive at intermediate radii. Gauss's law outside then gives exactly zero electric field and the chosen reference gives zero exterior voltage. A numerical inverse recovering only zero perturbation from exterior data is observationally consistent with both the absence of charge and this particular structured distribution. Integrating the polynomial with its correct $4\pi r^2 dr$ weight confirms the exact zero total charge independently.

For $a = 20$ mm, $V_g = 0.10$ V, the internal centre voltage differs by 100 mV while every ideal exterior detector, no matter how accurately calibrated, records no difference whatsoever. At $r = a/2$, $g = 0.0422$ V and the enclosed perturbation charge is 9.39×10^{-14} C. An internal measurement can therefore break this particular ambiguity. Moving external probes closer while keeping them outside the sphere cannot. Positivity restrictions on the total density can reduce ambiguity, but adding a sufficiently small signed

perturbation to a sufficiently positive background can preserve nonnegativity of both candidate densities and still leave their exterior data identical.

This example suggests a practical way to report results when full source reconstruction is impossible. Ask whether the quantity of interest changes along a silent perturbation. Total charge and all external moments stay unchanged here, whereas the central voltage and internal charge profile change. A claim about total charge can be appropriate even when detailed shell-by-shell densities are not identifiable. Conversely a fitted compact central peak may depend on the chosen smoothness penalty or positivity constraints even when every reported exterior measurement is reproduced.

A multiscale numerical exercise can demonstrate the effect reproducibly. Discretise both g and its associated $\delta\rho$, solve the independent forward Poisson problem, and evaluate internal and external probes. Coarse grids may show a small exterior signal if source deposition fails to preserve its neutral moments. Refine the source representation, plot the exterior residual separately from the interior voltage difference and compare with the analytic polynomial. A residual that tends to zero while the interior difference remains finite is the expected physical outcome. Using exactly the same discrete operator to manufacture data and to recover them can mask representation errors, so a second mesh, an analytic source integral or a differently implemented forward solver is especially valuable.

See which part of a specimen electrodes can resolve

Compare two contact configurations and their sensitivity to a local material change. An accurate potential at the electrodes does not necessarily resolve the interior.

Open this experiment online

Try the calculation

Inclusion depth (mm) 8

Sensing half-spacing (mm) 5

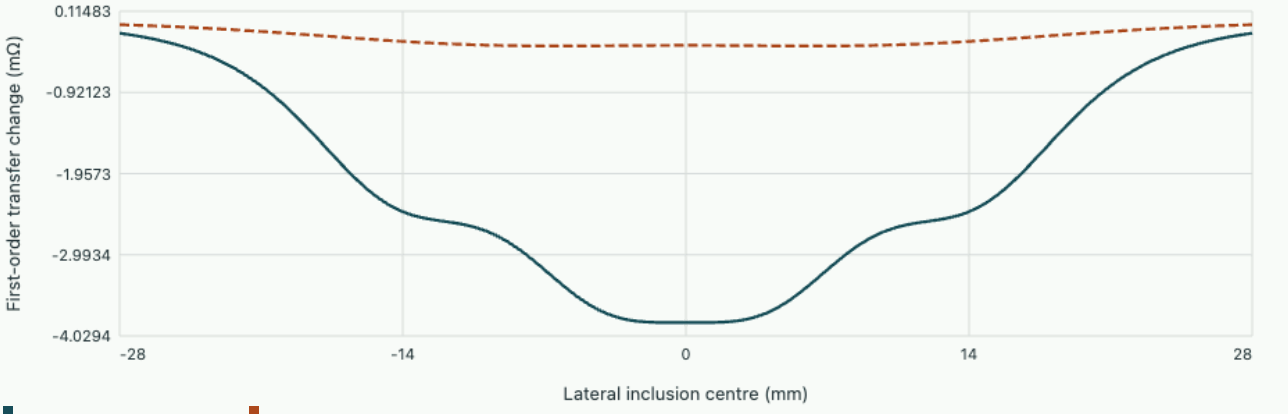

Centre perturbation -3.858 mΩ; unperturbed transfer 79.58 Ω. Sphere radius 1 mm, conductivity increase 0.020 S/m.

Can two independent estimates agree for the wrong reason?

Separate common uncertainty from independent noise in two height scans

A probe measures a 10 mm wavelength mode at heights 1.0 and 2.0 mm with negligible aperture. The two Fourier amplitudes are 5.34 and 2.85 mV, each with independent 0.10 mV random uncertainty, but they share an unknown common voltage gain. Estimate the boundary amplitude and its random error under unit gain. Decide what the agreement can establish about calibration.

▼ **Derive and check the result**

The two transfers are

$$H_1 = e^{-0.2\pi} = 0.5335,$$
$$H_2 = e^{-0.4\pi} = 0.2846.$$

Each individually predicts about 10.0 mV at the boundary. For independent equal-variance amplitude noise, minimise $\sum (y_i - H_i f)^2$. Its solution is $f = (H_1 y_1 + H_2 y_2)/(H_1^2 + H_2^2)$, and random standard deviation $0.10/\sqrt{H_1^2 + H_2^2} = 0.165$ mV. Simply averaging the two directly inverted amplitudes gives the noisier second inversion equal weight and hence a larger variance.

The measured amplitude ratio is about 0.534, as predicted by the additional 1 mm of propagation. A common multiplicative calibration factor cancels from this ratio. If the true voltage gain were 1.10, both unit-gain inversions would agree at about 10 mV even though the physical amplitude would be 9.1 mV. Repeated scans reduce the random uncertainty but cannot remove this systematic scale. A known reference electrode or independent calibrated voltage source is needed.

If instead both probes share a small additive voltage offset in every spatial sample, a full ideal Fourier analysis would place that constant entirely in the zero mode. Incomplete sampling, finite windows or background leakage can mix the offset into the fitted sinusoid. Including a constant nuisance term in a weighted least-squares fit is one way to test that effect directly. Identifying the form of a shared error is as important as quoting its magnitude: common gain, common offset and relative height uncertainty enter the inverse problem in different directions and respond to different calibration experiments.

Tutorial · compare an experimental redesign with a stronger prior

Resolve a window null without changing sample spacing

A voltage camera averages over $w = 4$ mm. A suspected boundary pattern has wavelength 4 mm. Find its measured transfer and propose a second window width that recovers sensitivity. Include the effect of a 1 mm measurement height.

▼ **Work through the solution**

At equal aperture and wavelength the sinc argument is π, giving zero. With a 2 mm window the aperture transfer becomes

$$\sin(\pi/2)/(\pi/2) = 2/\pi.$$

Height attenuation is $e^{-2\pi(1/4)} = 0.2079$, so the combined transfer is 0.132. A 20 mV boundary amplitude therefore gives 2.65 mV in the second scan and exactly zero in the first idealised scan. Collecting more centres with the original width would still give zero. Calibrating the second aperture and its orientation is part of the forward model, especially near a sinc null where small geometry errors strongly change inference.

Choose a regularisation level by its permitted bias

For a mode with transfer 0.20 and unit penalty weight, require the mean reconstructed amplitude to retain at least 80% of the true value. Find the allowed maximum α. For 2 mV noise in the measured coefficient, compare inverse standard deviations with and without this penalty.

▼ **Work through the solution**

Set $W = 0.04/(0.04 + \alpha^2) \geq 0.80$. This gives $\alpha \leq 0.10$. At the limiting value the noise gain is $0.20/(0.04 + 0.01) = 4$, so the reconstructed noise standard deviation is 8 mV. Without regularisation the inverse noise is 10 mV. This modest improvement costs a 20% amplitude bias. The calculated tradeoff may or may not be acceptable for the physical question. Stating both numbers allows a reader to decide whether this experiment can support a claimed amplitude difference.

Further reading

- Measure the transfer of two spatial frequencies
- Reconstruct a tensor from finite electrostatic observations
- MIT, Smith · electric-field inversion and models of interacting electrodes
- Christian Clason · Regularization of Inverse Problems, spectral filters and Tikhonov regularisation

Electrostatic field theory and measurement · 13. Which electrode sees a charge moving above a detector?

A point charge moves without touching the electrodes. Derive the induced charge on one strip from a second, source-free boundary problem. Use the two-dimensional map to distinguish motion across the detector from motion away from it.

Exchange the source and the measuring electrode

An infinite conducting plane is split into long parallel strips. The gaps have negligible width and every strip is held at zero potential during the measurement. Put one charge q at (x, z) above the plane. Computing the field separately for every position would be expensive. Instead consider an auxiliary problem with the measuring strip at unit potential, all other strips grounded and no charge above the plane. Call its dimensionless solution w.

Green's reciprocity pairs the electrode potentials of one problem with the charges of the other. The grounded real electrodes make one boundary contribution vanish. The test electrode gives Q_{strip} and the real point source gives $qw(x, z)$. Their sum vanishes, hence $Q_{\mathrm{strip}} = -qw$. For a strip occupying $-a < u < a$, the Poisson kernel of the upper half-plane integrates the boundary value into the interior:

$$w(x, z) = \frac{1}{\pi} \int_{-a}^{a} \frac{z\, du}{(u - x)^2 + z^2} = \frac{\arctan[(a - x)/z] + \arctan[(a + x)/z]}{\pi}.$$

This weighting potential is computed for the electrode geometry. It is independent of the test charge. Its gradient predicts the readout current as a charge travels through different weightings. Infinite strip length and an effectively infinite return plane are the assumptions that permit this two-dimensional construction.

Read a charge and a displacement separately

At the centre and at height $z = a$, the strip subtends a right angle, giving $w = 1/2$. A positive charge of 8 fC induces −4 fC on this electrode. At $x = a, z = a$ the weight is $\arctan(2)/\pi$, about 0.352. The change in measured charge can occur with the same charge and the same height. The peak and width of a lateral scan together carry more positional information than one sample. A finite insulating gap or a grounded back plane would change the boundary problem. A second measurement illustrates why electrode geometry matters for a current signal. Differentiate the central response $w(0, z) = 2 \arctan(a/z)/\pi$, giving $\partial_z w = -2a/[\pi(a^2 + z^2)]$. At $z = a = 1$ mm, an 8 fC charge moving upward at 1 mm/µs changes the induced charge at $+8/\pi$ fC/µs, or $+2.55$ nA. The sign here describes the time derivative of charge on the strip. The sign of an external current reading also depends on the chosen lead direction.

Summing the strip weights over an entire tiled plane gives one because the Poisson kernel integrates to one. Total induced charge on that plane is therefore $-q$, even as charge redistributes between individual electrodes. A finite numerical map can miss the long tails of the weighting function. Enlarge the lateral range and check the sum before interpreting a shortfall as an uncollected signal.

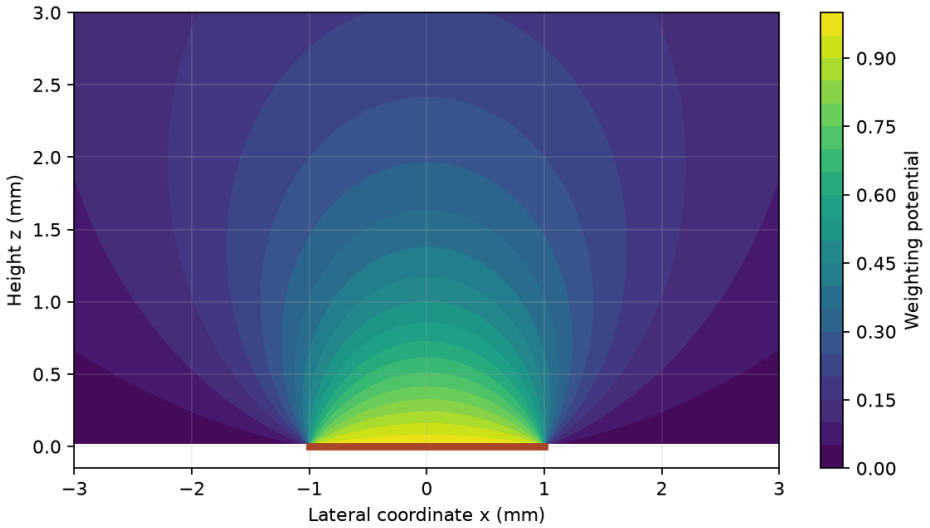

Contours show equal sensitivity to a point charge. The steepest change occurs close to an electrode edge.

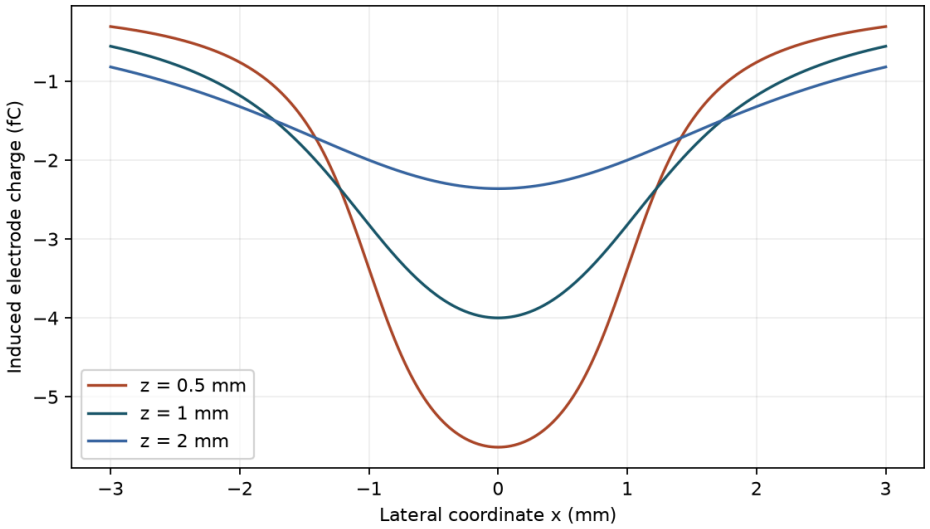

Move the charge at constant height and record the induced charge. The scan width can help distinguish a small nearby charge from a larger distant one.

Exercise · close the charge balance

If the entire plane is read out, how much induced charge do all electrodes collect together?

▼ Work through the solution

The full boundary integral runs from minus infinity to plus infinity. Its arctangent increases by π, so the weights sum to one and the total induced charge is $-q$. In the notebook, add the weights from neighbouring strips and watch the deficit shrink as the readout array grows.

Exercise · infer a height

A known charge above the centre produces a weight of one third. Find the height in units of the half-width.

▼ **Work through the solution**

At the centre $w = 2\arctan(a/z)/\pi$. Thus $a/z = \tan(\pi/6) = 1/\sqrt{3}$ and $z = \sqrt{3}a$. An unknown lateral offset would spoil this one-parameter inversion.

Try it · Strip charge

Change the inputs and compare the recalculated curves with the preceding derivation and baseline figure. The axes give the units; the numerical readout states the model assumptions and any limiting cases. Reset the inputs to return to the reference setting.

Open this live calculation

Try the calculation

Charge height / strip half-width 1

Point charge (fC) 8

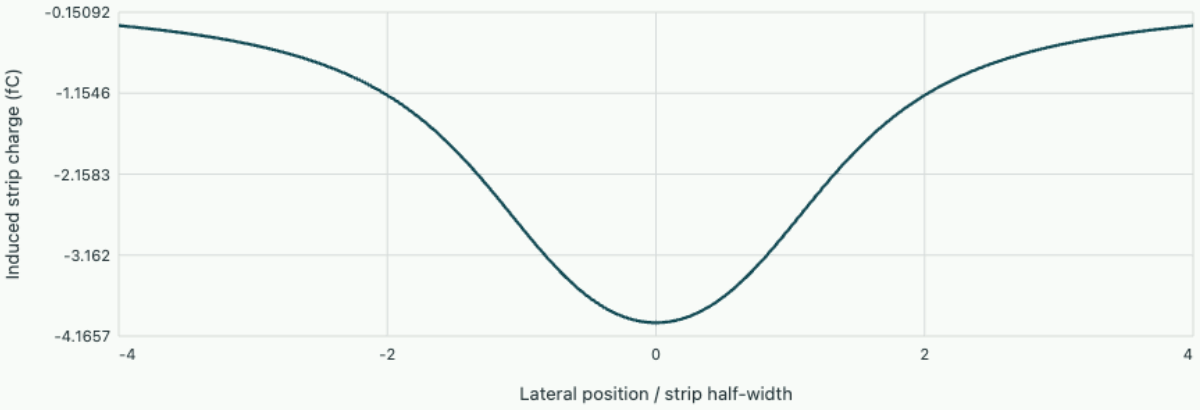

Grounded strip charge

At the centre the electrode receives -4 fC. Reciprocity converts the strip weighting potential into induced charge.

Download the corresponding editable notebook. The browser recalculates the reduced equations directly; the notebook exposes the full calculation and its checks.

Open editable notebook Download .ipynb

Electrostatic field theory and measurement · 14. Build the field operators in curved coordinates

Derive the geometric factors in gradient, divergence, curl and Laplacian, then use dimensional conversion to compare electromagnetic conventions.

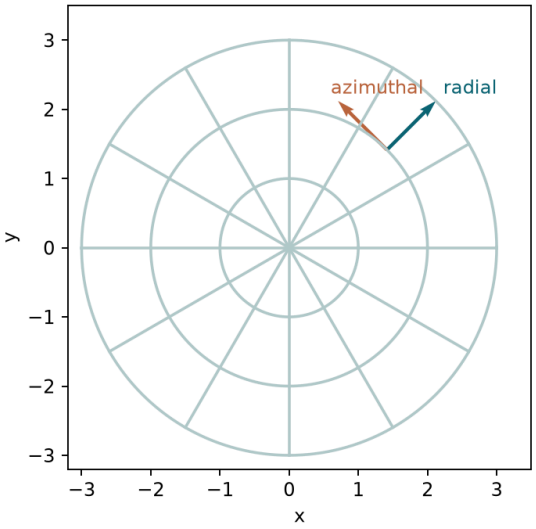

Cylindrical coordinate curves and local radial and azimuthal basis vectors. Equal angular increments span longer arcs at larger radius.

Try it · Cylindrical

Change the inputs and compare the recalculated curves with the preceding derivation and baseline figure. The axes give the units; the numerical readout states the model assumptions and any limiting cases. Reset the inputs to return to the reference setting.

Open this live calculation

Try the calculation

Fixed angle ϕ (degrees) 45

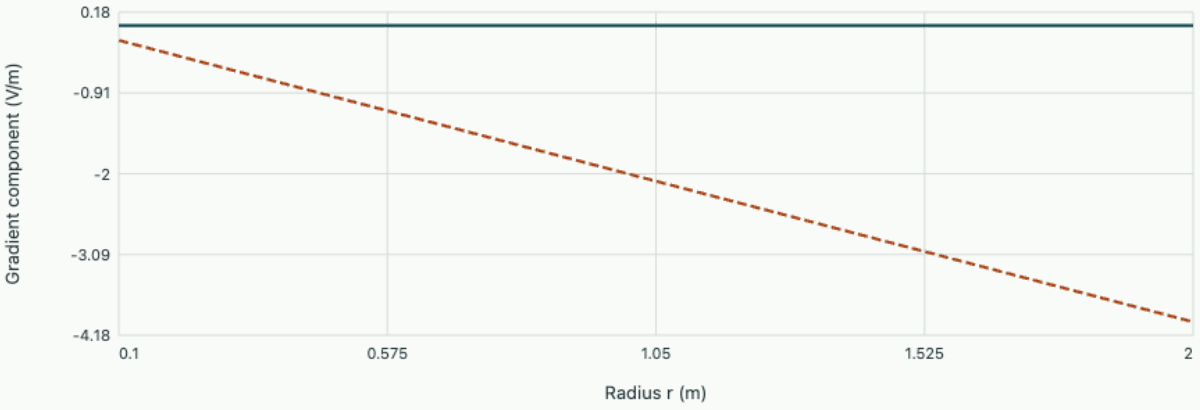

For V = (1 V/m²) r² cos(2ϕ), the Laplacian is zero: radial 4 cos(2ϕ) and angular −4 cos(2ϕ) cancel. The azimuthal derivative needs the metric factor 1/r.

Attach a length to a coordinate increment

Coordinates label points, while differential operators describe spatial change. In a right-handed orthogonal system q_1,q_2,q_3 write the position as r(q). The coordinate tangent vectors are mutually perpendicular. Define $h_i=|\partial r/\partial q_i|$ and unit vectors $e_i=(\partial r/\partial q_i)/h_i$. A small displacement is $\Sigma e_i h_i dq_i$. Matching $dV=\Sigma(\partial V/\partial q_i)dq_i$ with $dV=\nabla V\cdot dr$ gives the gradient.

$$\nabla V = \sum_i \frac{\mathbf{e}_i}{h_i}\frac{\partial V}{\partial q_i},$$

$$d\mathcal{V} = h_1 h_2 h_3\, dq_1 dq_2 dq_3.$$

For cylindrical coordinates (s,ϕ,z), r=(s cosϕ,s sinϕ,z). Differentiation gives h=(1,s,1), e_s=(cosϕ,sinϕ,0) and e_ϕ=(−sinϕ,cosϕ,0). Thus ∂ϕ e_s=e_ϕ and ∂ϕ e_ϕ=−e_s. For spherical coordinates (r,θ,ϕ), direct differentiation gives h=(1,r,r sinθ). The coordinate basis changes direction even if the components of a field stay constant.

Recall · Angle increments are dimensionless

An angular change dϕ corresponds to arc length s dϕ in a cylinder. Accordingly the azimuthal derivative of potential has physical component (1/s)∂ϕV. This has the same units, volts per metre, as ∂sV. Omitting the geometric factor changes both dimensions and the electric field.

Derive divergence by subtracting opposite face fluxes

A small face normal to e_1 has area $h_2h_3dq_2dq_3$. The two opposite faces have different field and potentially different area. Subtract their outward fluxes using a first-order expansion, sum over the three coordinate directions and divide by cell volume.

$$\nabla \cdot \mathbf{A} = \frac{1}{h_1 h_2 h_3}\left[\partial_1(h_2 h_3 A_1) + \partial_2(h_3 h_1 A_2) + \partial_3(h_1 h_2 A_3)\right].$$

The cylindrical radial term is (1/s)∂s(sA_s). The spherical radial term is $(1/r^2)\partial r(r^2A_r)$. These follow from circumference and surface area respectively. For A=Cr e_r in a sphere, the divergence is 3C. A sphere of radius R then encloses flux $4\pi CR^3$, matching the volume integral of 3C.

Derive curl from the oriented boundary of one face

Choose the q_2–q_3 face with positive normal e_1. Circulation along its four edges gives $\partial_2(h_3A_3)-\partial_3(h_2A_2)$, multiplied by dq_2dq_3. Divide by $h_2h_3dq_2dq_3$. Cyclic permutation supplies all three components.

$$(\nabla \times \mathbf{A})_1 = \frac{\partial_2(h_3 A_3) - \partial_3(h_2 A_2)}{h_2 h_3}.$$

In cylindrical symmetry A=Aϕ(s)eϕ yields (curl A)z=s^{-1}d(sAϕ)/ds. Aϕ=Bs/2 has curl B ez, the familiar vector potential for a uniform axial magnetic field. Aϕ=C/s has zero local curl away from the axis but a nonzero circulation 2πC around it. The excluded axis supplies the topological or singular information.

Remember · Zero local curl needs a domain condition

Stokes' theorem requires a spanning surface inside the region where the field is regular. A loop encircling an excluded axis need not have such a surface. To infer a single-valued potential from zero curl, check the domain as well as the local differential equation.

Compose the two operators

Insert the gradient components into the divergence formula. The scalar Laplacian is therefore

$$\nabla^2 V = \frac{1}{h_1 h_2 h_3} \sum_i \partial_i \left(\frac{h_1 h_2 h_3}{h_i^2} \partial_i V \right).$$

In spherical coordinates this becomes $r^{-2}\partial r(r^2\partial rV)+(r^2\sin\theta)^{-1}\partial\theta(\sin\theta\partial\theta V)+(r^2\sin^2\theta)^{-1}\partial\phi^2V$. For $V=r^2P_2(\cos\theta)$, the radial contribution is $6P_2$ and the angular contribution is $-6P_2$. The potential is harmonic even though neither contribution vanishes separately. This cancellation underlies separation into radial powers and angular eigenfunctions.

Convert a physical experiment between conventions

In SI vacuum electrostatics the point-source law is $E=q/(4\pi\varepsilon_0 r^2)$, with force qE. Gaussian conventions write the corresponding laws $E=q/r^2$ and $F=qE$, while magnetic force contains $v\times B/c$. The numerical values and dimensions of both charge and field change. To convert, equate a measurable force in the same physical experiment first. One statcoulomb is $3.335640952\times10^{-10}$ C, one statvolt/cm is 29979.2458 V/m, and one gauss is 10^{-4} T.

$$\nabla \cdot \mathbf{E}_{\mathrm{G}} = 4\pi\rho_{\mathrm{G}},$$

$$\nabla \times \mathbf{B}_{\mathrm{G}} = \frac{1}{c}\partial_t \mathbf{E}_{\mathrm{G}} + \frac{4\pi}{c}\mathbf{J}_{\mathrm{G}}.$$

Gaussian electric and magnetic fields share dimensions. Rationalised Heaviside–Lorentz conventions absorb the source factors 4π into the field and charge normalisation. A conversion must state whether c is retained or set to unity. The route from an equation to a voltage or force requires restoring that convention. A ratio E/B in SI is a velocity, whereas E_G/B_G for a plane vacuum wave equals one.

Exercises on geometry and conversion

1. Derive the cylindrical Laplacian and apply it to $V=s^2\cos2\phi$. What Cartesian polynomial does this represent?

▼ **Work through the solution**

The radial term is $4\cos2\phi$ and the angular term is $-4\cos2\phi$. Their sum vanishes. Since $s^2\cos2\phi=x^2-y^2$, the Cartesian Laplacian is $2-2=0$.

---

2. A plane wave has $E=300$ V/m. Determine B in tesla and gauss, then check the Gaussian electric-field number.

▼ **Work through the solution**

$B=E/c\approx1.00069$ μT$=0.0100069$ G. Dividing 300 V/m by 29979.2458 V/m per statvolt/cm gives 0.0100069 statvolt/cm, the same Gaussian number.

---

3. Evaluate the outward flux of C e_s/s through a cylindrical shell and explain why local zero divergence does not remove an axial source.

▼ Work through the solution

The curved outer face gives 2πCL for length L, independent of radius. A shell with both inner and outer faces has net zero flux. A solid cylinder includes the singular axis, where the distributional source supplies 2πC per unit length.